Award Number: W81XWH-12-2-0042

TITLE: Development of Injury Thresholds Pertaining to Under-Body Blasts

PRINCIPAL INVESTIGATOR: Robert S. Salzar

CONTRACTING ORGANIZATION:
Rector & Visitors of the University of Virginia
Charlottesville, VA 22903-4833

REPORT DATE: November 2013

TYPE OF REPORT: Final

PREPARED FOR: U.S. Army Medical Research and Materiel Command
Fort Detrick, Maryland 21702-5012

REPORT DOCUMENTATION PAGE			Form Approved OMB No. 0704-0188
Public reporting burden for this collection of information is estimated to average 1 hour per response, including the time for reviewing instructions, searching existing data sources, gathering and maintaining the data needed, and completing and reviewing this collection of information. Send comments regarding this burden estimate or any other aspect of this collection of information, including suggestions for reducing this burden to Department of Defense, Washington Headquarters Services, Directorate for Information Operations and Reports (0704-0188), 1215 Jefferson Davis Highway, Suite 1204, Arlington, VA 22202-4302. Respondents should be aware that notwithstanding any other provision of law, no person shall be subject to any penalty for failing to comply with a collection of information if it does not display a currently valid OMB control number. **PLEASE DO NOT RETURN YOUR FORM TO THE ABOVE ADDRESS.**			
1. REPORT DATE November 2013	**2. REPORT TYPE** Final		**3. DATES COVERED** 01 May 2012 – 30 November 2013
4. TITLE AND SUBTITLE Development of Injury Thresholds Pertaining to Under-Body Blasts			**5a. CONTRACT NUMBER** **5b. GRANT NUMBER** W81XWH-12-2-0042 **5c. PROGRAM ELEMENT NUMBER**
6. AUTHOR(S) Robert S. Salzar E-Mail: salzar@virginia.edu			**5d. PROJECT NUMBER** **5e. TASK NUMBER** **5f. WORK UNIT NUMBER**
7. PERFORMING ORGANIZATION NAME(S) AND ADDRESS(ES) Rector & Visitors of the University of Virginia 1001 N Emmet ST Charlottesville, VA 22903-4833			**8. PERFORMING ORGANIZATION REPORT**
9. SPONSORING / MONITORING AGENCY NAME(S) AND ADDRESS(ES) U.S. Army Medical Research and Materiel Command Fort Detrick, Maryland 21702-5012			**10. SPONSOR/MONITOR'S ACRONYM(S)** **11. SPONSOR/MONITOR'S REPORT NUMBER(S)**
12. DISTRIBUTION / AVAILABILITY STATEMENT Approved for Public Release; Distribution Unlimited			
13. SUPPLEMENTARY NOTES			
14. ABSTRACT Severe injuries are being reported from occupants of MRAP and other vehicles exposed to under-body blasts. Both the etiology of these injuries and an effective means to mitigate these injuries are not currently known or understood, although whole body accelerations and at least some limited seat-pan and toe-pan intrusions are expected. Furthermore, live-fire testing with the Hybrid-III instrumented crash test dummy has resulted in sensor data that is difficult to interpret due to the lack of this dummy's biofidelity in the blast range of loadings. This proposal teams the University of Virginia Center for Applied Biomechanics (UVA-CAB) with collaborators at the U.S. Army Aeromedical Laboratory (USAARL) to develop new, blast rate injury criteria applicable to those injuries typically seen in theater resulting from under-body blasts to vehicle occupants. These criteria will be used to develop injury criteria for the WIAMan blast test dummy, so that competing vehicle designs, interior injury mitigation strategies, and personal protective equipment can be evaluated using this test dummy. Preliminary testing of Hybrid-III has begun for comparison to live-fire and GenHull2 Hybrid-III response. Initial results show that the UVA ODYSSEY blast simulator represents well the UBB environment, and is sufficient for WIAMan development work.			
15. SUBJECT TERMS WIAMan, Lower Extremity, Pelvis, Thorax, Blast, Injury			

16. SECURITY CLASSIFICATION OF:			**17. LIMITATION OF ABSTRACT**	**18. NUMBER**	**19a. NAME OF RESPONSIBLE PERSON**
a. REPORT	**b. ABSTRACT**	**c. THIS PAGE**			**19b. TELEPHONE NUMBER**
U	U	U	UU	77	*(include area code)*

Table of Contents

Introduction

Severe lower extremity injuries are being reported from occupants of MRAP vehicles exposed to under-body blasts. Both the etiology of these injuries and an effective means to mitigate these injuries are not currently known or understood, although whole body accelerations and at least some limited toe-pan intrusion are expected. Furthermore, there is currently no objective test methodology to determine the risk of injury to the lower extremities due to foot-well intrusion from under-vehicle blast. The research that the University of Virginia's Center for Applied Biomechanics has undertaken aims to create injury criteria for such injuries as well as investigate the injury and response of vehicle occupants.

The research that is presently completed in this area by UVA involves the design of an under-vehicle blast test device capable of testing both whole body PMHS and manikins over a range of expected loading environments. Extensive research into this loading environment has discovered broad spectrum loading with magnitudes ranging from 300g to 1800g, to over 68,000g. The current test device is designed to replicate each of these loading scenarios.

In addition, a primary injury mode has been identified that has not been previously known, or, well understood. This primary injury mode has appeared in the current military conflicts as a result of the increasing size of improvised explosive devices used to defeat the more fortified vehicle armor. This combination has resulted in a high frequency load to the lower extremity that is capable of producing injuries being reported from theater.

While the bulk of the effort of the original project remained in the planning stages while the contract was under USMRMC control, significant research and knowledge was gained over this period. Since the contract has changed management, we fully expect this research to continue to advance the state of knowledge of the effects of underbody blast, as well as provide the data necessary to create a robust, biofidellic manikin for LFT&E test purposes. The following report outlines the final research outcomes and proposals required by the program that were completed during the period of performance of this contract.

1. Submitted Research Plans

1.1 WIAMan Research Plan 1: Develop biofidelity corridors for the knee-thigh-hip complex for under body blast

1.1.1 ABSTRACT

The goal of this study is to determine the sub-injurious biomechanical response of PMHS subjects under loading conditions seen in Under Body Blast (UBB). The results of this study will provide critical data and validate the biofidelity of available ATDs, and provide occupant response to the vehicle motion with a particular emphasis on the lower extremity. Whole body PMHS will be instrumented and tested at conditions representative of those seen in under-body blasts.

1.1.2 STUDY PERSONNEL

Personnel Name	Responsibilities
Robert Salzar	PI
Annie Bailey	Project Manager
Aaron Alai	Test Engineer
Kyvory Henderson	Test Engineer

1.1.3 STUDY LOCATION

This study will be performed at the University of Virginia-Center for Applied Biomechanics, Charlottesville, VA.

1.1.4 OBJECTIVES/SPECIFIC AIMS/RESEARCH QUESTIONS

The goal of this study is to determine the biomechanical response of available ATDs and PMHS subjects under the loading condition similar to an event of Under Body Blast (UBB). The results of this study validate the biofidelity of the available ATDs and provide the occupant response to the vehicle motion with a particular emphasis on the lower extremity. The ATDs and whole body PMHS will be instrumented and tested at conditions representative of those seen in under-body blasts.

1.1.5 WIAMan/MILITARY RELEVANCE

Mine Resistant Ambush Protected (MRAP) and other armored vehicles (such as the M-ATV) are designed to survive improvised explosive device (IED) attacks and ambushes. Initial reports have indicated the prevalence of lower extremity injuries resulting from under-body loads which can lead to life-threatening hemorrhages in the short term, and costly, painful debilitation in the long term. This study will begin the process of reducing these injuries by focusing on the whole body kinematics of PMHS during a UBB event, resulting in strain and transmissibility data to be used in developing WIAMan, and understanding the deficiencies in current dummy designs.

1.1.6 SCIENTIFIC BACKGROUND AND SIGNIFICANCE

There is currently no objective test methodology to determine the risk of injury to the lower extremities due to foot-well intrusion from an under-vehicle blast, but a significant body of research exists on lower extremity injuries resulting from automobile crashes that may be useful for this project. Lower limb injuries sustained in automobile crashes have been heavily researched due to their frequency and high likelihood of impairment and disability. A review of the literature suggest that lower limb injuries account for roughly one-third of all moderate-to-serious injuries sustained by motor vehicle occupants involved in frontal crashes (Otte et al., 1992); Crandall et al., 1994; Kruger et al., 1994). Since intrusion of the foot-well region is often postulated as the primary mechanism of below-knee lower limb injuries, intrusion characteristics such as toe-pan displacement, toe-pan acceleration, intrusion onset rate, intrusion duration, and intrusion initiation time have been examined for their potential to produce lower limb trauma. The UVA research team has performed much of the research effort studying the effects of intrusion on injury risk using both component tests (Funk et al., 2000; Funk et al., 2002; Bass et al., 2004) and sled tests (Crandall et al., 1995; Rudd et al., 2001).

The injury mechanisms of the lower limb associated with intrusion of the footwell include inertial loading, entrapment, excessive motion of the joints, and subsequent contact with other structures within the occupant compartment (Crandall et al., 1998). In terms of mechanisms associated with these injuries, the most severe trauma is normally sustained from axial loading of the limb. Biomechanical testing has been conducted to develop basic injury criteria for axial loading of the below-knee structures. Yoganandan et al. (1997) conducted a series of axial impact tests to the human foot-ankle complex and found a mean dynamic force at fracture (calcaneus and distal tibia) to be 15.1 kN. Funk et al. (2002) determined injury risk functions for axial loads to the foot/ankle complex from a study that included axial loads up to approximately 12 kN.

The research team proposed here has also documented other injury mechanisms and criteria for the lower limb structures including ankle dorsiflexion (Rudd et al, 2004), hindfoot xversion (Funk et al., 2002), bending of the tibia and fibula (Schreiber et al., 1998), and bending of the femur (Funk et al, 2004; Ivarsson et al., 2009). While these tests provide valid criteria for the automotive environment, they possess several critical limitations for use in the development of injury countermeasures in the under-body blast environment: they have not been developed at rates of loading indicative of the vehicle-blast environment and they have not included any footwear (in particular combat boots). The applicability of studies and criteria remain a key question to answer in the course of the proposed research.

Preliminary tests for the Lower Extremity Assessment Program (LEAP) performed by both the University of Virginia and the U.S. Army Institute for Surgical Research have developed procedures that may be useful in evaluating these types of blast-induced intrusion injuries (Crandall et al., 2000; Bass et al., 2004). Beyond the blast environment, UVA has evaluated lower limb loading that occurs at the relatively high rates of ejection seat testing where contact with the seat structure and/or other body regions occur (Paskoff et al., 2002).

Using their research experience and knowledge in the area of lower limb biomechanics, vehicle crash testing with intrusion, blast loading, and injury criteria development, the UVA and USAARL teams have proposed a comprehensive research program that culminates with the delivery of a test methodology, injury criteria for dummies, and recommendations for mitigation strategies.

1.1.7 Research Methodology

A. Description of Research Approach

For this project, an experimental test methodology using both Hybrid-III and PMHS is developed using the University of Virginia ODYSSEY blast rig. This sled system will allow the evaluation of intrusion parameters such as acceleration time-histories and toe-pan compliance on the kinematic patterns of PMHS bodies in a realistic vehicle environment.

Acknowledging that standard crash test dummies were designed by automobile manufacturers for primarily seated postures and load vectors commonly seen in frontal or lateral automobile crashes, these dummies were not designed for multi-axial loads including dominant vertical loading seen in under-body blasts. However, these dummies will continue to be widely used as an instrumentation platform for evaluating soldier survivability in free-field tests. The standard crash test dummy, the Hybrid-III, is a robust instrumentation platform that has the anthropometry of a 50th percentile male, although limited biofidelity in some very specific areas. For example, it is known that the Hybrid-III spine has little spine articulation (all focused at the pelvis/spine interface and the neck), and that the lower extremities are overly stiff with poor frequency response (Crandall et al., 1996). An improved dummy for automotive testing, Thor, has better thoracic response, along with an advanced lower extremity design (Thor LX) which may prove to be more biofidelic and predictive of injury in under-body blast loadings. While the THOR LX is the most advanced design known to the research team, other lower extremity dummy designs can be examined for their appropriateness to represent the lower extremity kinematics seen in theater.

For the proposed project, the Hybrid-III and whole body PMHS specimens will be used as both an instrumentation platform, and in the case of the PMHS, a biofidelic surrogate capable of modeling kinematics of human body.

B. Research Specimens/Components (Cadavers and/or ATDs as Applicable)

The specimens will be selected from male donors, which have no previous injuries to the flesh. The subjects will be tested for standard potential transmissible diseases. Only cadavers meeting all of the following criteria may be utilized in the study: (1) Males above the age of 18 years and below the age of 80 years. (2) Cadavers without existing unhealed bone or soft tissue injury. (3) Cadavers will not have evidence of wasting disease. (4) Cadavers tested negative for Hepatitis A, B, C and HIV. (5) Only remains obtained from an approved source. To limit cadaveric variation, specimens will be selected that have a stature of 1755±70mm and a mass of 85±14kg, which is based on U.S. Army anthropometric studies for the 50th percentile male.

Specimens' demographics and anthropometry will be precisely documented during the preparation process and pre- and post-test CT scans will be acquired from the specimens. Due to the nature of the research at the University of Virginia-Center for Applied Biomechanics, a large source of PMHS samples are available and more specimens are being acquired for the WIAMan project.

The standard 50% male Hybrid-III will be tested in matched pair tests in this effort.

C. Exposures, Setup, and Data

Using the University of Virginia ODYSSEY blast rig, the kinematics and internal forces/strains of the femur/patella/tibia-fibula complex will be determined in sub-injurious testing. Six whole body PMHS and an instrumented Hybrid-III will be used in this task. Each will be positioned on the test device with varying levels of knee extension, simulating common seating positions. Instrumentation in the Hybrid-III tests will be similar to that used in the main study, and listed here in Table 1. Instrumentation in the PMHS tests will be focused on the lower extremities, and listed in Table 2. Matched condition tests (x2 iterations) will be performed with the PMHS and the Hybrid-III for each seating position and loading condition, as outlined in Table 3. Three different knee angle positions will be tested at two different load levels. Each of the 6 PMHS will be tested 4 times at different sub-injurious load conditions. The test matrix has been developed such that 4 tests will be performed for each test condition, and so that comparisons can be made between each loading condition for each knee angle.

The load levels for these tests are shown in Table 4. The load levels have been determined based on previous PMHS testing using the ODYSSEY blast rig and the recommendations of the Pelvis Working Group. Note that the high loading condition is representative of the V1 condition in the N129 test matrix which is currently defined as a 5m/s in 5 ms rise time. Drawing from live fire data and Generic Hull 2 data, the acceleration for the seat pan should be a fraction of the toe pan acceleration; therefore the pulses summarized in Table 4 are based on this observation. The low load condition was developed based on the ranges produced by the Pelvis Working Group such that the probability of injury was greatly reduced. These load conditions may be slightly altered to fit the needs of the WIAMan project, but are recommended based on the necessity of keeping these tests sub-injurious so that the entire test matrix may be completed.

Since each PMHS will be tested multiple times, a rigorous set of checks will be performed between tests to determine whether injury has occurred and whether testing should continue on that body. These checks include preliminary analysis of the strain gage data or data from other pertinent sensor as well as visual inspection of the body and checks for laxity in joints. Pre- and post-test conditions will be well documented using photography as well as notes taken during visual inspection of the body. After all tests have been completed for a body, a post-test CT will be performed to verify that no injuries were incurred during testing.

Instrumentation for the ATD and PMHS testing has been chosen so as to make the best use of available data acquisition resources while meeting the requirements for biofidelity corridors. Therefore, based on observations from previous testing performed using the Odyssey blast rig, some accelerometers for the Y-axis have been removed from the instrumentation list as well as angular rate sensors for the X- and Z- axes. Table 2 shows the instrumentation list for the PMHS tests. The channels highlighted in green are channels which are required for creating the biofidelity corridors requested for the WIAMan project. The additional channels will enable a better understanding of the kinematics and response of the subject during the test without collecting data for unnecessary axes. Table 5 shows which of the biofidelity corridors can be developed from this series of tests. Strain gage locations for the pelvis are to be determined based on the results from component pelvis tests.

Table 5 indicates that spinal compression (video), femur bone-load cell FX, and foot accel Z biofidelity corridors will not be satisfied by these tests. Because Vicon is not included or budgeted for on these tests, spinal compression will not be possible to analyze. Determining the femur FX load would require the implantation of a femur load cell by removing a portion of the femur diaphysis. This is not recommended due to the disruption of the load path as well as the possibility of creating artifactual fractures. Instead, strain gages will be placed along the length of the tibia, which will allow for detection of bending in the femur. Finally, foot acceleration in the z-direction will not be measured due to difficulties with attaching the sensor in an appropriate location which would provide useful data. The logical position for this sensor would be to rigidly attach it to the calcaneus, but due to its irregular geometry it would be difficult to attach the sensor without creating artifactual injuries from screwing directly into the bone.

Ideally this test series would be able to fulfill part of the N129 test matrix (specifically WB 31 and 32), though this series of testing was originally part of the Jumpstart effort aimed at gaining knowledge about the appropriate loading conditions. However, this test series does not include PPE as is required for WB 31 and 32, and the test conditions are set for a lower velocity than the 7 m/s in 5ms as are required in the N129 test matrix, so as to insure that no injury is incurred during testing. Our test equipment has the capability to meet the requirements of WB 31 and 32 in the N129 test matrix, however, because of the risk of injury at the required loading condition as well as the possibility that the presence of the medium PPE may tie the kinematic results to that particular set of PPE which would be less useful to dummy development.

Table 1. Hybrid-III Test Instrumentation

MEASURAND	SEN.	SENSOR Type	AXIS	MAX	UNIT
Acceleration	Left hindfoot	7264B	X	2000	G
Acceleration		7270	Z	6000	G
Acceleration	Left midfoot	7264B	X	2000	G
Acceleration		7270	Z	6000	G
Acceleration	Right Mid-	7264B	X	2000	G

	Tibia				
Acceleration		7270	Z	6000	G
Acceleration	Left Mid-Tibia	7264B	X	2000	G
Acceleration		7270	Z	6000	G
Acceleration	Hybrid-III Head CG	7264B	X	2000	G
Acceleration		7264B	Y	2000	G
Acceleration		7264B	Z	2000	G
Angular rate		8k ARS	X	8k	Deg/s
Angular rate		8k ARS	Y	8k	Deg/s
Acceleration	Hybrid-III T1	7264B	X	2000	G
Acceleration		7264B	Z	2000	G
Angular rate		8k ARS	X	8k	Deg/s
Angular rate		8k ARS	Y	8k	Deg/s
Acceleration	Hybrid-III Pelvis	7264B	X	2000	G
Acceleration		7264B	Y	2000	G
Acceleration		7264B	Z	2000	G
Angular rate		8k ARS	X	8k	Deg/s
Angular rate		12k ARS	Y	8k	Deg/s
Acceleration	Toe pan	7270	Z	6000	G
Acceleration	Seat pan	7270	Z	6000	G
Belt tension load	Left shoulder belt				N
Belt tension load	Right shoulder belt				N
Belt tension load	Lap belt				N
Forces/moments	Hybrid-III lumbar spine	Den1842	XYZ		N, Nm
Forces/moments	Hybrid-III Left Femur	Den1914	XYZ		N, Nm
Forces/moments	Mil-LX Right Upper Tibia		XYZ		N, Nm
Forces/moments	Hybrid-III Left Upper Tibia	Den3785J	XYZ		N, Nm
Forces/moments	Mil-LX Right Lower Tibia		XYZ		N, Nm
Forces/moments	Hybrid-III Left Lower Tibia	Den3785J	XYZ		N, Nm
Forces/moments	Hybrid-III Upper Neck	Den1716A	XYZ		N, Nm

Table 2. PMHS Instrumentation Matrix

Measurand	Location	Instrument	Axis	Range	Units	BRC
Acceleration	Right Distal Tibia	7264B	X	2000	G	
Acceleration		7270	Z	6000	G	Tibia Accel Z
Angular rate		18k ARS	Y	18k	Deg/s	
Acceleration	Left Distal Tibia	7264B	X	2000	G	
Acceleration		7270	Z	6000	G	Tibia Accel Z
Angular rate		18k ARS	Y	18k	Deg/s	

Acceleration	Right Distal Femur	7264B	X	2000	G	Femur Accel X
Acceleration		7264B	Z	2000	G	
Angular rate		8k ARS	Y	8k	Deg/s	
Acceleration	Left Distal Femur	7264B	X	2000	G	Femur Accel X
Acceleration		7264B	Z	2000	G	
Angular rate		8k ARS	Y	8k	Deg/s	
Acceleration	Pelvis (Lumbar Spine)	7264B	X	2000	G	Pelvis Accel Z, Pelvis Resultant Accel
Acceleration		7264B	Y	2000	G	Pelvis Resultant Accel
Acceleration		7264B	Z	2000	G	Pelvis Resultant Accel
Angular rate		8k ARS	Y	8k	Deg/s	Pelvis Rotation
Acceleration	Head	7264B	X	2000	G	
Acceleration		7264B	Y	2000	G	
Acceleration		7264B	Z	2000	G	
Angular rate		8k ARS	X	8k	Deg/s	
Angular rate		8k ARS	Y	8k	Deg/s	
Angular rate		8k ARS	Z	8k	Deg/s	
Acceleration	T1 Vertebra	7264B	X	2000	G	
Acceleration		7264B	Z	2000	G	T1 Accel Z
Angular rate		8k ARS	Y	8k	Deg/s	T1 Rotation
Acceleration	T4 Vertebra	7264B	X	2000	G	
Acceleration		7264B	Z	2000	G	T4 Accel Z
Angular rate		8k ARS	Y	8k	Deg/s	T4 Rotation
Acceleration	T12 Vertebra	7264B	X	2000	G	
Acceleration		7264B	Z	2000	G	T12 Accel Z
Angular rate		8k ARS	Y	8k	Deg/s	T12 Rotation
Acceleration	Sternum	7264B	X	2000	G	
Acceleration	Sternum	7264B	Z	2000	G	
Acceleration	Seat hammer	7270A	Z	6000	G	
Acceleration	Toe hammer	7270A	Z	6000	G	
Belt tension load	Left shoulder belt	Belt tension LC			N	
Belt tension load	Right shoulder belt	Belt tension LC			N	

Belt tension load	Lap belt	Belt tension LC			N	
Acceleration	Toe pan	7270	Z	6000	G	
Acceleration	Seat pan	7270	Z	6000	G	
Acceleration	Toe pan	Loffi	Z		G	
Acceleration	Seat pan	Loffi	Z		G	
Strain	Right Anterior Distal Femur	Vishay SG	Z			
Strain	Right Anterior Mid-Femur	Vishay SG	Z			
Strain	Right Anterior Proximal Femur	Vishay SG	Z			
Strain	Left Anterior Distal Femur	Vishay SG	Z			
Strain	Left Anterior Mid-Femur	Vishay SG	Z			
Strain	Left Anterior Proximal Femur	Vishay SG	Z			
Strain	Right Distal Anterior Tibia	Vishay SG	Z			Tibia Force Z
Strain	Left Distal Anterior Tibia	Vishay SG	Z			Tibia Force Z
Strain	Right Distal Medial Tibia	Vishay SG	Z			Tibia Force Z
Strain	Left Distal Medial Tibia	Vishay SG	Z			Tibia Force Z
Strain	Right Distal Lateral Tibia	Vishay SG	Z			Tibia Force Z
Strain	Left Distal Lateral Tibia	Vishay SG	Z			Tibia Force Z
Strain	Right Distal Posterior Tibia	Vishay SG	Z			Tibia Force Z
Strain	Left Distal Posterior Tibia	Vishay SG	Z			Tibia Force Z
Strain	Left Anterior Mid- Tibia	Vishay SG	Z			
Strain	Left Anterior Proximal	Vishay SG	Z			

	Tibia					
Strain	Right Calcaneus	Vishay SG	Z			
Strain	Left Calcaneus	Vishay SG	Z			
Strain	Right 4th Rib	Vishay SG				
Strain	Left 4th Rib	Vishay SG				
Strain	Right 8th Rib	Vishay SG				
Strain	Left 8th Rib	Vishay SG				
Acoustic Emission	Right Tibia	Vishay SG				
Acoustic Emission	Left Tibia	Vishay SG				
Strain	Pelvis TBD	Vishay SG				
Strain	Pelvis TBD	Vishay SG				
Strain	Pelvis TBD	Vishay SG				
Strain	Pelvis TBD	Vishay SG				

Table 3. Test matrix of whole body tests

Test Condition			**Specimen Numbers**		
No PPE					
	WB 18		**1,2,3**		
7 m/s	**8 ms**	**90/90/90**			
	WB 14		**7,8,9**		
7 m/s	**5 ms**	**90/90/90**			
	WB 20		**13, 14, 15**		
7 m/s	**2 ms**	**90/90/90**			
Medium PPE					
	WB 17		**4, 5, 6**		
7 m/s	**8 ms**	**90/90/90**			
	WB 16		**10, 11, 12**		
7 m/s	**5 ms**	**90/90/90**			
	WB 19		**16, 17, 18**		
7 m/s	**2 ms**	**90/90/90**			
			Velocity	**Time to Peak**	**KTH Angles**

Table 4. Loading conditions for kinematics tests.

Load Level	Foot Pan Acceleration (G) in (ms)	Foot Pan Velocity (m/s) in (ms)	Seat Pan Acceleration (G) in (ms)	Seat Pan Velocity (m/s) in (ms)
Low	100 in 2.5	3.3 in 6.8	90 in 6.4	3.5 in 8.5
High	450 in 1.5	5.6 in 4.8	370 in 2.3	6.7 in 6

Biofidelity corridors will be reported at the conclusion of this task, and will be used to assess both the appropriateness of the Hybrid-III for this loading regime, as well as to identify potentially less injurious seating positions during under body blast scenarios.

The kinematics will be documented using high speed camera footage. An overhead and side view will be recorded with NAC high speed cameras. Video analysis of markers placed on the test subject will be used to obtain the required biofidelity corridors.

Table 5. Coordination with Biofidelity Corridor Requirements

Velocity	Low	High (V1)
PPE	boots	boots
Posture (knee angle in degrees)	84, 90, 106	84, 90, 106
Corridors		
Head Accel Z	Yes	Yes
Head Accel Resultant	Yes	Yes
Head Rotation (ARS)	Yes	Yes
Motion of Head (video)	Yes	Yes
Spinal compression (video)	No	No
Motion of Shoulder (video)	Yes	Yes
T1 Spinal Accel Z	Yes	Yes
T1 Spinal Rotation (ARS)	Yes	Yes
T4 Spinal Accel Z	Yes	Yes
T4 Spinal Rotation (ARS)	Yes	Yes
T12 Spinal Accel Z	Yes	Yes
T12 Spinal Rotation (ARS)	Yes	Yes
Pelvis Accel Z	Yes	Yes
Pelvis Accel Resultant	Yes	Yes
Pelvis rotation (ARS)	Yes	Yes
Femur Accel X	Yes	Yes
Femur Bone-Load Cell FX	No	No
Tibia Accel Z	Yes	Yes
Tibia Bone-load cell FZ	Yes	Yes
Foot Accel Z	No	No
Head rotation relative to torso (XZ Plane)	Yes	Yes
Head rotation relative to pelvis (XZ Plane)	Yes	Yes
Motion of knees (video)	Yes	Yes
Motion of feet (video)	Yes	Yes

1.1.8 ANALYSIS PLAN

The kinematics of the PMHS and ATD subjects will be collected and the local forces and accelerations will be calculated. The results of this study evaluate the biofidelity of the available ATDs and also provide the occupant response to the WIAMan developer in an event of UBB. Biofidelity corridors relevant to the WIAMan project will be developed according to the methods of Lessley, et al. (2004). All data will be mass scaled and length scaled when appropriate.

1.1.9 SCHEDULE, PRODUCTS, AND MILESTONES

The experimental part of this study is planned start early March 2013 and concluded by September 31, 2013, with data analysis concluded by January 31, 2013. By the end of this period the kinematics of the lower leg components along with all the experimental data will be delivered as the final product of this study.

1.1.10 ASSUMPTIONS AND RISKS

Cadaver protocol documents submitted to U.S. Army, and are currently under review.

1.2 WIAMan Research Plan 2: Develop uni-axial injury criteria for the pelvis subject to load vectors and rates seen in live-fire testing

1.2.2 ABSTRACT

This task undertakes the development of a pelvic injury criterion subject to under-body vertical loads at rates similar to those seen in live-fire tests. These tests will provide structural response and injury data sufficient to develop a biofidelic pelvis for WIAMan along with the required sensors (accelerometers and load cells) necessary to interpret the applied dummy loads.

1.2.3 STUDY PERSONNEL

Personnel Name	Responsibilities
Robert S. Salzar	PI
Jake Christopher	Project Manager
Kyvory Henderson	Test Engineer
Dennis Roethlisberger	Data Integrity Engineer
Sara Heltzel	Biological Materials Specialist

1.2.4 STUDY LOCATION

All aspects of this task will be performed at the Center for Applied Biomechanics at the University of Virginia

1.2.5 OBJECTIVES/SPECIFIC AIMS/RESEARCH QUESTIONS

This task undertakes the development of a pelvic injury criterion subject to under-body vertical loads at rates similar to those seen in live-fire tests. These tests will provide structural response and injury data sufficient to develop a biofidelic pelvis for WIAMan along with the required sensors (accelerometers and load cells) necessary to interpret the applied dummy loads. This task includes first article testing (and limited material characterization) of WIAMan pelvis designs. The testing of injury mitigation strategies such as seat cushions with the final WIAMan design is not within the scope of this proposal, but is anticipated as follow-on research.

1.2.6 WIAMan/MILITARY RELEVANCE

This task will provide high rate material properties of the pelves through the combination of applied force/acceleration and resulting strain, human biofidelity corridors from the iliac wing displacement, and human injury risk curves from the resulting survival analysis of the pelves. Matched pair testing of first article WIAMan pelves and the PMHS pelves tested in this task will provide sufficient data to develop IARCs for the WIAMan pelvis.

1.2.7 SCIENTIFIC BACKGROUND AND SIGNIFICANCE

Severe injuries are being reported from occupants of MRAP and other vehicles exposed to under-body blasts. Both the etiology of these injuries and an effective means to mitigate these injuries are not currently known or understood, although whole body accelerations and at least some limited seat-pan and toe-pan intrusions are expected. Furthermore, live-fire testing with the Hybrid-III instrumented crash test dummy has resulted in sensor data that is difficult to interpret due to the lack of this dummy's biofidelity in the blast range of loadings. This proposal tasks the University of Virginia Center for Applied Biomechanics (UVA-CAB) to develop new, blast rate injury criteria applicable to those injuries typically seen in theater resulting from under-body blasts to vehicle occupants. These criteria will be used to develop injury criteria for the WIAMan blast test dummy, so that competing vehicle designs, interior injury mitigation strategies, and personal protective equipment can be evaluated using this test dummy. All testing proposed in this document will utilize previous test data and acquired knowledge gained during the execution of the original contracted effort. In preparation of the original contracted effort, two under-body blast simulation devices (one whole body and one component – based) were developed and constructed to deliver the input accelerations seen in live fire testing to the toe-pan and seat-pan of the vehicle occupant. This blast simulator allows the reproduction of vehicle accelerations within a laboratory environment and without live explosives. This enables full visualization of the impact event using high-speed video cameras, VICON motion capture systems, high-speed x-ray, full instrumentation, and access to PMHS that have not obtained permissions from the donor's next of kin for live-fire testing.

The baseline loading conditions to be used in the execution of this test series include a low and high-rate linear impactor configuration (component pelvis testing), and a low, medium, and high-rate UBB simulator configuration (whole body PMHS testing). The range of these load profiles are shown in Figure 1.

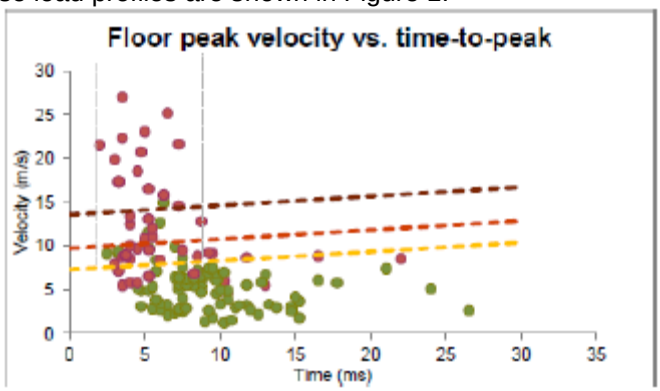

Figure 1. Loading targets to be used in the evaluation of PMHS and WIAMan (i.e. 7, 10, and 15 m/s).

1.2.8 RESEARCH METHODOLOGY

A. Description of Research Approach

Most injury research involving the pelvis has been performed for the automotive industry, due to the prevalence and severity of these injuries. Moffat et al. (1990) estimated that, in 1985 alone, 15,300 pelvic fractures occurred during motor vehicle crashes in the United States. The mortality rate for such injuries may be as high as 50% (Gocken et al, 1994) due to concurrent intra-abdominal hemorrhaging and puncturing of the abdominal viscera. In addition to the complex treatment and extensive rehabilitation frequently required to treat pelvic ring and acetabular fractures, incomplete reduction can lead to post-traumatic osteoarthritis (Hoffman et al., 1984).

Studies have shown that pelvic injury patterns correlate significantly with the direction of impact (States, 1986; McCoy et al., 1989; Pattimore et al., 1991; Dischinger et al., 1993; Siegel et al., 1993). Recent studies indicate that there are approximately 15,000 hip injuries annually caused by frontal crashes in the United States alone (Rupp et al., 2002). Kuppa and Fessahaie (2003) emphasized that knee-thigh-hip injuries are the most common form of lower extremity injuries. The distribution of lower extremity injuries in motor vehicle crashes reveals a recent increase in the prevalence of hip injuries compared to knee/thigh injuries (Rupp et al., 2003). Otte (1996) surveyed 6,985 car crashes and found combinations of femoral and pelvic fractures in frontal impacts. Severe open book pelvic fractures resulting from frontal impacts involve complete disruption of the pubic symphysis. Pelvic instability caused by pubic symphysis laxity has been associated with pelvic pain (LaBan et al., 1978) and sacral stress fractures (Albertson et al., 1995) in non-traumatic patients.

Near-side automotive impacts (where the vehicle strikes the occupant side) are the number one cause of pelvic injuries (Gokcen et al., 1994; Samaha and Elliott, 2003). Side impacts tend to produce lateral compression fractures on the pelvic ring that involve the pubic rami, sacrum, and iliac wing. Although seat belts and airbags are effective in preventing automotive fatalities and reducing injury severity in frontal impacts, they provide minimal benefits against pelvic injury during side impacts (Loo et al., 1996). In a clinical study on pelvic injuries in side impacts, States and States (1968) found predominantly pubic rami fractures and sacral crush. Acetabular fractures with central dislocation of the femoral head were noted among a small percentage of side impact victims. Grattan and Hobbs (1969) studies hip joint injuries in side impacts and also found predominantly pubic rami fractures, along with some centrally dislocated acetabular fractures. Other clinical data indicate that acetabular fractures do occur in automotive side impacts (Schmidtke et al., 1995; Dakin et al., 1999). Gokcen et al. (1994), in a surveillance study of pelvic fractures resulting from car crashes found a mortality rate of roughly 50% and unsatisfactory treatment among one-third of the survivors. They found that despite the fact that frontal collisions outnumbered lateral collisions, more pelvic fractures occurred in lateral collisions. Otte (1996) found isolated pelvic fractures in lateral impacts in both car and object collisions. Thomas and Frampton (1999) determined that fractures of the pelvis and lower extremity scored higher than other forms of injury on the HARM scale (Malliaris et al., 1985), which reflects economic costs associated with long-term outcome.

Automotive accidents including frontal and side collisions (Nordhoff, 2005) and car-to-pedestrian impacts (Teresinski and Madro, 2001) are a leading cause of injury to sacroiliac joints and the surrounding ligaments. Guillemot et al. (1997) found that near-side impacts account for 94% of the sacroiliac joint injuries. Under very high energy impacts, an unstable fracture of the pelvis such as open book pelvic fractures usually occurs, with failure of the SI ligaments. So far, little information is available about the injury mechanisms of the SI joint in automotive collisions, and the role of accessory ligaments on the SI joint stability and mobility is still not well understood.

Guillemot and Cuny (2005) examined the LAB-CEESAR database for belted drivers and front seat passengers in frontal impacts as well as occupants involved in lateral impacts who sustained pelvic injuries (Table 1). Frontal impacts produced mostly iliac wing and acetabulum fractures each in approximately one-third of the cases whereas lateral impacts produced rami fractures in 57% of the cases.

Table 1. Pelvic injuries sustained in frontal and lateral crashes.

Injuries	Frontal		Side	
	n	%	n	%
Iliac Wing	21	31	12	11
Pubic Rami	11	16	60	57
Acetabulum	22	33	14	13
Hip	6	9	2	2
Ilium	-	-	1	1
Ischium	-	-	2	2
Sacroiliac Joint	1	1	7	7
Sacrum	4	6	4	4
Symphysis	3	4	3	3
Total	68	100	105	100

Summary:

- Fractures of the pubic rami are the most common fractures in side impacts, followed by fractures of the acetabulum, sacrum, and iliac wing.
- In lateral collisions, the most frequent fracture sites are the rami and iliac wing.
- Frontal collisions are commonly associated with acetabular fractures but they can also be produced in lateral impacts.
- In severe frontal collisions, disruption of the sacro-iliac joint occurs.

Salzar et al. (2006) developed a position-dependent injury tolerance of the pelvis for a frontal impact direction. This study found an axial injury tolerance based on peak force to be 6,850N for the extended, neutral seated position, and 4,090N in the flexed, neutral position. From the flexed neutral orientation, the peak axial force increased 18% for 20° abduction and decreased 6% for 20° adduction. This variation in fracture tolerance due to femur position indicates the need for further refinement of pelvic injury criteria.

Salzar et al. (2009) further investigated load path distribution through the pelvis from a lateral load in order to help design a more representative biofidelic pelvis for an automobile manufacturer.

There is evidence that multiple fractures to the pelvis are being seen during a UBB event. These injuries include to the pelvic ring, as well as the ischium; a fracture that is not commonly seen during an automotive impact (Figure 2). Each possible fracture mechanism will be investigated in this task for the purpose of providing sufficient biofidelity and injury data for the development of a new instrumented pelvis for WIAMan.

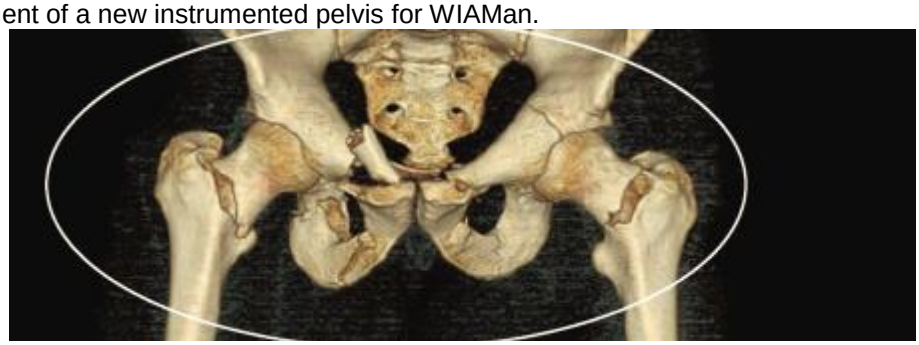

Figure 2. Pelvic fractures due to a UBB event. Note femoral neck fractures indicative of femoral shaft loading, ischium fractures likely due to vertical loading, and pelvic ring instability.

B. Research Specimens/Components (Cadavers and/or ATDs as Applicable)

- Task 1.1 (femur loading of pelvis) **Not funded**
  Task 1.2 (posterior loading of pelvis) Specimens quantity: 6-component pelvis (**funding based on priorities**)
  Task 1.3 (lateral loading of pelvis) Specimens quantity: 12 component pelvis (**funding based on priorities**)
  Task 1.4 (vertical loading of pelvis) Specimens quantity: 18 component pelves, 8 whole body PHMS (**Currently Funded**)
- Specimens will be procured from approved sources and will focus on 50% males between the ages of 18 and 65 years of age. Specimens will be procured for this task, as all on-hand specimens do not meet the current Army's approval for informed consent. Depending on anthropometry range of specimens, scaling based on the decisions of the Army Biomedical IPT will be used in the post-processing of the resulting data.

- Inclusion criteria for this Task:
  - Negative for communicable Hep B, Hep C, and HIV (testing by supplier preferred or the Center prior to acceptance)
  - No known medical history of active TB, MRSA, or sudden onset dementia
  - For whole bodies – height and weight proportional, no evidence of abnormalities that might affect the mechanical properties of the thorax, recent thoracic surgery, known thoracic cancer or metastases to thorax, rib fractures due to aggressive CPR.
  - For components – no known history of trauma to the extremity or metastatic disease that might affect bone strength
- Limited medical histories are available for each specimen. However, these will be reviewed. DEXA will be taken on each specimen to quantify bone quality.
- Depending on anthropometry range of specimens, scaling based on the decisions of the Army Biomedical IPT will be used in the post-processing of the resulting data.

C. Exposures, Setup, and Data (original Task 1.4)

This Task will use a combination of the UVA Odyssey underbody blast simulator and the UVA linear impactor-based component UBB simulator (TELEMACHUS) (Figure 3). Using the knowledge and data developed in previous whole body PMHS work, parallel load rates produced in the whole body tests will be reproduced on the component level.

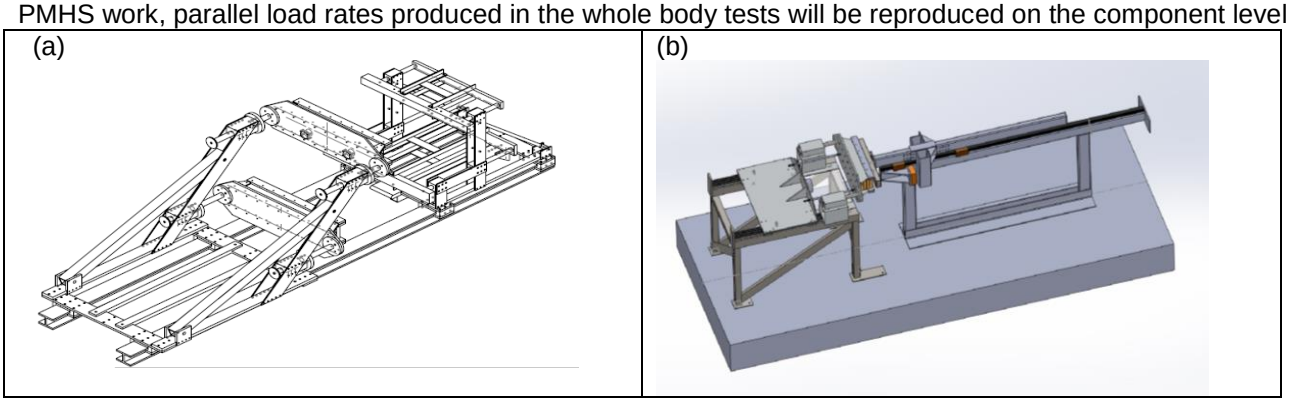

Figure 3. Schematic of UVA (a) ODYSSEY sled-based whole body UBB simulator; and (b) TELEMACHUS linear impactor-based component UBB simulator.

The primary injury directions to the pelvis of occupants of vehicles subject to under body blast is likely to be vertical as the seat-pan accelerates into the pelvic complex. The response of the pelvis in the vertical direction is not well researched by the automotive community since this is not a common loading vector. Vertical loads to the pelvis are seen in military aviators subject to both crashes and ejection pulses. In ejection seat tests performed at the University of Virginia, the vertical acceleration pulse used has a much longer duration with a much smaller peak than that seen in UBB events (Figure 4) (Salzar et al., 2009).

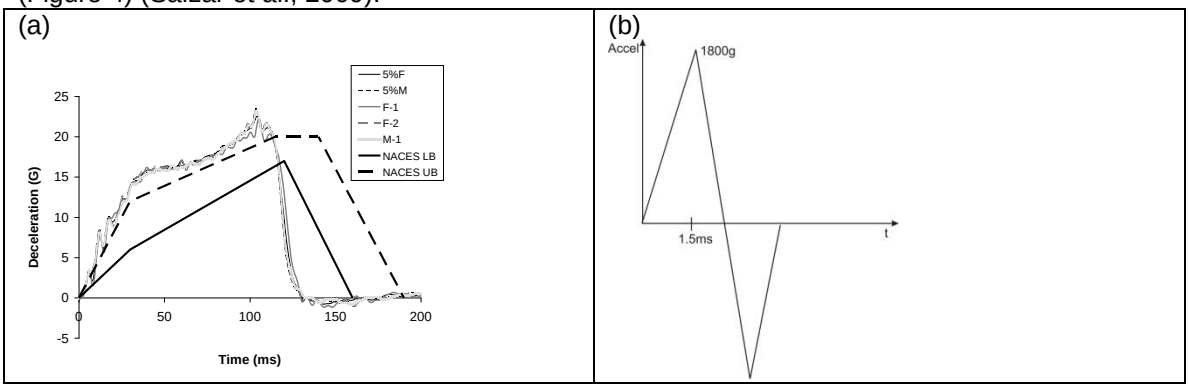

Figure 4. (a) Ejection seat pulse used in Salzar et al. (2009); (b) Idealized UBB pulse modeled by the UVA whole body UBB simulator.

D. Test Matrices

There are two critical body parts that are susceptible to both phases of loading from a UBB event. The first are the foot and lower extremities. The second are the lower torso and pelvis in contact with the seat-pan of the vehicle. Both of these critical areas can be subject to inertial loading from up to the 1800g vertical acceleration pulse, but also to the low momentum, high energy compression wave that propagates from the shock wave into the steel structure of the vehicle, and then into any body part in contact with that vehicle. Of course, this compression wave is potentially mitigated by any damped seat, but for the purpose of this study, an idealized steel seat will be used to model the worst case scenario.

Both the UVA-UBBS and the linear impactor will be used to examine the vertical load paths and failure stresses/strains seen in the pelvis during an under body blast event. For the lower range of loads, component tests will be performed on the UVA linear impactor UBB device (Figure 5). Two different load rates will be explored on the linear impactor, along with three different seated postures. The testing of first article designs of the WIAMan pelvis is included in this task using the same test rig. Limited material characterization testing on candidate pelvis materials supplied by the dummy manufacturer is included in this task.

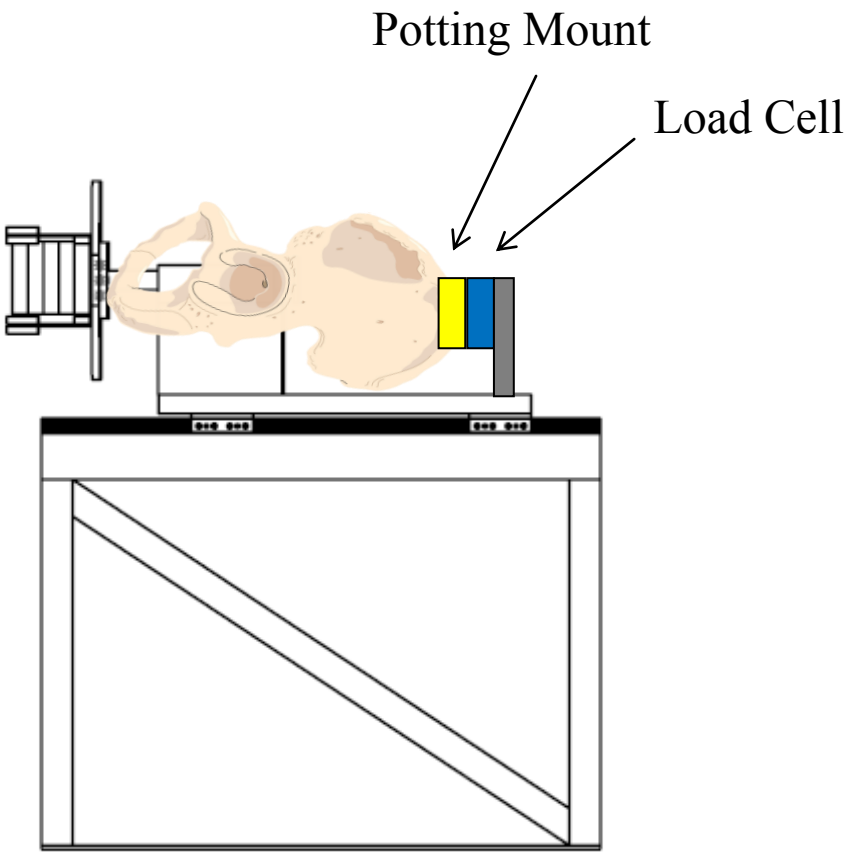

Figure 5. Pelvis loading configuration using the UVA component UBB simulator.

The test matrix for the component tests is shown in Table 2.

Table 2. Test matrix for vertical loading of pelvis (component PMHS tests)

PV02 (w/ flesh)		
Test #	**Specimen #**	**Velocity**
1	Specimen #1	V0
2	Specimen #1	V0

3	Specimen #1	BRC V1
4	Specimen #1	V0
5	Specimen #1	BRC V2
6	Specimen #1	V0
7	Specimen #1	BRC V3
8	Specimen #1	V0
1	Specimen #2	V0
2	Specimen #2	V0
3	Specimen #2	BRC V1
4	Specimen #2	V0
5	Specimen #2	BRC V2
6	Specimen #2	V0
7	Specimen #2	BRC V3
8	Specimen #2	V0
1	Specimen #3	V0
2	Specimen #3	V0
3	Specimen #3	BRC V1
4	Specimen #3	V0
5	Specimen #3	BRC V2
6	Specimen #3	V0
7	Specimen #3	BRC V3
8	Specimen #3	V0

PV12 (w/o flesh)		
Test #	**Specimen #**	**Velocity**
1	Specimen #1	V0
2	Specimen #1	V0
3	Specimen #1	BRC V1
4	Specimen #1	V0
5	Specimen #1	BRC V2
6	Specimen #1	V0
7	Specimen #1	BRC V3
8	Specimen #1	V0
9	Specimen #1	V4
1	Specimen #2	V0
2	Specimen #2	V0
3	Specimen #2	BRC V1
4	Specimen #2	V0

5	Specimen #2	BRC V2
6	Specimen #2	V0
7	Specimen #2	BRC V3
8	Specimen #2	V0
9	Specimen #2	V5
1	Specimen #3	V0
2	Specimen #3	V0
3	Specimen #3	BRC V1
4	Specimen #3	V0
5	Specimen #3	BRC V2
6	Specimen #3	V0
7	Specimen #3	BRC V3
8	Specimen #3	V0
9	Specimen #3	V6

PV14 (w/ flesh)

Test #	**Specimen #**	**Velocity**	**Test #**	**Specimen #**	**Velocity**	**Test #**	**Specimen #**	**Velocity**
1	Specimen #4	V0	1	Specimen #7	V0	1	Specimen #10	V0
2	Specimen #4	V0	2	Specimen #7	V0	2	Specimen #10	V0
3	Specimen #4	BRC V1	3	Specimen #7	BRC V1	3	Specimen #10	BRC V1
4	Specimen #4	V0	4	Specimen #7	V0	4	Specimen #10	V0
5	Specimen #4	BRC V2	5	Specimen #7	BRC V2	5	Specimen #10	BRC V2
6	Specimen #4	V0	6	Specimen #7	V0	6	Specimen #10	V0
7	Specimen #4	BRC V3	7	Specimen #7	BRC V3	7	Specimen #10	BRC V3
8	Specimen #4	V0	8	Specimen #7	V0	8	Specimen #10	V0
9	Specimen #4	V4	9	Specimen #7	V4	9	Specimen #10	V4
1	Specimen #5	V0	1	Specimen #8	V0	1	Specimen #11	V0
2	Specimen #5	V0	2	Specimen #8	V0	2	Specimen #11	V0
3	Specimen #5	BRC V1	3	Specimen #8	BRC V1	3	Specimen #11	BRC V1
4	Specimen #5	V0	4	Specimen #8	V0	4	Specimen #11	V0
5	Specimen #5	BRC V2	5	Specimen #8	BRC V2	5	Specimen #11	BRC V2
6	Specimen #5	V0	6	Specimen #8	V0	6	Specimen #11	V0
7	Specimen #5	BRC V3	7	Specimen #8	BRC V3	7	Specimen #11	BRC V3
8	Specimen #5	V0	8	Specimen #8	V0	8	Specimen #11	V0
9	Specimen #5	V5	9	Specimen #8	V5	9	Specimen #11	V5
1	Specimen #6	V0	1	Specimen #9	V0	1	Specimen #12	V0
2	Specimen #6	V0	2	Specimen #9	V0	2	Specimen #12	V0
3	Specimen #6	BRC V1	3	Specimen #9	BRC V1	3	Specimen #12	BRC V1
4	Specimen #6	V0	4	Specimen #9	V0	4	Specimen #12	V0

5	Specimen #6	BRC V2		5	Specimen #9	BRC V2		5	Specimen #12	BRC V2
6	Specimen #6	V0		6	Specimen #9	V0		6	Specimen #12	V0
7	Specimen #6	BRC V3		7	Specimen #9	BRC V3		7	Specimen #12	BRC V3
8	Specimen #6	V0		8	Specimen #9	V0		8	Specimen #12	V0
9	Specimen #6	V6		9	Specimen #9	V6		9	Specimen #12	V6

PV04 (w/ flesh)		
Test #	**Specimen #**	**Velocity**
1	Specimen #13	V0
2	Specimen #13	V0
3	Specimen #13	BRC V2 @ 2ms
4	Specimen #13	V0
5	Specimen #13	BRC V2 @ 8ms
6	Specimen #13	V0
7	Specimen #13	V4, V5, or V6
1	Specimen #14	V0
2	Specimen #14	V0
3	Specimen #14	BRC V2 @ 2ms
4	Specimen #14	V0
5	Specimen #14	BRC V2 @ 8ms
6	Specimen #14	V0
7	Specimen #14	V4, V5, or V6
1	Specimen #15	V0
2	Specimen #15	V0
3	Specimen #15	BRC V2 @ 2ms
4	Specimen #15	V0
5	Specimen #15	BRC V2 @ 8ms
6	Specimen #15	V0
7	Specimen #15	V4, V5, or V6
1	Specimen #16	V0
2	Specimen #16	V0
3	Specimen #16	BRC V2 @ 2ms
4	Specimen #16	V0
5	Specimen #16	BRC V2 @ 8ms
6	Specimen #16	V0
7	Specimen #16	V4, V5, or V6

PV06 (w/ flesh)		
Test #	**Specimen #**	**Velocity**
1	Specimen #17	V0

2	Specimen #17	V0
3	Specimen #17	BRC V2 @ 5ms, Posture 1
4	Specimen #17	V0
5	Specimen #17	BRC V2 @ 5ms, Posture 2
6	Specimen #17	V0
7	Specimen #17	V4, V5, or V6
1	Specimen #18	V0
2	Specimen #18	V0
3	Specimen #18	BRC V2 @ 5ms, Posture 1
4	Specimen #18	V0
5	Specimen #18	BRC V2 @ 5ms, Posture 2
6	Specimen #18	V0
7	Specimen #18	V4, V5, or V6
1	Specimen #19	V0
2	Specimen #19	V0
3	Specimen #19	BRC V2 @ 5ms, Posture 1
4	Specimen #19	V0
5	Specimen #19	BRC V2 @ 5ms, Posture 2
6	Specimen #19	V0
7	Specimen #19	V4, V5, or V6
1	Specimen #20	V0
2	Specimen #20	V0
3	Specimen #20	BRC V2 @ 5ms, Posture 1
4	Specimen #20	V0
5	Specimen #20	BRC V2 @ 5ms, Posture 2
6	Specimen #20	V0
7	Specimen #20	V4, V5, or V6

PV08 (w/ flesh)		
Test #	**Specimen #**	**Velocity**
1	Specimen #21	V0
2	Specimen #21	V0
3	Specimen #21	BRC V2 @ 5ms, 5kg added
4	Specimen #21	V0
5	Specimen #21	BRC V2 @ 5ms, 10kg added
6	Specimen #21	V0

7	Specimen #21	V4, V5, or V6
1	Specimen #22	V0
2	Specimen #22	V0
3	Specimen #22	BRC V2 @ 5ms, 5kg added
4	Specimen #22	V0
5	Specimen #22	BRC V2 @ 5ms, 10kg added
6	Specimen #22	V0
7	Specimen #22	V4, V5, or V6
1	Specimen #23	V0
2	Specimen #23	V0
3	Specimen #23	BRC V2 @ 5ms, 5kg added
4	Specimen #23	V0
5	Specimen #23	BRC V2 @ 5ms, 10kg added
6	Specimen #23	V0
7	Specimen #23	V4, V5, or V6
1	Specimen #24	V0
2	Specimen #24	V0
3	Specimen #24	BRC V2 @ 5ms, 5kg added
4	Specimen #24	V0
5	Specimen #24	BRC V2 @ 5ms, 10kg added
6	Specimen #24	V0
7	Specimen #24	V4, V5, or V6

Eight whole body PMHS will also be used in this task. Instrumentation will include the accelerometers in the seat pan, along with the strain gages along the rami and iliac wings (see Section 8E). The loading configuration for these tests is shown in Figure 6.

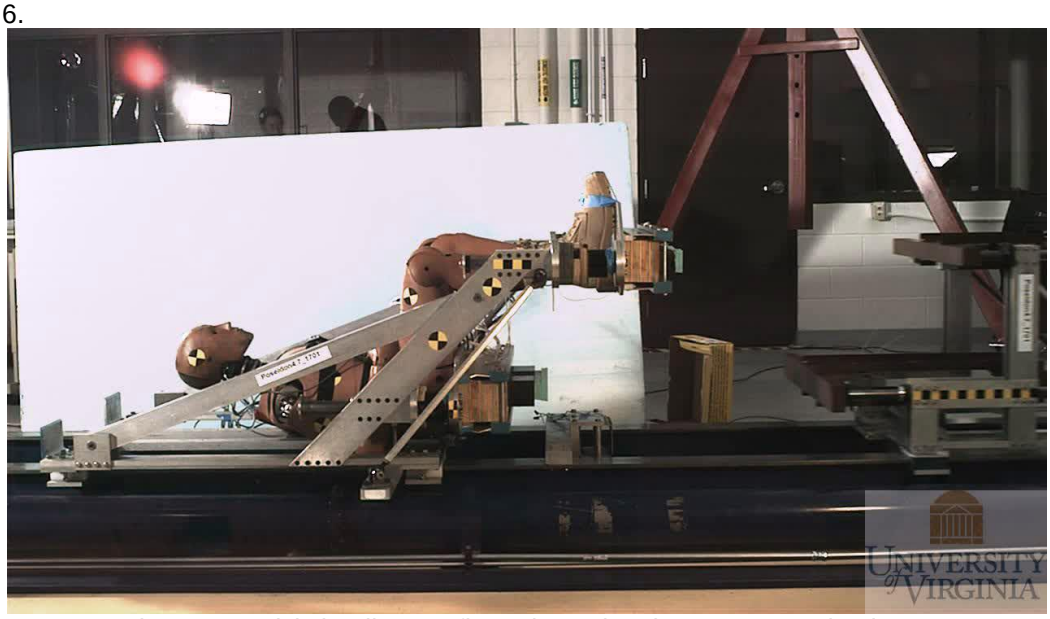

Figure 6. Pelvis loading configuration using the UVA UBB simulator.

The test matrix for this subtask is shown in Table 3. The testing of first article designs of the WIAMan pelvis is included in this task using the same test rig. Limited material characterization testing on candidate pelvis materials supplied by the dummy manufacturer is included in this task.

Table 3. Test matrix for vertical loading of pelvis (whole body PMHS tests)

Test	Load Rate
Specimen 1	15 m/s
Specimen 2	7 m/s
Specimen 3,4,5	10 m/s ± depending on results from test 1 and 2
Specimen 6,7,8	10 m/s ± depending on results from test 1 through 5

E. Instrumentation and Biofidelic Response Corridors (BRCs)

The primary measurand of this test series are the axial forces being transmitted to, and through, the pelvis. Accelerometers and angular rate sensors will be rigidly attached to the body are prescribed locations for this task. Acoustic crack detection sensors will be located in proximity of the acetabulum and the sacroiliac joint, along with the use of high speed x-ray for crack initiation (Figure 7). In addition, strain gages will be placed in strategic locations around the pelvis in order to track the distribution of strain, and to attempt to identify the time and location of first fracture.

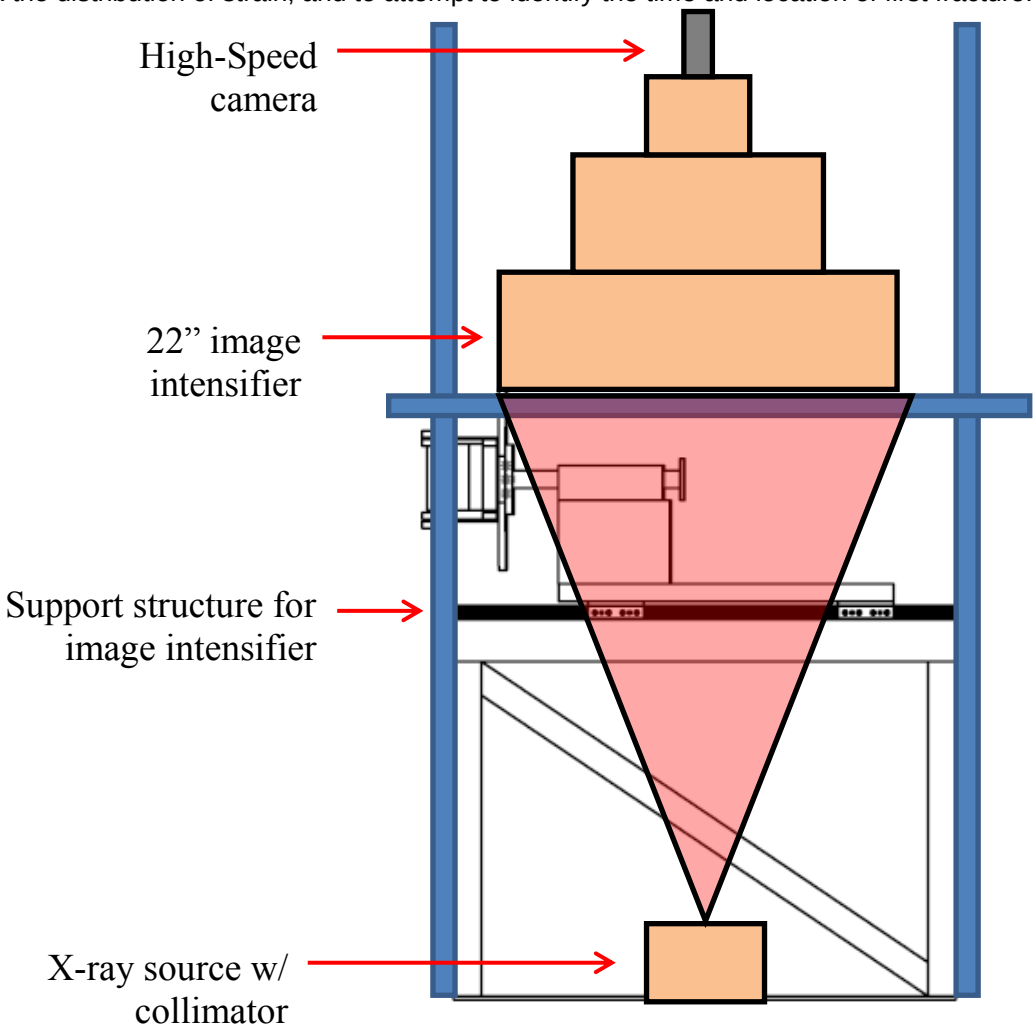

Figure 7. High speed x-ray test configuration on component level tests.

For the component tests, focused instrumentation will be placed in and around the pelvis to stratify the project’s requirements. Table 4 lists the instrumentation and corresponding BRCs for the component tests. Figure 8 details the locations of the strain gages on the component tests.

Table 4. Biomechanical Measurements (component tests)

BIO PT proposed measurements	**UVa’s Plan for instrumentation**

Pelvis accel measured at sacrum; core: Az; secondary: Ax, Ay; in sacrum local x, y, z axis	*A six-axis cube comprised of three linear accels and three angular rate sensors*
Pelvis accel resultant	*use the six-axis cube at sacrum to derive resultant acceleration*
Pelvis rotation (ARS) measured at Sacrum Core: wy; Secondary: wx, wz ; in sacrum local x, y, z axis	*A six-axis cube comprised of three linear accels and three angular rate sensors*
Pelvis displacement & rotations in relative to the seat from motion tracking of Sacrum & Seat; Secondary: Dz, qy, Dx, Dy, qx, qz, in seat local x, y, z axis	*Use point track on high-speed video, VICON motion capture system.*
Contact forces & Moments between pelvis/seat; Core: Fz; Secondary: Fx, Fy, Mx, My, Mz; X, Y, Z in seat coordinate system	*No plans to accommodate this proposed measurement because it is not a feasible measurement to obtain*
Forces & Moments measured at Sacrum; Core: Fz; Secondary: Fx, Fy, Mx, My, Mz; in sacrum local x, y, z axis	*A six-axis load cell will be rigidly mounted at the sacrum*
	A suite of at least 10 strain gauges, 8 of which are tri-axial, will be mounted on the pelvis to help derive load path and identify local deflections in the pelvis

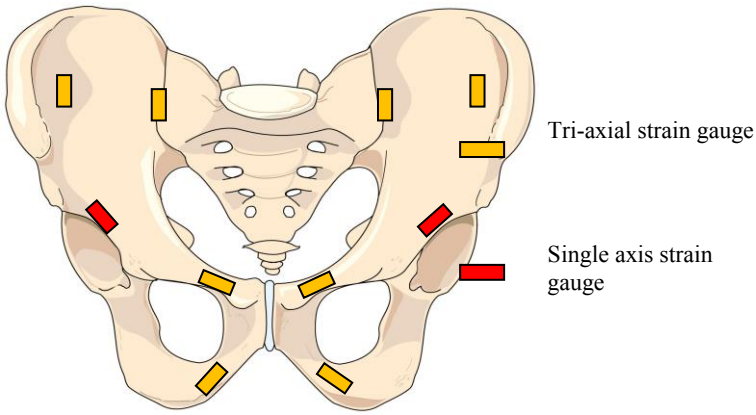

Figure 8. Location of strain gages on component pelvic test specimens.

For the whole body tests, focused instrumentation will be placed in and around the pelvis to stratify the project's requirements (in addition to the usual whole body instrumentation suite, Table 6). Table 5 lists the instrumentation and corresponding BRCs for the whole body tests. Figure 9 details the locations of the strain gages on the whole body tests.

Table 5. Biomechanical Measurements (whole body tests)

BIO PT proposed measurements	**UVa's Plan for instrumentation**
Head accel Z	*A six-axis cube comprised of three linear accels and three angular rate sensors*
Head accel resultant	*use the six-axis cube at sacrum to derive resultant acceleration*
Head rotation (ARS)	*A six-axis cube comprised of three linear accels and three angular rate sensors*
Motion of head (video)	*Use point tracking on high-speed video*
Spinal compression (video)	*This cannot be satisfied in whole body testing*
Motion of shoulder (video)	*Use point tracking on high-speed video*
T1 spinal accel Z	*A linear accel will be mounted in Z and X directions, and an ARS measuring rotations about Y will be mounted.*
T1 spinal rotation (ARS)	*A linear accel will be mounted in Z and X directions, and an ARS measuring rotations about Y will be mounted.*
T4 spinal accel Z	*A linear accel will be mounted in Z and X*

	directions, and an ARS measuring rotations about Y will be mounted.
T4 spinal rotation (ARS)	*A linear accel will be mounted in Z and X directions, and an ARS measuring rotations about Y will be mounted.*
T12 spinal accel Z	*A linear accel will be mounted in Z and X directions, and an ARS measuring rotations about Y will be mounted.*
T12 spinal rotation (ARS)	*A linear accel will be mounted in Z and X directions, and an ARS measuring rotations about Y will be mounted.*
Pelvis accel Z	*A six-axis cube comprised of three linear accels and three angular rate sensors*
Pelvis accel resultant	*A six-axis cube comprised of three linear accels and three angular rate sensors*
Pelvis rotation (ARS)	*A six-axis cube comprised of three linear accels and three angular rate sensors*
Femur accel X	*A linear accel will be mounted in Z and X directions, and an ARS measuring rotations about Y will be mounted.*
Femur bone-load cell FX	*No plans to accommodate this proposed measurement*
Tibia accel Z	*A linear accel will be mounted in Z and X directions, and an ARS measuring rotations about Y will be mounted.*
Tibia bone-load cell FZ	*This will be accommodated using strain gages*
Foot accel Z	*No plans to accommodate this proposed measurement*
Head rotation relative to torso (XZ plane)	*A six-axis cube comprised of three linear accels and three angular rate sensors*
	A suite of at least 6 tri-axial strain gauges will be mounted on the pelvis to help derive load path and identify local deflections in the pelvis, especially along the rami and iliac wings

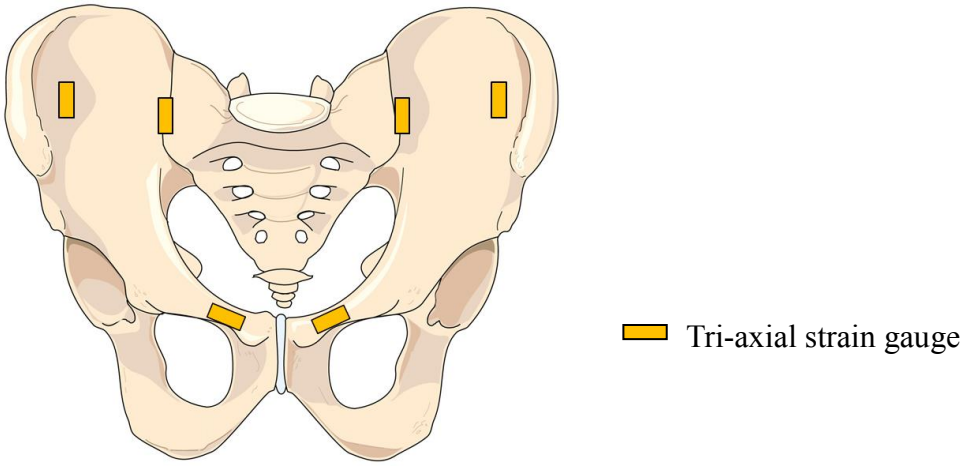

Figure 9. Location of strain gages on whole body pelvic test specimens.

Table 6 – Whole Body instrumentation list

Measurand	Location	Instrument	Axis	Range	Units	BRC
Acceleration	Right Distal Tibia	7264B	X	2000	G	
Acceleration		7270	Z	6000	G	Tibia Accel

						Z
Angular rate		18k ARS	Y	18k	Deg/s	
Acceleration	Left Distal Tibia	7264B	X	2000	G	
Acceleration		7270	Z	6000	G	Tibia Accel Z
Angular rate		18k ARS	Y	18k	Deg/s	
Acceleration	Right Distal Femur	7264B	X	2000	G	Femur Accel X
Acceleration		7264B	Z	2000	G	
Angular rate		8k ARS	Y	8k	Deg/s	
Acceleration	Left Distal Femur	7264B	X	2000	G	Femur Accel X
Acceleration		7264B	Z	2000	G	
Angular rate		8k ARS	Y	8k	Deg/s	
Acceleration	Pelvis (Lumbar Spine)	7264B	X	2000	G	Pelvis Accel Z, Pelvis Resultant Accel
Acceleration		7264B	Y	2000	G	Pelvis Resultant Accel
Acceleration		7264B	Z	2000	G	Pelvis Resultant Accel
Angular rate		8k ARS	Y	8k	Deg/s	Pelvis Rotation
Acceleration	Head	7264B	X	2000	G	
Acceleration		7264B	Y	2000	G	
Acceleration		7264B	Z	2000	G	
Angular rate		8k ARS	X	8k	Deg/s	
Angular rate		8k ARS	Y	8k	Deg/s	
Angular rate		8k ARS	Z	8k	Deg/s	
Acceleration	T1 Vertebra	7264B	X	2000	G	
Acceleration		7264B	Z	2000	G	T1 Accel Z
Angular rate		8k ARS	Y	8k	Deg/s	T1 Rotation
Acceleration	T4 Vertebra	7264B	X	2000	G	
Acceleration		7264B	Z	2000	G	T4 Accel Z
Angular rate		8k ARS	Y	8k	Deg/s	T4 Rotation
Acceleration	T12 Vertebra	7264B	X	2000	G	
Acceleration		7264B	Z	2000	G	T12 Accel Z
Angular rate		8k ARS	Y	8k	Deg/s	T12 Rotation
Acceleration	Sternum	7264B	X	2000	G	
Acceleration	Sternum	7264B	Z	2000	G	
Acceleration	Seat hammer	7270A	Z	6000	G	
Acceleration	Toe	7270A	Z	6000	G	

	hammer					
Belt tension load	Left shoulder belt	Belt tension LC			N	
Belt tension load	Right shoulder belt	Belt tension LC			N	
Belt tension load	Lap belt	Belt tension LC			N	
Acceleration	Toe pan	7270	Z	6000	G	
Acceleration	Seat pan	7270	Z	6000	G	
Acceleration	Toe pan	Loffi	Z		G	
Acceleration	Seat pan	Loffi	Z		G	
Strain	Right Anterior Distal Femur	Vishay SG	Z			
Strain	Right Anterior Mid-Femur	Vishay SG	Z			
Strain	Right Anterior Proximal Femur	Vishay SG	Z			
Strain	Left Anterior Distal Femur	Vishay SG	Z			
Strain	Left Anterior Mid-Femur	Vishay SG	Z			
Strain	Left Anterior Proximal Femur	Vishay SG	Z			
Strain	Right Distal Anterior Tibia	Vishay SG	Z			Tibia Force Z
Strain	Left Distal Anterior Tibia	Vishay SG	Z			Tibia Force Z
Strain	Right Distal Medial Tibia	Vishay SG	Z			Tibia Force Z
Strain	Left Distal Medial Tibia	Vishay SG	Z			Tibia Force Z
Strain	Right Distal Lateral Tibia	Vishay SG	Z			Tibia Force Z
Strain	Left Distal Lateral Tibia	Vishay SG	Z			Tibia Force Z
Strain	Right Distal Posterior Tibia	Vishay SG	Z			Tibia Force Z
Strain	Left Distal Posterior	Vishay SG	Z			Tibia Force Z

	Tibia					
Strain	Left Anterior Mid- Tibia	Vishay SG	Z			
Strain	Left Anterior Proximal Tibia	Vishay SG	Z			
Strain	Right Calcaneus	Vishay SG	Z			
Strain	Left Calcaneus	Vishay SG	Z			
Strain	Right 4th Rib	Vishay SG				
Strain	Left 4th Rib	Vishay SG				
Strain	Right 8th Rib	Vishay SG				
Strain	Left 8th Rib	Vishay SG				
Acoustic Emission	Right Tibia	Vishay SG				
Acoustic Emission	Left Tibia	Vishay SG				
Strain	Pelvis	Vishay SG				
Strain	Pelvis	Vishay SG				
Strain	Pelvis	Vishay SG				
Strain	Pelvis	Vishay SG				
Strain	Pelvis	Vishay SG				
Strain	Pelvis	Vishay SG				

Military Medical Needs
This subtask will provide WIAMan designers with human biofidelity corridors of the human pelvis loaded in the vertical directions, high-rate material properties of the rami and ischium, and human injury risk (or threshold tolerance) curves for the pelvis.

First article testing of WIAMan pelvis under all tested configurations
After the development of the first generation pelvis by WIAMan designers, the pelvis will be tested in each of the load configurations in Task 1 for the purpose of evaluation and the development of IARCs for the WIAMan pelvis. This work is included in the above task.
Military Medical Needs
Matched pair testing of first article WIAMan pelves and the PMHS pelves tested in this task will provide sufficient data to develop IARCs for the WIAMan pelvis.

1.2.8 ANALYSIS PLAN

The kinematics of the PMHS will be collected and the local forces and accelerations will be calculated. The results of this study evaluates the biofidelity of the available ATDs and also provide the occupant response to the WIAMan developer in an event of UBB. Each data plot will be filtered according to the Army approved procedure.

Raw (unfiltered) data for each channel will be delivered to the sponsor.

Filtered data will be delivered for each channel, as well as plotted in an Excel files for easy reference.

Biofidelity corridors will be developed for each key response as a function of pelvic angle. This information will be used by dummy developers to identify and design each key component of WIAMan to be as biofidelic as possible.

1.2.9 SCHEDULE, PRODUCTS, AND MILESTONES

Gant chart for this task attached in Appendix.

- Delivery Date: Task 1.4 - Component test (9 months from approval); Whole body tests (15 months from approval)
- Final report (including IRC's) (3 months from end of testing of each test group)

1.2.10 ASSUMPTIONS AND RISKS

The only significant outstanding risk in this research is the successful procurement of adequate PMHS. This should be the only limiting factor to success of this project.

1.3 WIAMan Research Plan 3: Develop multi-axial injury criteria for the femur complex

1.3.1 ABSTRACT

The goal of this study is to determine the biomechanical response of PMHS component femurs under loading conditions seen in Under Body Blast (UBB). The results of this study will provide critical data for the force transmissibility of the femur, as well as the kinematic response of the femur under UBB loads. Component PMHS femurs will be instrumented and tested at conditions representative of those seen in under-body blasts.

1.3.2 STUDY PERSONNEL

Personnel Name	Responsibilities
Robert Salzar	PI
Brandon Perry	Project Manager
Kyvory Henderson	Test Engineer

1.3.3 STUDY LOCATION

All aspects of this task will be performed at the Center for Applied Biomechanics at the University of Virginia

1.3.4 OBJECTIVES/SPECIFIC AIMS/RESEARCH QUESTIONS

The goal of this study is to determine the biomechanical response of available ATDs and PMHS subjects under the loading condition similar to an event of Under Body Blast (UBB). **Testing will be performed in accordance with Series ID # UL01, UL02, and UL03 prescribed in table 10 of the ITM Draft with the exception of flesh.** The results of this study will validate the biofidelity of the available ATDs and provide the occupant response to the vehicle motion with a particular emphasis on the femur. The ATDs and whole body PMHS will be instrumented and tested at conditions representative of those seen in under-body blasts.

1.3.5 WIAMan/MILITARY RELEVANCE

Mine Resistant Ambush Protected (MRAP) and other armored vehicles (such as the M-ATV) are designed to survive improvised explosive device (IED) attacks and ambushes. Initial reports have indicated the prevalence of lower extremity injuries resulting from under-body loads which can lead to life-threatening hemorrhages in the short term, and costly, painful debilitation in the long term. This study will begin the process of reducing these injuries by focusing on the biomechanics and injury thresholds of PMHS during a UBB event, resulting in strain and transmissibility data to be used in developing WIAMan, and understanding the deficiencies in current dummy designs.

1.3.6 SCIENTIFIC BACKGROUND AND SIGNIFICANCE

This task will focus on developing an injury criterion for the femur appropriate for use in studying under body blasts. By examining past studies in the literature, and performing supplemental tests at high rate, the newly developed injury

criterion will be useful for both upcoming WIAman development, as well as future validation of numerical models of the human femur.

Loading rate is used as a primary criterion to evaluate previous studies. Five of the previous studies report results from tests conducted at quasi-static loading rates, which may significantly underestimate the bending tolerance of the femur under impact loading (Carter and Hayes, 1977, and McElhaney, 1966). Carter and Hayes (1977) estimate that both strength and modulus of cortical bone were proportional to the strain rate raised to the 0.06 power. While this suggests bone may experience a strain rate sensitivity of fracture tolerance, this effect may be smaller than inter-specimen variation when strain rates vary by less than an order of magnitude. Table 1 shows related femoral tolerance values found in the literature.

Table 1. Summary of previous studies on the structural bending strength of the femur.

Study	Sample size	Mean failure moment (Nm)	Notes
Weber, 1859 in Nyquist, 1986	9 (4 M, 5 F)	233/182 Nm (m/f)	– Quasi-static
Messerer, 1880 in Nyquist, 1986	12 (6 M, 6 F)	310 /180 Nm (m/f)	– Quasi-static, Lateral direction
Mather 1968a, 1968b	145 (91 M, 54 F)	318/202 Nm (m/f)	– Load rate affects energy absorption
Motoshima, 1960 in Nyquist, 1986	35 Total (M & F)	211 Nm	– Quasi-static, Females 5/6 moment of males, Tolerance same in all directions
Martens, 1986	33 (26 M, 7 F)	373/275 Nm (mid/dist fx)	– <200 ms load time, 4-point bend tests
Stromsoe, 1995	14 (10 M, 4 F)	185/125 Nm (m/f)	– Deflection rate = 1 mm/min
Kress, 2001	604	100–500 Nm	– Dynamic, Fracture study, Mostly embalmed
Kerrigan, 2003	8 (4 Pairs, 3F, 1M)	412 Nm	– 1 Quasi-static, 7 Dynamic (1.2 m/s), With surrounding flesh, L-M direction
Funk, 2004	15 (7 pairs +1 M)	458 Nm	– Dynamic, Tolerance same in all directions
Kennedy, 2004	45	395 Nm (50%, 50th Male)	– Dynamic (5 m/s), Tolerance same in all directions, All Data RIGHT censored
Kerrigan, 2004	34 (7 thigh/mid, 6 thigh/dist. Third, 18 femur/mid, 3 femur/dist third)	50% Risk: 447 Thigh/Mid 372 Thigh/Dist 387 Femur/Mid 322 Femur/Dist	– Dynamic (1.5 m/s), P-A and L-M tolerance same for femora

Since the femur has a slight curvature in the sagittal plane, a compressive axial load on the femoral shaft induces a bending moment in the structure. While this condition has been previously studied using thirty-eight specimens by UVA in both quasi-static (1 mm/s) and dynamic (1.5 m/s) test conditions, the effect of an axial tensile load, seen in Hybrid-III femurs during live-fire testing, has not been evaluated in PMHS femurs. UVA has developed appropriate testing hardware and protocol to examine similar phenomenon for axial compressive loadings, and will modify the existing test device for axial tensile loads.

Using their research experience and knowledge in the area of lower limb biomechanics, vehicle crash testing with intrusion, blast loading, and injury criteria development, the UVA and USAARL teams have proposed a comprehensive research program that culminates with the delivery of a test methodology, injury criteria for dummies, and recommendations for mitigation strategies.

1.3.7 RESEARCH METHODOLOGY

A. Description of Research Approach

For this project, an experimental test methodology using component PMHS femurs is developed using the UVA impactor with appropriate fixation of femurs. This impactor system will allow the evaluation of intrusion parameters such as knee acceleration time-histories on the kinematic patterns of the PMHS femurs in a realistic UBB environment. Acknowledging that standard crash test dummies were designed by automobile manufacturers for primarily seated postures and load vectors commonly seen in frontal or lateral automobile crashes, these dummies were not designed for multi-axial loads including dominant vertical loading seen in under-body blasts. However, these dummies will continue to be widely used as an instrumentation platform for evaluating soldier survivability in free-field tests. The standard crash test dummy, the Hybrid-III, is a robust instrumentation platform that has the anthropometry of a 50th percentile male, although limited biofidelity in some very specific areas. For example, it is known that the Hybrid-III spine has little spine articulation (all focused at the pelvis/spine interface and the neck), and that the lower extremities are overly stiff with poor frequency response (Crandall et al., 1996). An improved dummy for automotive testing, Thor, has better thoracic response, along with an advanced lower extremity design (Thor LX) which may prove to be more biofidelic and predictive of injury in under-body blast loadings. While the THOR LX is the most advanced design known to the research team, other lower extremity dummy designs can be examined for their appropriateness to represent the lower extremity kinematics seen in theater.

For the proposed project, the Hybrid-III and component PMHS specimens will be used as both an instrumentation platform, and in the case of the PMHS, a biofidelic surrogate capable of modeling kinematics of human body.

B. Research Specimens/Components (Cadavers)

The specimens will be selected from male donors, less than 60 years in age, and have no previous injuries to the flesh. The subjects will be tested for standard potential transmissible diseases. Only cadavers meeting all of the following criteria may be utilized in the study: (1) Males above the age of 18 years and below the age of 60 years. (2) Cadavers without existing unhealed bone or soft tissue injury. (3) Cadavers will not have evidence of wasting disease. (4) Cadavers tested negative for Hepatitis A, B, C and HIV. (5) Only remains obtained from an approved source. To limit cadaveric variation, specimens will be selected that are similar in stature and mass to a 50th percentile male based on the ongoing U.S. Army anthropometric studies.

Specimens' demographics and anthropometry will be precisely documented during the preparation process and pre- and post-test CT scans will be acquired from the specimens. Due to the nature of the research at the University of Virginia-Center for Applied Biomechanics, a large source of PMHS samples are available and more specimens are being acquired for the WIAMan project.

C. Exposures, Setup, and Data

Using the impactor device, the kinematics and internal forces/strains of the femur complex will be determined in injurious and none injurious testing (Figure 1). **Fifty-four (54) component PMHS femurs will be used in this task. PMHS and H-III femur will be tested at three sub-injurious and three injurious velocities (Table 2). Loading will be consistent with UL01, UL02, and UL03 of Table 10 of the ITM.** Each will be potted, instrumented, and positioned in the test device and tested to determine the threshold fracture tolerance under realistic UBB conditions as determined from whole body ODYSSEY testing. Instrumentation in the H-III will be comprised of the test fixture load cell and acceleration/angular rate measurements, in addition to the H-III femur load cell (Table 3). Instrumentation in the PMHS tests will be comprised of 6-DOF load cells, accelerometers and angular rate sensors, strain gages, and acoustic sensors, appropriate to create biofidelic corridors and injury risk functions (Table 4). The load cells and accelerometers satisfy BP-47 and -48 for femur testing in Appendix C of the ITM.

Figure 1. Left: Impactor schematic of femur loading event. Right: 3-D drawing of femur loading apparatus.

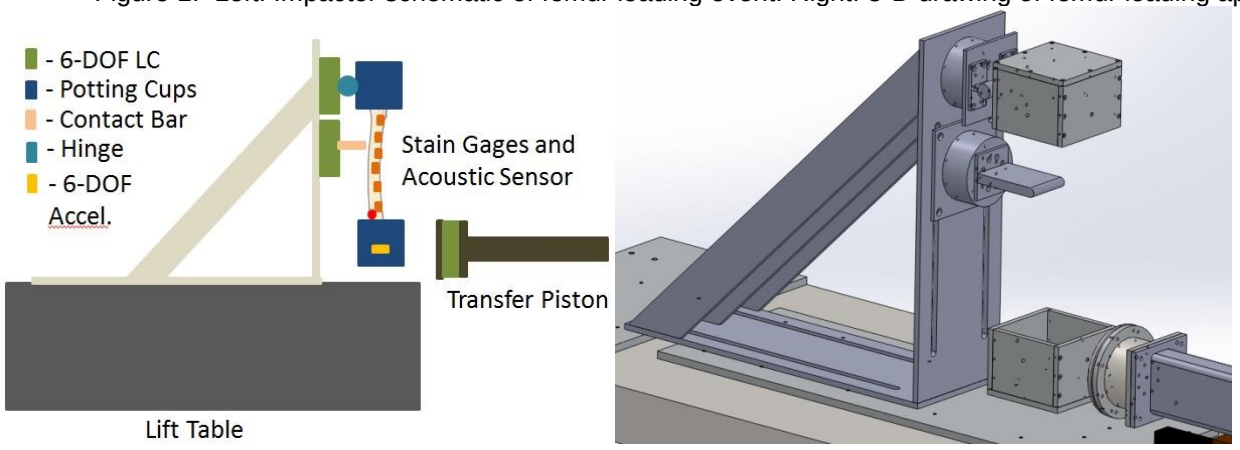

Table 2. Test matrix of sub-injurious position and load conditions for the leg.

Velocity	1/3 Proximal Femur P-A Loading (UL01)	1/3 Proximal Femur M-L Loading (UL02)	1/3 Proximal Femur L-M Loading (UL03)
V_1	3 PMHS/3 H-III	3 PMHS/3 H-III	3 PMHS/3 H-III
V_2	3 PMHS/3 H-III	3 PMHS/3 H-III	3 PMHS/3 H-III
V_3	3 PMHS/3 H-III	3 PMHS/3 H-III	3 PMHS/3 H-III
I_1	3 PMHS/3 H-III	3 PMHS/3 H-III	3 PMHS/3 H-III
I_2	3 PMHS/3 H-III	3 PMHS/3 H-III	3 PMHS/3 H-III
I_3	3 PMHS/3 H-III	3 PMHS/3 H-III	3 PMHS/3 H-III

Table 3. H-III Instrumentation List

CHANNEL COUNT	**MEASURAND**	**SEN.**	**SEN. Type**	**AXIS**	**MAX**
1-6	Load Cell	Femur Cup	Denton 3868	X,Y,Z	22kN
7-12	Load Cell	Femur	Denton Femur LC	6-DOF	
7	Accelerometer	Eff. Mass	7264B	Z	5000G
8	Angular rate	Eff. Mass	8k ARS	Y	8k
9	Accelerometer	Distal Femur	7264B	Z	5000G
10	Angular rate	Distal Femur	8k ARS	Y	8k

Table 4. PMHS Instrumentation List

CHANNEL COUNT	**BIO PT Proposed Measurements**	**MEASURAND**	**SEN.**	**SEN. Type**	**AXIS**	**MAX**
1	Femur Bone-Load Cell FX **(BP-48)**	Load cell	Femur Cup	Denton 3868	X	22kN
2		Load cell	Femur Cup	Denton 3868	Y	11kN
3		Load cell	Femur Cup	Denton 3868	Z	11kN
4		Load cell	Femur Cup	Denton 3868	X	565Nm
5		Load cell	Femur Cup	Denton 3868	Y	1130Nm
6		Load cell	Femur Cup	Denton 3868	Z	1130Nm
7		Load cell	Transfer Piston	Denton 3868	X	22kN
8		Load cell	Transfer Piston	Denton 3868	Y	11kN
9		Load cell	Transfer Piston	Denton 3868	Z	11kN
10		Load cell	Transfer Piston	Denton 3868	X	565Nm
11		Load cell	Transfer Piston	Denton 3868	Y	1130Nm
12		Load cell	Transfer Piston	Denton 3868	Z	1130Nm
13		Load cell	Contact Bar	Denton 3868	X	22kN
14		Load cell	Contact Bar	Denton 3868	Y	11kN

15		Load cell	Contact Bar	Denton 3868	Z	11kN
16		Load cell	Contact Bar	Denton 3868	X	565Nm
17		Load cell	Contact Bar	Denton 3868	Y	1130Nm
18		Load cell	Contact Bar	Denton 3868	Z	1130Nm
19	Femur Accel. X **(BP-47)**	Accelerometer	Eff. Mass	7264B	Z	5000G
20		Angular rate	Eff. Mass	8k ARS	Y	8k
21		Accelerometer	Distal Femur	7264B	Z	5000G
22		Angular rate	Distal Femur	8k ARS	Y	8k
23-43		Strain Gages	A/P/L/M	350 ohm	multiaxial	-
44		Acoustic Sensor				

While the above instrumentation is currently planned for these tests, changes may be made to accommodate the recommendations of the instrumentation working group in effort to standardize with the rest of the bio-performers. Further information about instrumentation application techniques will be presented at the Test Readiness Review.

Biofidelity corridors will be reported at the conclusion of this task, and will be used to assess the appropriateness of the Hybrid-III for this loading regime.

1.3.8 ANALYSIS PLAN

The kinematics of the PMHS subjects will be collected and the local forces and accelerations will be calculated. The ultimate result of this study will evaluate the biofidelity of the available ATDs and also provide the occupant response to the WIAMan developer in an event of UBB. Each data plot will be filtered according to the Army approved procedure.

Raw (unfiltered) data for each channel will be delivered to the sponsor.

Filtered data will be delivered for each channel, as well as plotted in Excel files for easy reference.

Biofidelity corridors and injury risk functions will be developed as a function of shear stresses and bending moments at the proximal third of the femur. This information will be used by dummy developers to identify and design the femur component of WIAMan to be as biofidelic as possible.

Scaling is anticipated to be minimal since anthropometry will be kept to tight tolerances. In the advent of the need for scaling, the mass scaling schemes of Eppinger et al. (1984) will be used.

1.3.9 SCHEDULE, PRODUCTS, AND MILESTONES

The experimental part of this study is planned start early July 2013 and concludes by September 30, 2013, with data analysis concluded by December 31, 2013 (Figure 2). By the end of this period the kinematics and fracture tolerance of the femur along with all the experimental data will be delivered as the final product of this study. Interim reports and interim results will be provided to the sponsor throughout the test series, as sufficient numbers of specimens may be a problem. Raw data will be submitted within five days of test completion and filtered data within seven days. Data analysis will be submitted 30 days after testing concludes. The final report will be submitted within three months of testing.

Figure 2. Timeline for WIAMan femur testing.

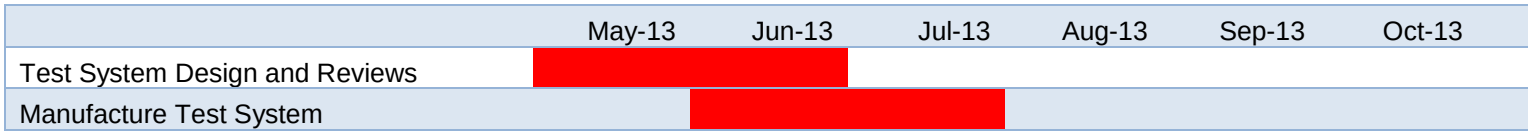

Testing to Support Threshold Critical BRC	[redacted]
Conduct PMHS Testing	[redacted]
Review and Analyze Data	[redacted]
Submit Data to FTP Site	[redacted]
Develop Threshold Upper Leg BRC	[redacted]

1.3.10 ASSUMPTIONS AND RISKS

The only significant outstanding risk in this research is the successful procurement of adequate PMHS. This should be the only limiting factor to success of this project.

1.4 DEVELOPMENT OF INJURY CRITERIA FOR THE FORE-FOOT FOR GLOBAL-LINEAR AND LOCAL-ANGULAR ACCELERATIONS TYPICAL IN LIVE-FIRE TESTS

1.4.1 ABSTRACT

The goal of this study is to determine the biomechanical response of PMHS component femurs under loading conditions seen in Under Body Blast (UBB). The results of this study will provide critical data for the force transmissibility of the femur, as well as the kinematic response of the femur under UBB loads. Component PMHS femurs will be instrumented and tested at conditions representative of those seen in under-body blasts.

1.4.2 STUDY PERSONNEL

Personnel Name	Responsibilities
Robert Salzar	PI
Aaron Alai	Project Manager
Brandon Perry	Test Coordinator
Dennis Roethlisberger	Data Integrity Engineer
Sara Heltzel	Biological Materials Specialist

1.4.3 STUDY LOCATION

All aspects of this task will be performed at the Center for Applied Biomechanics at the University of Virginia

1.4.4 OBJECTIVES/SPECIFIC AIMS/RESEARCH QUESTIONS

Research in the automotive field investigating injury to lower extremities as a function of foot-well intrusion has yielded an increasing linear relationship between the two phenomena (Petit et al. 1996). Currently though, there is no objective test methodology to determine the transmission of forces, nor the risk of injury to the lower extremities due to foot-well intrusion from an under-vehicle blast. In order to investigate the injuries of the forefoot caused by pedal/foot-rest loadings and floor-pan loadings the University of Virginia-Center for Applied Biomechanics (UVA-CAB) has planned to initiate a series of component tests to characterize the response of lower limb under high rate loading conditions, and to investigate the biofidelity of available ATD's. This series of tests aims to:

- Investigate the failure properties of lower limb components in high rate loading conditions.
- Investigate the rate dependent transmissibility of lower limb components.
- Evaluate the biofidelity of available ATDs.

1.4.5 WIAMan/MILITARY RELEVANCE

The results of this study will provide local strength and damping properties of the bones in the forefoot (high-rate material properties), in addition to load rate dependent injury risk curves for the PMHS foot (human injury risk curves). Experimentation with existing ATD feet will provide a basis of comparison between current technology and the ability to

discern these foot injuries. First article testing of WIAMan will allow injury prediction of the bones in the forefoot using matched pair tests (injury assessment reference curves).

1.4.6 SCIENTIFIC BACKGROUND AND SIGNIFICANCE

Loading of the foot and ankle by the floor, foot-rest, or gas/brake pedal of a military vehicle subject to an under-body blast has been shown to be a common mode of injury and responsible for serious injuries seen in theater. The occupant of a vehicle will commonly ride with the forefoot on either the gas/break (vehicle driver) or foot-rest/floor (back passenger) with the Achilles tendon actively engaged. During the blast event, these supports may induce dorsiflexion and axial loading of the ankle due to local deformation, toepan intrusion and/or occupant acceleration and initial foot position. This type of loading can produce a variety of injuries that differ from pure vertical/axial loadings; that is, the differing load paths and active musculature have shown to produce different injury patterns. Previous testing of the whole foot placed on a loading platen resulted in calcaneus and distal tibia fractures while talus and fibula fractures were not seen. This is in contradiction to previous automotive-rate testing where the simulation of active musculature resulted in significant talus and fibula fracture, in addition to tibia and calcaneus fractures (see Rudd et al., 2004).

In order to investigate the injuries though the forefoot caused by pedal/foot-rest loadings and floor-pan loadings, high-rate impact tests will be conducted. This particular study is focused on injuries that occur on one's forefoot in a blast event with the Achilles tendon active during the loading event.

The leg below the knee consists of two long bones, the tibia and fibula (Figure 1). The tibia is the larger of these two bones, and is the primary bone responsible for weight bearing. The fibula is situated posterolaterally to the tibia, and is connected to the tibia both proximally and distally by synarthrodial joints that allow limited motion. The distal portions of the tibia and fibula have bony extensions termed the medial malleolus and lateral malleolus, respectively. The malleoli combine with the distal articulating surface of the tibia, called the tibial plafond or pilon, to form the ankle mortise. The talus, an irregularly shaped bone whose surface is composed largely of articular cartilage, rotates within the ankle mortise to form the talo-crural, or ankle joint. The anterior extension of the talus, which articulates with the navicular, is termed the talar head. The talar neck connects the talar head to the body of the talus. Below the talus is the calcaneus, or heel bone. The joint between these two bones is called the talo-calcaneal, or subtalar joint. The combined motions of the ankle and subtalar joints are collectively referred to as hindfoot motion. The talus and calcaneus articulate with several midfoot bones collectively known as tarsals, which connect to the metatarsals and then to the phalanges, or toes.

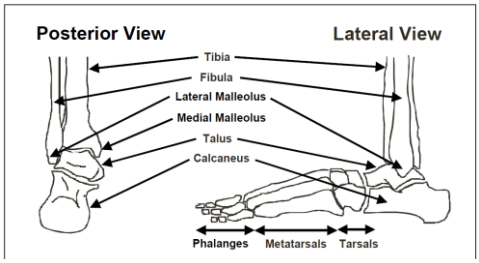

Figure 2. Anatomy of the foot and ankle.

Motion of the foot with respect to the leg is described by a three-dimensional coordinate system (Figure 2). The origin of the coordinate system is the ankle center, defined as the midpoint between distal tips of the malleoli (Inman, 1976). The X-axis points anteriorly through the second metatarsal, and motion about this axis is called eversion (lateral side of the foot moves towards the leg) or inversion (medial side of the foot moves towards the leg). The Y-axis points to the right and motion about this axis is called dorsiflexion (toes move towards the leg) or plantarflexion (toes move away from the leg). The Z-axis points down along the same direction as the long axis of the tibia and motion about this axis is termed internal (toes move medially) or external (toes move laterally) rotation.

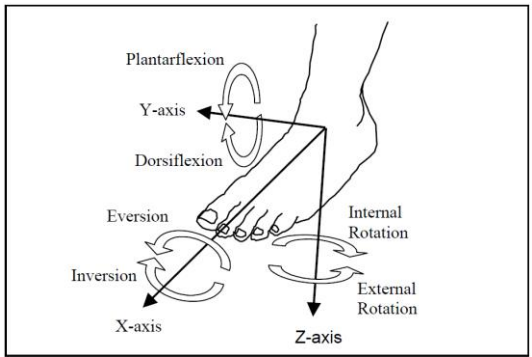

Figure 3. Diagram of the foot and ankle showing the SAE sign convention and common nomenclature used to describe ankle rotations.

The morphology of the ankle joint reflects the competing goals of mobility and stability. Mobility is accomplished primarily by rotation about the ankle joint. The largest muscles and tendons of the leg are located in the posterior compartment and are responsible for plantarflexion, which propels the body forward during gait. In the sagittal plane, the superior surface of the talus is convex and the inferior surface of the tibia is concave. Joint congruity between the talus and tibial plafond is very tight and is maintained throughout the entire range of motion about the flexion axis. Ligamentous structures offer very little resistance within this range of motion. In fact, ankle joint motion is virtually unconstrained about the flexion axis except by passive muscle tension until the extremes of the range of motion are reached (Norkin and Levangie, 1992).

Studies have found that the lower extremity is the most commonly injured body region after the head in road traffic accidents (RTA) (Pattimore et al., 1991; States, 1986), accounting for approximately 20% to 30% of moderate to severe injuries (Pattimore et al., 1991; Morgan et al., 1991; Dischinger et al., 1994; Pilkey et al., 1994). Though not life-threatening, lower limb injuries are often the most severe injuries sustained in a crash (Pattimore et al., 1991), and may be the most common cause of long-term impairment and disability (Morgan et al., 1991). Lower extremity injuries are associated with a 19% complication rate, and a long-term decrease in earning power of 26% (Otte et al., 1992).

Although above-knee injuries are generally the most serious lower extremity injuries, below-knee injuries can be just as serious and are more common (Pattimore et al., 1991; Ward et al., 1992). The most frequently injured region of the lower limb is the foot and ankle. Foot and ankle injuries comprise approximately 30% to 40% of all lower extremity injuries (Pattimore et al., 1991; Morgan et al., 1991; Morris et al., 1997; Pilkey et al., 1994; Jibril et al., 1998; Ward et al., 1992), and up to 10% of all reported injuries in automobile crashes (Crandall et al., 1996; Morgan et al., 1991). Seatbelts and airbags have been shown to provide some protection against above knee lower extremity injuries (Karlson et al., 1998; Loo et al., 1996), but little or no protection against below knee injuries (Crandall et al., 1994; Morgan et al., 1991; Lestina et al., 1992; Otte et al., 1992; Dischinger et al., 1992; Burgess et al., 1995). As seatbelt and airbag restraint systems continue to improve and further reduce the incidence of life-threatening injuries to the head and thorax, the relative importance of lower limb injuries, particularly below-knee injuries, will only increase (Crandall et al., 1994).

Several investigators have published detailed breakdowns of the frequency of specific below-knee fractures sustained in motor vehicle crashes (Figure 3). Comparing data from multiple epidemiological studies is sometimes difficult due to the diverse sources of data and the different injury codings employed by the various investigators. In spite of these differences, most studies are in good agreement about the incidence of particular below-knee fractures. All studies agree that malleolar fractures are the commonest below-knee injury, accounting for 20% - 30% of all moderate to serious injuries. Injuries to the midfoot or forefoot region make up around 15% - 25% of below-knee fractures, making it the second most frequently injured substructure of the below-knee complex. Calcaneal fractures are the next most common below-knee injury (15-20% of the total), followed by tibial pilon fractures (10-15% of the total). Fractures of the tibial plateau and tibial shaft each account for about 10% of below-knee fractures. Most studies report a low incidence of talus fractures, at around 5% of the total. No epidemiological study of ankle injuries sustained in automobile crashes has specified whether location of talus fracture was at the talar neck or talar body.

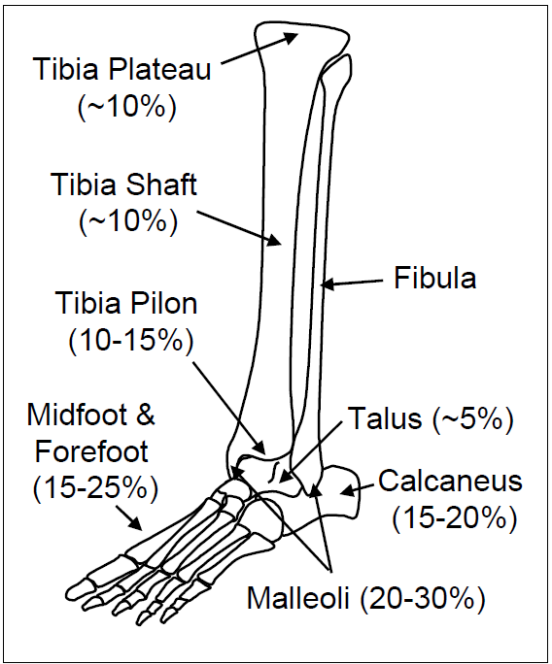

Figure 4. Location and frequency of below-knee injuries sustained in car crashes.

Injury exposure information provided to this researcher has shown that foot injuries in the form of fractures and dislocations with and without associated tibia fractures are a frequent injury mode of UBB (Figure 4, 5).

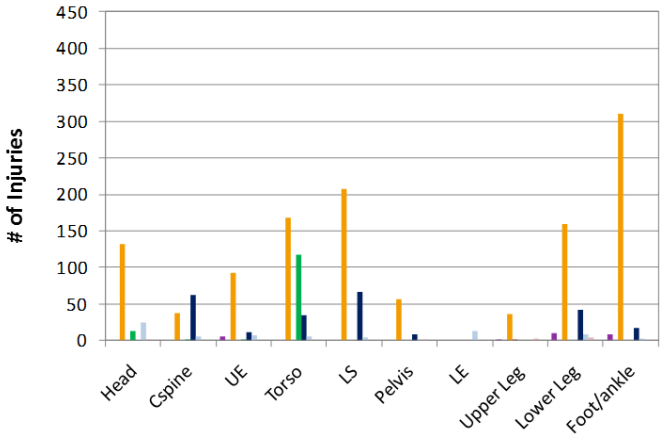

Figure 5. WIA injury distributions from UBB.

Figure 6. X-ray image of injured mid- and forefoot from a nonspecific UBB event.

There have been few investigations into the response of the foot and ankle complex as a function of forefoot loading, more specifically with an active force applied to the Achilles tendon. In a study by Manning et al. (1998) forefoot loading during hard breaking was measured in volunteers undergoing simulation driving, and the resulting force on the Achilles tendon was calculated to be approximately 1.5kN. While loading of the forefoot during experimentation on cadaveric lower limbs, the Achilles tendon had one of three loads applied; 0N, 960N, and 1.5kN. Lower limbs were fitted with a load cell replacing a portion of the tibial shaft, and the forefoot was loaded with a 1.25kg pendulum at velocities of 2, 4, and 6m/s. Researchers found a 1.5kN and 2.3kN mean difference in the tibial load cell between 0N/960N and 0N/1.5kN respectively of applied force to the Achilles tendon. Indicating that testing with an active Achilles tendon changes the response of the lower leg during loading events.

In a study by Smith et al. (2003), again with varying levels of active tension on the Achilles tendon, two possible mechanisms of injury were tested. The first simulating the driver braking hard with the foot on the brake pedal at 0 degree plantar flexion. The second injury mechanism simulated a driver's hard braking action by impacting the ball of the foot with the foot plantar-flexed 35 to 50 degrees. Five of the feet tested in the plantar flexed configuration had a stretched, ruptured, or avulsed injury to the Lisfrac ligament. The most common injury was multiple metatarsal fractures and the most common injury severity level was AIS 3. In the data analysis, the loads causing tarsometatarsal injuries to the feet ranged from 4.5 to 14.7 kN. The impact velocity ranged from 4.5 to 15.5 m/s. The impactor acceleration ranged from 80 to 349 g. Funk et al. (2002) did not necessarily load the forefoot, but did apply on average a 1.8kN force to the Achilles tendon then loaded the entire foot bottom. Their results indicate a greater number of pilon fractures with respect to no Achilles tension (1/3 of specimens), and that fractures initiated at the distal tibia more frequently in tests with Achilles tension than tests without Achilles tension.

The goal of this study is to determine the injury mechanisms, high-rate material properties, and injury risk curves to the feet and the individual bones of the feet while loading the forefoot and applying a prescribed load to the Achilles tendon. Because the seating posture of the vehicle occupants can vary from the nominal 90 degree angle position, to vehicle driver with foot on pedals, to vehicle occupants with feet on foot-rest structures, and since each of these postures will result in a different set of foot/ankle injuries, the WIAMan dummy must be robust in the foot/ankle area and should predict injury across these loading conditions. The injury information from theater shows that both metatarsal and calcaneus injuries occur at equal rates, with both injuries leading to foot amputation or severe lifetime pain, the WIAMan dummy should predict these injuries with high precision, implying that the WIAMan foot should exhibit this level of resolution.

1.4.7 RESEARCH METHODOLOGY

A. Description of Research Approach

Twenty fresh-frozen postmortem human surrogate (PMHS) will be obtained for this test series through the Virginia State Anatomical Board and other tissue suppliers accredited by the American Association of Tissue Banks and approved by the US Army as a supplier to this program. The test protocols will be subjected to review by the University of Virginia Cadaver Use Committee. Specimens will be sectioned below the patella and the proximal epiphysis of the tibia and the proximal fibula will be potted using Fast Cast (Goldenwest Manufacturing, Cedar Ridge, CA).

Specimens will be instrumented with twenty-five strain gages (Micro-Measurements C2A-06-062LW-350) attached circumferentially around the distal tibia and fibula to form bone cells, at the proximal/distal ends of the tibia and fibula (anterior/medial on tibia and anterior/lateral on fibula) , on the calcaneus, and metatarsals, using cyanoacrylate adhesive to capture strains in the SAE-Z direction and to assist in the observation of fracture times (Figures 6 and 7). Four accelerometers (Endevco 7264B-2000), at the proximal/mid/distal tibia and the dorsal surface of the navicular bone (attached with screws); and two angular rate sensors (ARS-8k) attached to the dorsal mid/distal tibia using a nonintrusive worm hose screw clamp design, will capture the motion of the tibia. The navicular bone's articulation with the talus and calcaneus ensure that the bone experiences similar accelerations to the calcaneus and talus which are directly in the loading path. However, the navicular's position outside of the loading path helps ensure shielding from forces which would cause fracture in the bone, and thus inaccurate acceleration traces. Acoustic transducers (S9225 acoustic miniature sensor from Physical Acoustics) will be affixed to the distal end of the tibial shaft and media calcaneus to observe fracture time.

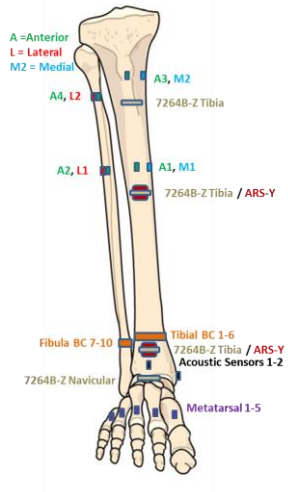

Figure 7. Instrumented lower leg.

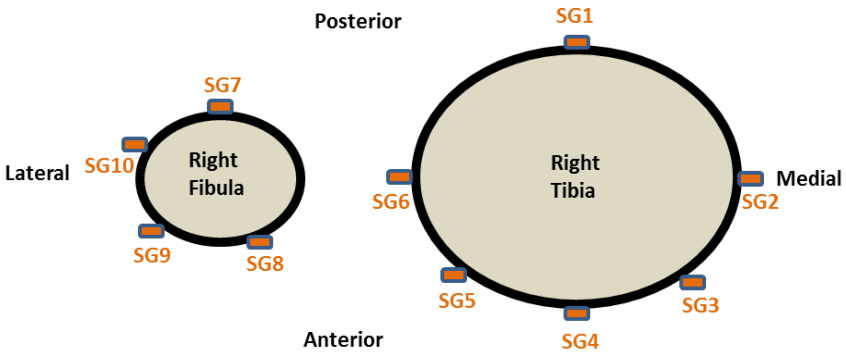

Figure 8. Bone cell strain gage configuration.

Lower legs will be tested on UVA's Telemacus linear impactor. A 6-axis load cell (Denton 3868) will be affixed to the loading plate, which will be constricted to translations in the SAE-Z direction, and below an interfacing member between the load cell and the forefoot (Figure 8). A 6-axis load cell (Denton 3868) will be attached to the potting cup at the proximal end of the tibia and attached to a massed stand (to mimic the mass of the upper leg) constrained to translations in the SAE-Z direction. The specimen will be placed with the lateral/medial side parallel to the earth; facilitating easy access to the Achilles tendon and X-Ray filming of the specimen during loading; dorsiflexion of the foot will be measured in X-Ray footage using metal angle markers affixed to the substrate on which the leg rests.

The Achilles tendon will be manipulated using the device below (figure 9), whereby the tendon will be sandwiched between two textured aluminum surfaces that are bolted together. A prescribed amount of force will be applied to the tendon by means of a constant force spring which will reside on the same platform as the distal load cell. The prescribed amount of tension applied to the Achilles Tendon will be calculated for each specimen thusly: the force exerted on the forefoot (assuming no hindfoot is in contact with the resting substrate) in a sitting position is estimated to be the sum of the upper and lower leg masses multiplied by gravity (F_{UL}); the force to exert on the Achilles tendon is then the ratio of the distances from the forefoot (X_{FF}) to the origin of the ankle complex and Achilles Tendon (X_{AT}) to the origin of the ankle complex, multiplied by the force calculated at the forefoot; $((X_{FF})/(X_{AT}))*(F_{UL})$. By applying tension to the Achilles tendon in this fashion we mimic the natural forces seen in the tendon as if a live specimen were sitting with their forefoot on the loaded substrate only.

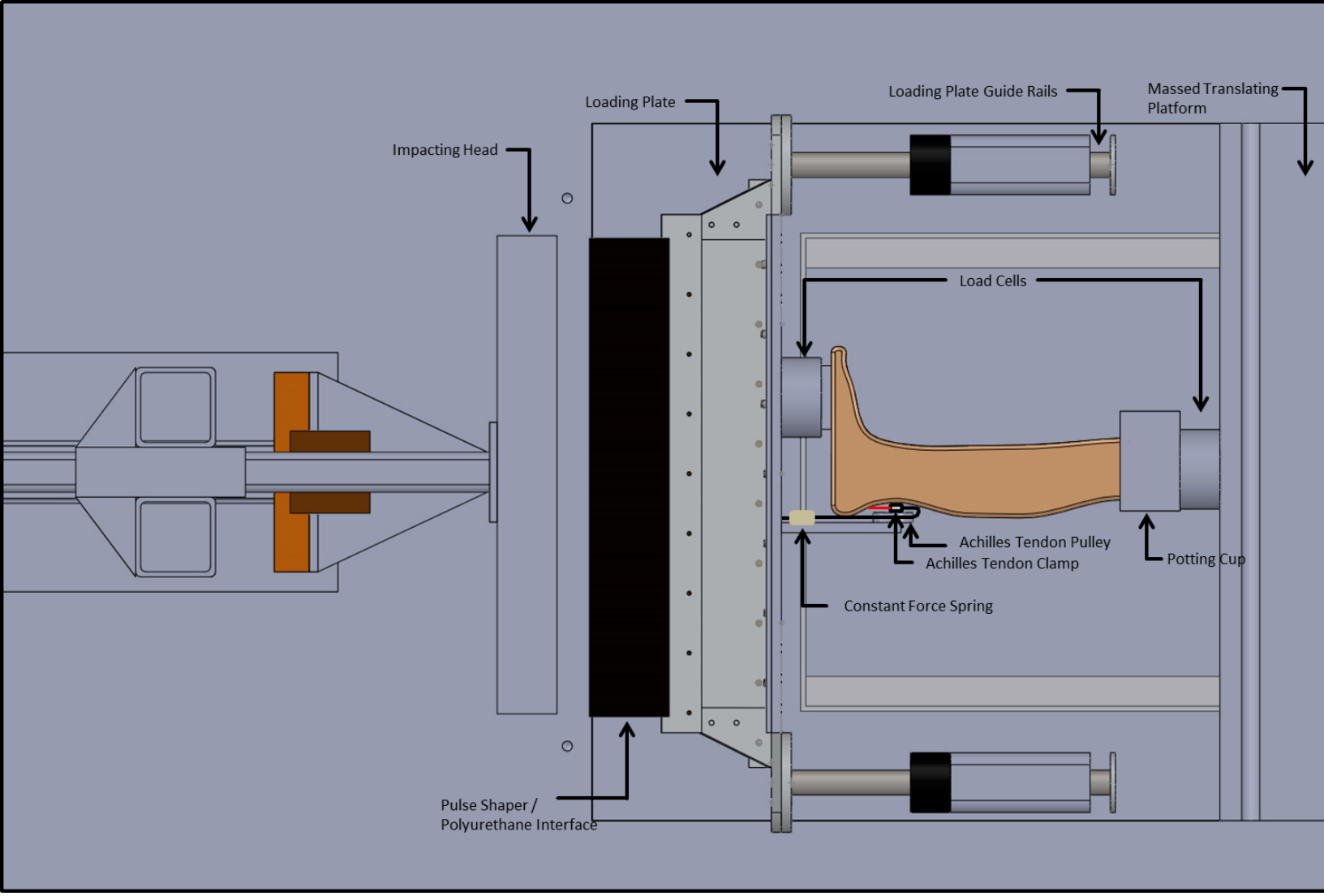

Figure 9. PMHS specimen in Telemachus linear impactor apparatus; viewed from above looking down from the perspective of the X-Ray emitter.

Figure 10. Textured aluminum clamping device to grip Achilles tendon.

The results of this task will provide local strength and damping properties of the bones in the forefoot (high-rate material properties); in addition to load rate dependent injury risk curves for the PMHS foot (human injury risk curves) all under normal loads to the Achilles tendon. Including existing ATD feet will provide a basis of comparison between current technology and the ability to discern these foot injuries. First article testing of WIAMan will allow injury prediction of the bones in the forefoot using matched pair tests (injury assessment reference curves).

B. Research Specimens/Components (Cadavers and/or ATDs as Applicable)

The number of specimens was estimated to acquire power of 80% in the data analysis and is subjected to changes in the data analysis process. The specimens will be selected from male donors, less than 60 years in age, and have no previous injuries to the flesh. The subjects will be tested for standard potential transmissible diseases. Only cadavers meeting all of the following criteria may be utilized in the study: (1) Males above the age of 18 years and below the age of 60 years. (2) Cadavers without existing unhealed bone or soft tissue injury. (3) Cadavers will not have evidence of wasting disease. (4) Cadavers tested negative for Hepatitis A, B, C and HIV. (5) Only remains obtained from an approved source. To limit cadaveric variation, specimens will be selected that are similar in stature and mass to a 50th percentile male based on the ongoing U.S. Army anthropometric studies.

Specimens' demographics and anthropometry will be precisely documented during the preparation process and pre- and post-test CT scans will be acquired from the specimens. Due to the nature of the research at the University of Virginia-Center for Applied Biomechanics, a large source of PMHS samples are available and more specimens are being acquired for the WIAMan project.

C. Exposures, Setup, and Data

Specimens will be instrumented with twenty-five strain gages (Micro-Measurements C2A-06-062LW-350) attached circumferentially around the distal tibia and fibula to form bone cells, proximal/distal ends of the tibia and fibula (anterior/medial on tibia and anterior/lateral on fibula), calcaneus, and metatarsals, using cyanoacrylate adhesive to capture strains in the SAE-Z direction and assist in observing fracture times (Figures 6 and 7). Acoustic transducers (S9225 acoustic miniature sensor, from Physical Acoustics) will be affixed to the distal end of the tibial shaft and medial calcaneus to observe fracture times. Four accelerometers (Endevco 7264B-2000) attached to the proximal/mid/distal tibia and dorsal surface of the navicular bone will measure accelerations in the SAE-Z direction, combined with two angular rate sensors (ARS-8k) attached to the mid/distal tibia will capture the motion of the tibia. The navicular bone's articulation with the talus and calcaneus ensure that the bone experiences similar accelerations to the calcaneus and talus which are directly in the loading path. However, the navicular's position outside of

the loading path helps ensure shielding from forces which would cause fracture in the bone, and thus inaccurate acceleration traces.

A 6-axis load cell (Denton 3868) will be attached to both the constrained loading plate and the potting cup at the proximal end of the tibia. The proximal load cell will be affixed to a massed stand that is constrained to translations in the SAE-Z axis. The stroke of the impact plate in the Z-direction will be limited by the use of inserts that fit around the shafts of the impact plate.

The impactor velocity, input acceleration (impact plate acceleration), times of fracture, stain and force along the tibial and fibula long axes, acceleration and rotation of the tibia, the reaction force at the knee, and both high speed film and X-Ray images of the bones during loading will be recorded; dorsiflexion of the foot will be measured in X-Ray footage using metal angle markers affixed to the substrate on which the leg rests. In addition CT images pre and post-test will be acquired. After each tests a complete autopsy will be performed on the specimens and all the injuries will be documented according to AIS and AFIS injuries codes. Injury risk functions based on the kinematics of the vehicle in an event of UBB will be developed based on the energy of the floor pan and the forces experienced during the impact.

To validate the biofidelity of the available ATDs University of Virginia-Center for Applied Biomechanics is planning to perform a series of tests on the available ATD's and at this point requests a MIL-LX lower limb. Total number of 10 tests will be performed on the MIL-LX lower leg during Fall of 2013.

University of Virginia Center for Applied Biomechanics has been heavily involved in cadaveric testing for more than 20 years and has developed a unique coding system to keep record of the specimens over the past years. Currently over 200 whole body and component PMHS specimens are kept at the center and are being handled by a fulltime biological material specialist.

All the testing protocols at the Center for Applied biomechanics are reviewed and approved by a testing protocol committee in term of all the safety aspects of the experimental procedures.

Instrumentation	Range	Axis	Location/Description Of Use	Biomechanical Parameters	BRC
Strain gauge (C2A-06-062LW-350)		Z	25 to measure strain in the SAE-Z direction and to assist in observing fracture times on metatarsals; 6 elements placed circumferentially at the distal tibia (bone cell), 4 elements placed circumferentially at the distal fibula (bone cell); 2 elements on medial/anterior and medial/lateral portions of the distal and proximal ends of the tibia and fibula respectively (total 8), 2 on the calcaneus; 1 on each metatarsal (total 5). Strain elements on tibia and fibula will be used in an attempt to measure the loads transmitted through the long bones.	BP-51: Tibia shaft loads FZ. Load cells placed directly into the tibial shaft are not used as they have a likely chance of creating artificial fractures at the load cell/bone interface.	Tibial Force Z
Accelerometer (Endevco 7264B-2000)	2000 g's	Z	4 placed on the proximal/mid/distal tibia, the other on the dorsal surface of the navicular bone, to measure accelerations in the SAE-Z direction for both the tibia and foot respectively.	BP-50: Tibia Accel Z BP-53: Foot Accel Z	Tibial Accel Z
Angular Rate Sensor (ARS-8K)	8000 deg/sec	Y	2 placed at the mid/distal tibia, will measure rotation of the long bone in the SAE-Y direction.		Tibial Rotation Y
Acoustic Sensor (PICO mini sensor)	200-750 kHz		2 will be affixed to the distal end of the tibial shaft and medial calcaneus to observe fracture times.		
Load Cell (6-Axis Denton 3868)	FX:22K N FY&FZ: 11K N MX: 565 N MY&MZ: 1130 N	X,Y,Z	2; one will be placed distally and measure loads between the forefoot and load plate, the other will be placed proximally and measure the transmitted load through the entire lower leg.		Tibial Force Transmission X,Y,Z
Camera (NAC GX-1)/X-Ray Film	1000 fps on both cameras	Y	To capture the motion of the foot and ankle compression, NAC will be obliquely positioned to capture general motion and compression, and X-Ray film will observe SAE-Y axis.	BP-54&55: Motion of the foot and compression of the ankle respectively.	

Table 1. Instrumentation and applicability to WIAman Project description.

While the above instrumentation is currently planned for these tests, changes may be made to accommodate the recommendations of the instrumentation working group in effort to standardize with the rest of the bio-performers. Further information about instrumentation application techniques will be presented at the applicable Test Readiness Review.

Velocity	Fore-foot loading Posture=90-90-90; Compression using foot w/ flesh and PPE
V_1	3 PMHS
V_2	3 PMHS
V_3	3 PMHS
I_1	4 PMHS
I_2	4 PMHS

Table 2. Test matrix of sub-injurious and injurious velocities.

1.4.8 ANALYSIS PLAN

A spring-dashpot model will be developed based on the recorded accelerations and forces that will identify the transmissibility of the lower leg components during high rate deformation. Also, based on the calculated local tibia force and the energy at boundary, injury risk curves will be developed. The results of this study are the first to predict the behavior of the lower limb forefoot components with active tension in the Achilles tendon to estimate the risk of injury in in high rate deformation.

1.4.9 SCHEDULE, PRODUCTS, AND MILESTONES

The experimental part of this study is planned to be started beginning of July 2013 and concluded by September 30th, 2013 and data analysis will be concluded by Dec 31, 2014. By the end of this period injury risk curves for the lower limb components and transmissibility models along with all the experimental data will be delivered as the final product of this study.

Objectives	20-May	30-Jun	31-Jul	31-Aug	30-Sep	31-Oct	30-Nov	31-Dec
Test System Design and Reviews								
Manufacture Test System								
Testing to Support Threshold Critical BRC								
Conduct PMHS Testing								
Review and Analyze Data								
Submit Data to FTP Site								
Develop Threshold Lower Leg BRC								

Table 3. Proposed project timeline.

1.4.10 ASSUMPTIONS AND RISKS

The only significant outstanding risk in this research is the successful procurement of adequate PMHS. This should be the only limiting factor to success of this project.

2. Finite Element Modeling of Lower Extremity Fractures in Occupants Subject to Under-Vehicle Blasts

Introduction

Severe fractures to the foot-ankle-lower leg account for over 80% of all skeletal injuries found in occupants of armored vehicles that were exposed to a blast (Ramasamy, 2011). Battlefield epidemiology suggests that these injuries are caused by axial loading to the lower extremities from contact between the deforming vehicle body and the occupant's feet. Axial loading to the foot-ankle complex is also an injury mechanism associated with a large number of severe injuries caused by frontal automotive impacts (Crandall, 1994). A well-established body of research into automotive lower extremity injuries (where the University of Virginia has been a major contributor) can be used to improve our knowledge of the risks and preventions of under-vehicle blast injuries. One such contribution that can be leveraged from the automotive field is validated computational models. Computational models are well-suited to help study and predict the high-rate dynamics of the lower extremities caused by automotive impacts, and have the potential for investigating the biomechanical responses to under-vehicle blasts.

This study focuses on predicting mechanical response and injury outcomes from high-rate axial impacts to the lower leg using the Global Human Body Model Consortium (GHBMC) finite element (FE) model. The GHBMC lower extremity model, developed by the University of Virginia, was previously validated for a multitude of loading conditions typically associated with automotive impacts. The current study extends the capabilities of the Phase 1 GHBMC FE model for use with under-vehicle blast loading. This is achieved by comparing the foot-ankle-lower leg FE model to impact tests performed on 18 post-mortem human surrogate (PMHS) lower legs. Modifications to the automotive-based FE model are made to improve the biofidelity of the model at higher loading rates. The modified FE model is evaluated for its reproduction of the complex internal and external loading characteristics of the PMHS. This effort established the early stages of a larger research strategy to develop biofidelic computational tools that can be used to assess injury risk and evaluate future designs for injury prevention.

Methods

The Phase I lower extremity FE model of the GHBMC 50th percentile male was integrated into a FE model of the University of Virginia drop-tower (Figure 11). The foot-ankle-leg model (Figure 12) was developed and validated for a wide range of loading conditions by Shin, et al. (2011, 2012). This model was simulated under conditions stemming from 11 of the 18 lower leg impact experiments performed by Henderson, et al. (2013). In that study, each leg was sectioned above the proximal epiphysis of the tibia and fibula, and instrumented with accelerometers, strain gauges, and load cells. The lower legs were mounted at the bottom of a drop tower equipped with an impactor capable of producing axial loading on the PMHS foot up to 600 g's acceleration over 1.5 ms duration. The FE model included a preload of 100 N corresponding to the impact plate resting on top of the foot prior to impact in the experiment (Figure 13). A free plate attached to the potted end of the tibia via a load cell element was included in the model. Comparison between the FE model and the physical tests were made by focusing on load cell force and distal tibia strain. Each simulation case was run for 20 ms using LS-DYNA V971 R6.1.1.

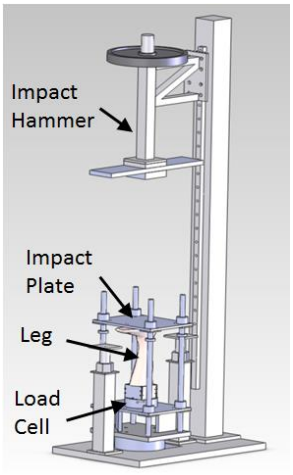

Figure 11. Drop-tower assembly used to obtain the experimental results.

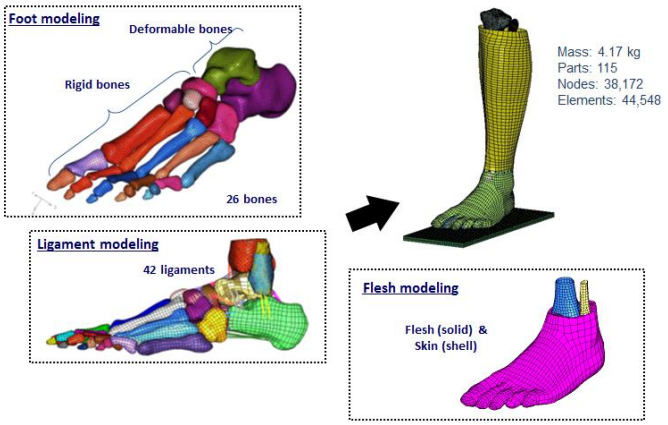

Figure 12. GHBMC foot-ankle-leg model validated by Shin, et al. (2011)

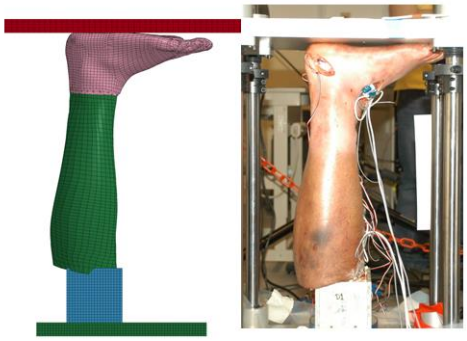

Figure 13. Comparison of the finite element model and the test setup for the drop-tower experiments by Henderson, et al. (2013)

An initial series of simulations were running using the original unmodified version of the lower leg model to establish a baseline comparison with the experimental results. After this analysis, the model was modified to better reflect the experimental data. Modifications included adding viscoelasticity to the foot flesh using a visco-hyperelastic constitutive model to capture the dynamic heel-pad mechanics (Natali, et al, 2010; Figure 14). Additionally, the original model's bone tissue meshes were refined to produce more accurate geometry, and to better model bony fracture (Figure 15, Table 5). Additionally, this modification increased the number of through-thickness elements in the fibula and tibia shafts to two, thereby improving the tibia bending stiff to a more biofidelic response. The simulations were rerun using the modified model with the same input conditions as the original model and the results were compared.

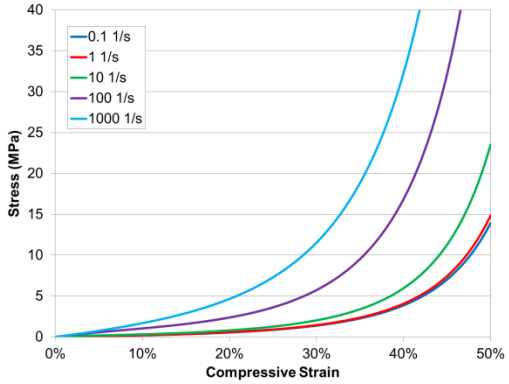

Figure 14. Visco-hyperelastic model used for the heel-pad (Natali, et al., 2010)

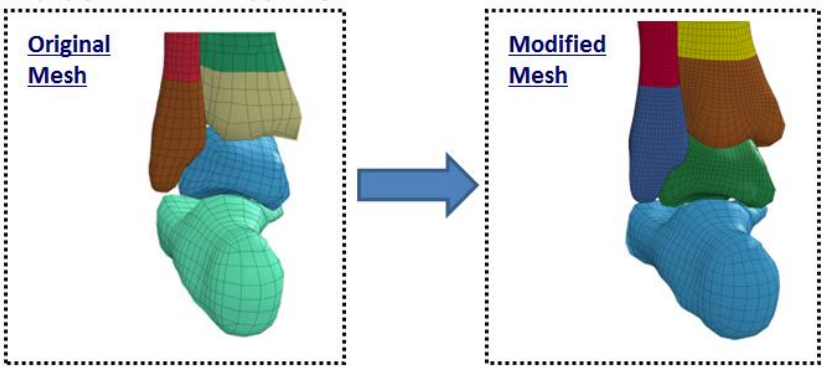

Figure 15. Modifications made to the model mesh

Table 5. Re-meshing characteristics

Bone	Original Mesh Size	Modified Mesh Size
Tibia	3.8 mm	1.9 mm
Fibula	2.2 mm	1.1 mm
Calcaneus	4.7 mm	4.7 mm
Talus	4.1 mm	2.3 mm

Results

The results from the original model greatly under-estimate both the proximal tibia force and strain, even as far as predicting tensile strain in the anterior tibia when compressive loading was demonstrated in the experimental study (Figure 16 to Figure 18). Additionally, a significant phase delay existed between the experimental and model traces.

Figure 16. Two typical cases of proximal tibia force-time history plots comparing the original and modified FE model results with the experimental data by Henderson et al., (2013).

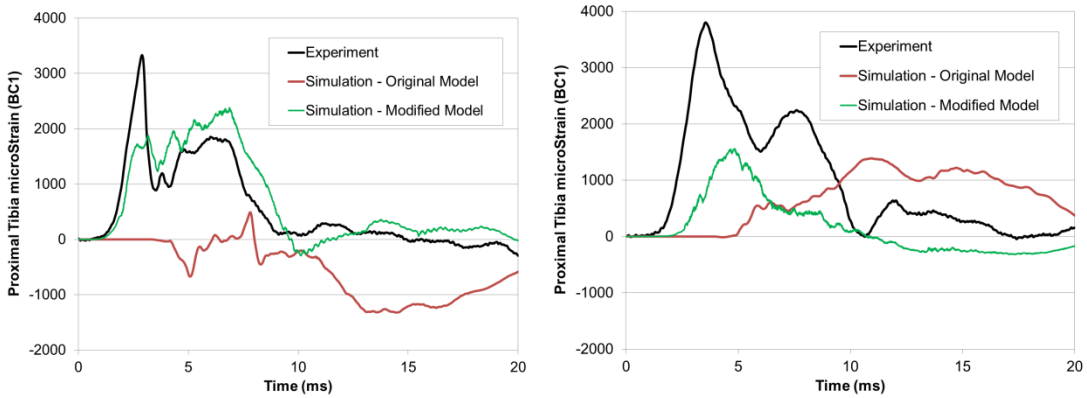

Figure 17. Two typical cases of distal anterior tibia strain time-history plots comparing the original and modified FE model results with the experimental data by Henderson et al., (2013).

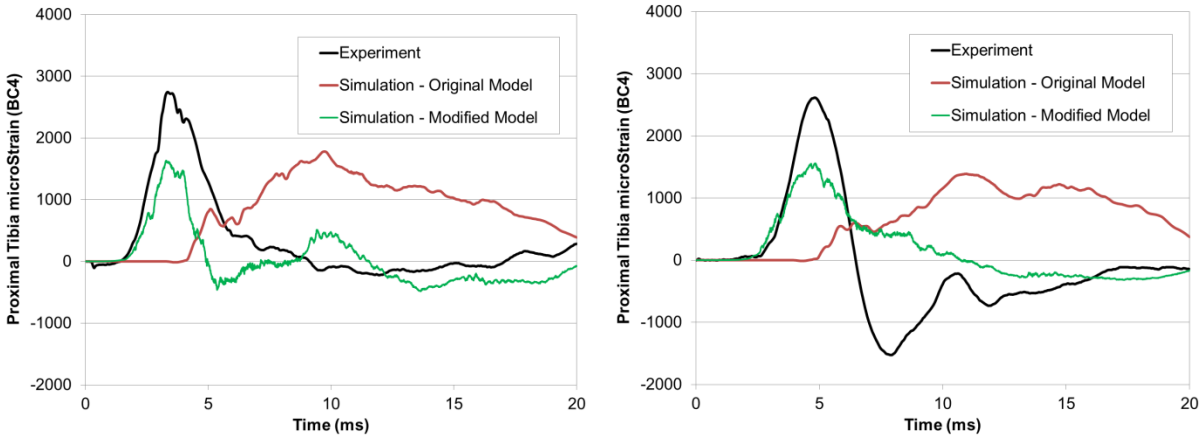

Figure 18. Two typical cases of distal posterior tibia strain time-history plots comparing the original and modified FE model results with the experimental data by Henderson et al., (2013).

Changes to the original model greatly improved the model biofidelity. Force amplitudes were slightly higher in the modified model than the experimental data (Figure 19), but were sufficiently close to consider them as representative. Loading rates were greatly improved, and issues with differences in phase lag were almost eliminated. Modified model response had an average (over the 11 cases) correlation coefficient with the experimental data of 0.85.

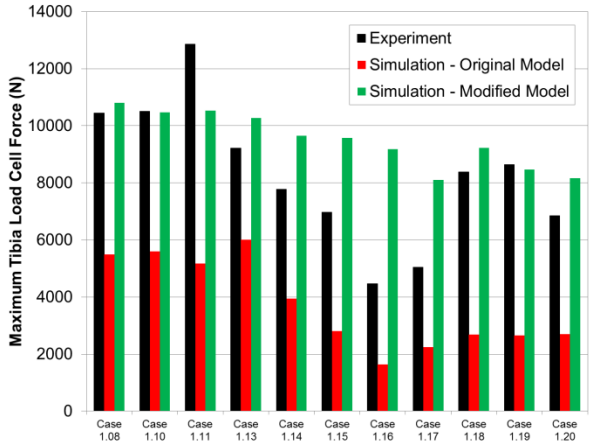

Figure 19. Comparison of peak tibia load cell force for the experiment, and the original and modified models.

Anterior and posterior tibia strain also greatly improved with the modifications to the original FE model; However, the FE model continued to under-estimate the maximum amplitude of the strain over all the cases (Figure 20). Phase response improved for the FE model, and the average correlation coefficients of the 11 cases simulated was 0.44 and 0.52 respectively.

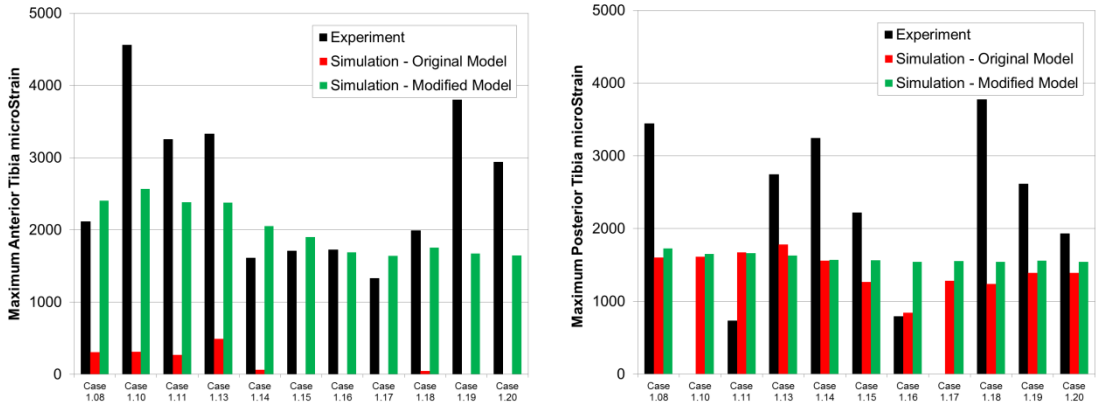

Figure 20. Comparison of peak anterior (left) and posterior (right) tibia strain for the experiment, and the corresponding strains measured in the original and modified FE models.

In addition to being able to reproduce similar force response, and reasonably close strain values, the modified model was also able to reproduce injuries similar to those observed in the drop-tower experiment. Similar fracture patterns were produced by both the model and the experiment for the calcaneus (Figure 21). Over all the cases simulated, the modified model predicted only calcaneus fractures which was the most common injury response seen in the experimental data (Table 6). The model did not predict talus or distal tibia fractures (found in a few cases in the

experimental data) but upon further review of the simulation results, these components experienced high levels of stress but below the define threshold for injury. Furthermore, it is apparent that the model can provide some level of distinction between injurious and sub-injurious cases, as evidenced by the existence of failure in only the cortical shell elements for some of the latter cases where injury was not reported. Failure of the cortical shell elements may be analogous to an incomplete fracture (or "hairline fracture") that may not have been apparent in the post-test autopsy of the experimental specimens.

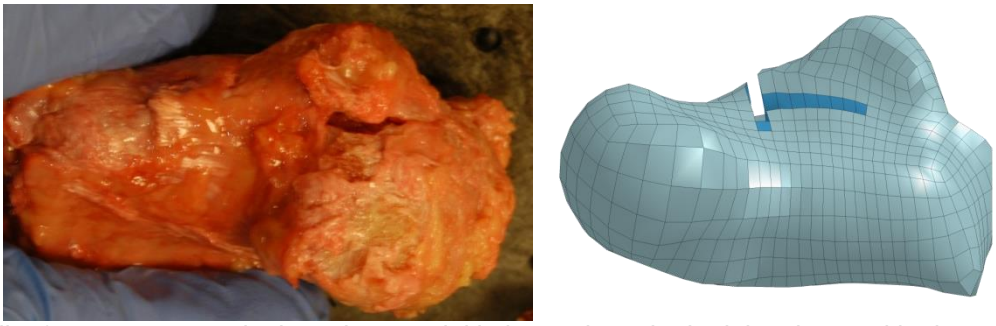

Figure 21. Similar fracture patterns in the calcaneus initiating at the subtalar joint observed in the modified model and experiment.

Table 6. Comparison of injuries observed in the experiment and the modified finite element model.

Case	Hammer Mass (kg)	Velocity (m/s)	Injuries reported	Simulation Injury
1.08	61.2	5.73	Calcaneus: fx line into one joint surface	Calcaneus fx
1.10	61.2	4.09	Distal Tibia: fx, partial articular	Calcaneus fx
1.11	61.2	5.57	Talus: fx NFS Calcaneus: fx NFS	Calcaneus fx
1.13	61.2	5.35	Distal Tibia: fx, partial articular Calcaneus: fx, extra articular	Calcaneus fx
1.14	34.2	5.46	Calcaneus: fx line into one joint surface Talus: fx NFS	Calcaneus fx
1.15	34.2	5.46	Calcaneus: fx NFS	Calcaneus fx
1.16	34.2	4.98	Calcaneus: fx, extra articular	Calcaneus fx, shell only
1.17	34.2	4.44	Calcaneus: fx, extra articular	Calcaneus fx, shell only
1.18	34.2	4.93	None	Calcaneus fx, shell only
1.19	34.2	4.66	None	Calcaneus fx, shell only
1.20	34.2	4.70	None	Calcaneus fx, shell only

Discussion

While great strides were made to convert an FE model of the lower extremities for automotive impacts into a biofidelic model for high rate military impacts, this effort is ongoing. Many areas of the model have been identified as potential components for further improvement in model biofidelity. Firstly, the constitutive models for bone must account for the high strain rate regimes achieved in military-type impacts. Early works on human bone mechanical properties by McElhaney (1966) and Carter and Hayes (1977) showed that the elastic response of bone was sensitive to loading rate (a phenomenon known as viscoelasticity), the yield strength and ultimate strength of bone was sensitive to loading rate (a phenomenon known as viscoplasticity), and both of these responses were dependent on bone density. Most constitutive models used for modeling bone were developed for modeling the elastic-plastic response of metals, and they often

include viscoelastic or viscoplastic material response but not both. Incorporating more appropriate constitutive models for bone should improve the biofidelity of the model in the areas of stress wave propagation and dissipation along the tibia (we see a decrease in strain amplitude from the distal end to the proximal end following the axial impact).

Additionally, variations in the ankle bone properties can strongly affect the fracture response and load transmission through the leg, and thus must be addressed. The strength and stiffness of cancellous bone in the calcaneus, talus, and tibia are strongly regional dependent (e.g., Jensen et al., 1988; Sabry et al., 2000). Variations in bone strength undoubtedly affect the fracture pattern and tolerance of the bone, which will affect the timing and magnitude of the peak force sustained in the lower leg. PMHS specific parameters such as age and anthropometry are also variations that are not considered in the current version of the model. Adjusting the material properties based on patient specific biometrics such as bone mineral density should improve correlation between the FE model and the specific experimental result.

Finally, am area which must be addressed in future lower leg models is ankle joint laxity. Since no cartilage exists in the FE model, contact between ankle bones may not be as tightly coupled, and the ankle kinematics resulting from an axial load may be affected. Ankle laxity in the FE model is believed to cause the ankle to prematurely roll and induce a lateral component to the loading on the tibia. This is believed to affect the corresponding tibia strain response. The experimental strain response demonstrates nearly pure axial loading of the tibia, with similar strain amplitudes around the circumference of the tibial shaft (as measured with the bone cell). However, the strain response in the FE suggests some amount of bending may be occurring since the variation of strain amplitude around the circumference of the tibial shaft is large. More experimentation, potentially with the use of a high-speed x-ray system, may be necessary to validate the kinematics of the ankle model, and to determine whether the tibia bending phenomenon is accurate or just a result of the ankle roll in the FE model.

Conclusions

This study focused on predicting mechanical response and injury outcomes from high-rate axial impacts caused by under-vehicle blast to the lower leg using an FE model of the human lower leg, foot, and ankle that was originally developed for automotive applications. While the original model was well validated in a multitude of loading conditions typically associated with automotive impacts, it failed to capture the axial loading response for high rate, short stroke impacts. Modifications to the FE model in the areas of material properties and mesh discretization substantially improved the biofidelity of the model at these higher loading rates. The modified FE model reproduced the complex internal (strain) and external (force) loading characteristics of the PMHS tests with reasonably good accuracy. The work in this study was constituted some of the preliminary steps required for the development of an effective and biofidelic modeling tool that can be used for evaluating future systems designed to mitigate injury in under-vehicle blast events.

3. Sub-Calcaneal Heel Pad Component Testing

BACKGROUND

In the instance of a high rate axial load to the lower limb, the soft tissue layer in the plantar region of the foot is the first structure engaged. A material characterization of this structure under such loading conditions would provide a better understanding of the load paths to the lower extremity, and accurate material properties for the development of biofidelic anthropometric test devices (ATDs) and finite element models (FEM) of the foot. The current Hybrid-III ATD is known to lack accurate heel compression characteristics for high rate loads (Kuppa, 1998). Therefore the university of Virginia Center for Applied Biomechanics (UVA-CAB) has initiated a series of component tests on human sub-calcaneal heel pad to characterize the tissue under high rate compressive loading. The objective of this test series is to characterize and compare the mechanical response of both the human sub-calcaneal heel pad and Hybrid III skin.

METHODS

Materials

Protocols for the handling of biological materials were approved by the University of Virginia's Institutional Biosafety Committee. Eight heel pads were collected from the hind foot region of four post mortem human surrogates (PMHS). Heel pads were flash frozen and stored in a morgue freezer at -20°C until materials testing could be performed. Five to eight tissue samples were cut to approximately 10mm in diameter and 10mm in height from each whole heel pad using a cylindrical boring tool. For ease of cutting, the heel pads were left partially frozen while being prepared. Samples were cut perpendicular to the skin surface and from four different regions of the pad (Miller-Young, 2002). Sample dimensions were measured with a micrometer and used to calculate tissue stresses and strains. The quality of each sample was evaluated and those that were not of good cylindrical shape were discarded.

Instrumentation

Tissue samples were tested using a bench-top test machine (ElectroForce® 3100 Test Instrument, Bose Corporation – ElectroForce Systems Group, Eden Prairie, MN). Samples were placed on an aluminum stage mounted atop a 250gram capacity force transducer (Model 31 Low, Honeywell International Inc., Golden Valley, MN), and beneath a flat aluminum load platen mounted to a linear actuator equipped with an LVDT to measure displacement. Excess compliance in the test frame due to the motion of the actuator induced an inertial based force response in the load cell. A 500g linear accelerometer (Model#: 7264B-500, Humanetics Innovative Solutions, Plymouth, MI) was mounted to the test

stage to subtract off this effect. Force, displacement, and acceleration data were acquired at 20kHz (DEWE-2010, Dewetron Inc., Wakefield, RI).

Compression Tests

Samples were subjected to a battery of ramp and hold stress relaxation tests. Prior to each test, the load platen and test stage were lubricated with a thin layer of saline to reduce the friction between the sample and boundaries. The load platen was then lowered at a rate of 0.01mm/s toward the top surface of the sample until a tare load of approximately 2gram force was measured. The actuator was stopped for a total of two minutes to verify contact between the sample and platen. During this time the initial, unstrained height of the sample was measured and recorded as the distance between the platen and test stage and used to calculate tissue strain. After two minutes had passed, the load platen was rapidly pressed into the tissue and held for 30s to measure the relaxation. Samples were compressed up to 20% engineering strain at peak displacement rates between (150-350)mm/s approximately (10-30)s^{-1}. Some samples were retested and in this case five minutes were allotted for the tissue to recover in between subsequent tests.

Mathematical Modeling

All data were filtered in accordance to the SAE-J211 standard, CFC 1000, using a zero-phase, digital IIR 8 pole butterworth filter at a Low Pass frequency of 1650Hz. The data were resampled in a logarithmically scaled time step to give equal weights to both ramp and hold portions of the test. Samples were assumed to be incompressible and isotropic. Engineering stress and strain were calculated from the force and displacement data through the following expressions:

$$\sigma = \frac{F}{A_o} \qquad \varepsilon = \frac{\Delta l}{l_o} \tag{1}$$

where F is the compressive force measured by the load cell, A_o and l_o are the initial, un-deformed cross sectional area and tissue length respectively, and Δl is the tissue displacement acquired by the LVDT. The stress response, $\sigma(\varepsilon, t)$,$\mathrm{F(h,t)}$ to an arbitrary strain input, $\varepsilon = \varepsilon(t)$,$\mathrm{h = h(t)}$ can be modeled using a quasi-linear viscoelastic (QLV) mathematical framework (Fung, 1993) :

$$\sigma(\varepsilon, t) = \int_0^t G(t-t')\frac{\partial \sigma^e(\varepsilon)}{\partial \varepsilon}\frac{\partial \varepsilon}{\partial t'}dt' \tag{2}$$

where $\sigma^e(\varepsilon)$ is the instantaneous elastic response of the tissue and $G(t-t')$ is the reduced or normalized relaxation function, $0 \le G(t) \le 1$. The elastic behavior of the tissue was modeled using two different constitutive equations. The first is a 3rd order polynomial relationship between stress and strain:

$$\sigma^e(\varepsilon) = a_1\varepsilon + a_2\varepsilon^2 + a_3\varepsilon^3 \tag{3}$$

where a_i are constants. For the second model the tissue was assumed to be incompressible and isotropic and modeled using an exponential strain energy density function (SEDF) (Beatty, 1996).

$$W = \frac{\mu_o}{2\gamma}\left[e^{\gamma(I_1-3)} - 1\right] \tag{4}$$

where μ_o is the elastic shear modulus, γ is the nonlinearity coefficient, and I_1 is the first invariant of the right Cauchy-Green strain tensor. The relationship between stress and strain from expression 4 is:

$$\sigma^e(\lambda) = \frac{\mu_o e^{\left[\gamma\left(\lambda^2+\frac{2}{\lambda}-3\right)\right]}(\lambda^3-1)}{\lambda^3} \tag{5}$$

where $\lambda = \varepsilon + 1$ is the stretch ratio. A six term prony series with five time constants was chosen to model the relaxation behavior $G(t)$ of the tissue:

$$G(t) = G_\infty + \sum_{i=1}^{5} G_i \cdot e^{-\frac{t}{\tau_i}} \tag{6}$$

where G_i's are the normalized relaxation coefficients of the corresponding time decades and G_∞ is the coefficient of the steady-state response. Values for the thirteen coefficients a_1, a_2, a_3, μ_o, γ, G_i, for i=1 to 5 and G_∞ were determined through a reduced gradient algorithm (Excel Solver®, Microsoft®, Redmond, WA) that was used to minimize the sum squared error between the model-predicted force, resulting from numerical integration of (2), and the experimental data from expression (1). To increase the stability of the model during the fitting procedure, the time constants were fixed at decades, τ_1 = 0.001s, τ_2 = 0.01s, τ_3 = 0.1s, τ_4 = 1s, and τ_5 = 10s.

RESULTS

Seventeen total compression tests were performed on the tissue samples and an average $\sigma^e(\varepsilon)$ and $G(t)$ were determined for expressions (3), (5), and (6) respectively, Figure 1. Average values for the coefficients of the exponential and polynomial models are provided in Table 1. Stress and strain time histories for an arbitrary chosen compression test are provided in figure 2. The constant a_2 was set equal to zero to ensure physically realistic stress strain behavior.

A **B**

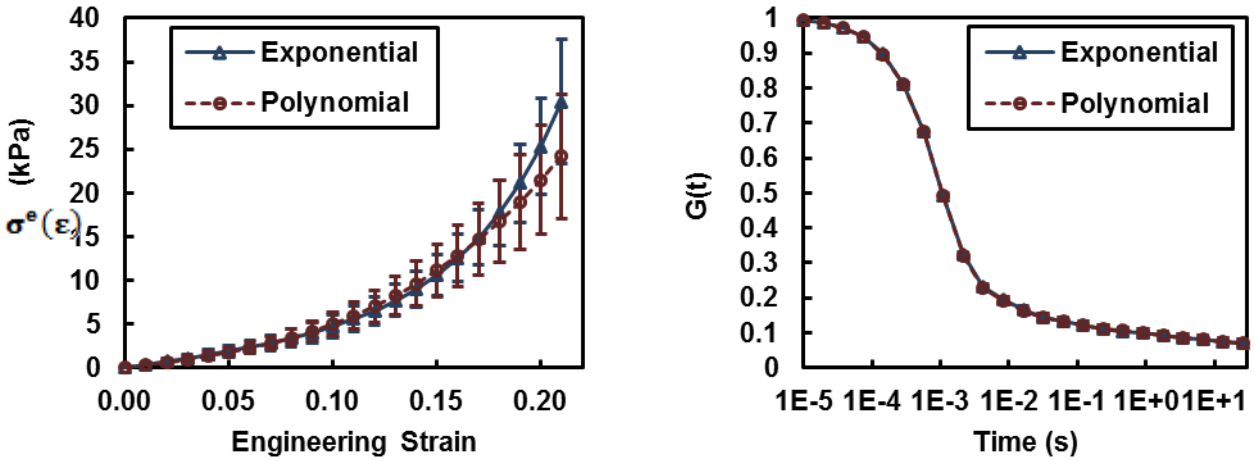

Figure 1: Average A) instantaneous elastic response, $\sigma^e(\varepsilon)$ and B) reduced relaxation function, $G(t)$.

Table 1: Average values for the polynomial and exponential model fits to the experimental data.

Polynomial			Exponential		
Unit	Coef	Value ± 95%CI	Unit	Coef	Value ± 95%CI
kPa	a_1	31.2 ± 7.8	kPa	μ	12.6 ± 3.7
kPa	a_2	0.00 ± 0.0	-	γ	14.7 ± 2.3
kPa	a_3	1903 ± 624			
-	G_1	0.744 ± 0.009	-	G_1	0.741 ± 0.007
-	G_2	0.108 ± 0.015	-	G_2	0.110 ± 0.010
-	G_3	0.033 ± 0.005	-	G_3	0.034 ± 0.004
-	G_4	0.023 ± 0.002	-	G_4	0.023 ± 0.002
-	G_5	0.021 ± 0.001	-	G_5	0.022 ± 0.001
-	G_∞	0.070 ± 0.010	-	G_∞	0.070 ± 0.010

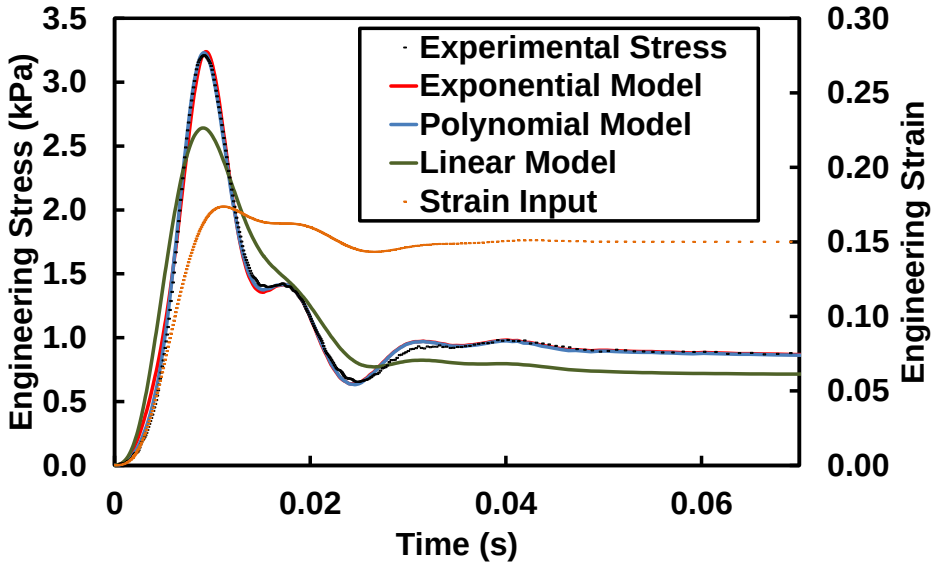

Figure 2: Examples of the QLV models (exponential and polynomial) fit to the experimental data for the ramp portion of an arbitrarily chosen compression test. The QLV models followed the experimental data more closely than the linear model during the ramp, peak, and initial relaxation of the tissue. A similar result was observed when modeling other experimental data. The increase in force near 16ms and 30ms is due to the increase in displacement of the compression platen into the tissue at these times.

DISCUSSION

The tissue behaved viscoelastic and spatially nonlinear, Figure 2. Above 17% engineering strain the exponential model predicted a higher value of stress when compared to the polynomial model. Below 17% strain the models were

approximately equal, Figure 1. In sixteen out of seventeen tests, the polynomial model resulted in higher R^2 values and lower Sum Squared Error indicating a better fit. The reduced relaxation function, $G(t)$ was nearly identical for both models. The instantaneous elastic shear modulus was determined to be (12.6 ± 3.7)kPa, which is in agreement with values reported in the literature (8-16)kPa for similar compression rates (Weaver, 2005; Erdemir, 2006). A linear viscoelastic constitutive model was fit to the experimental data, in addition to both QLV models however, the linear model did not capture the data during the ramp, peak stress, and initial tissue relaxation, Figure 2. The assumption of QLV was justified using the method of isochrones (Laksari, 2012). Three isochrones were chosen: t_1= 0.03s, t_2= 0.10s, and t_3= 5s after the peak stress at 10ms, Figure 2. Stress vs. strain data for each isochron were plotted and fit with an exponential function $y_i(\varepsilon) = \alpha\left(e^{\beta\varepsilon} - 1\right)$, which provided a better fit over a linear function, $i = 1, 2, 3$ for each time t_i. Dividing the isochronous curves $y_i(\varepsilon)$ resulted in approximately constant values indicating that the data exhibited no temporal nonlinearities up to 20% engineering strain and that the choice of a QLV model was valid.

Limitations

There are a number of experimental factors that may affect overall tissue response. First, the tissue samples were mechanically cut from whole heel pads. Through this process the tissue at the boundaries was damaged, which may have significantly altered the values of coefficients used to fit the experimental data, Table 1. Studies on brain and liver tissues suggest that the stiffness of soft biological tissues differ by up to (30-50)% when tested in vitro, excised outside the body, compared to in vivo or in situ, inside the body (Gefen, 2004; Kerdok, 2006). Therefore the results presented in this study are an approximation to those of healthy living tissue. Second, ensuring a flat and uniform boundary condition between the loading surface and tissue sample was challenging. The tissue samples were of approximate cylindrical shape with varying depth and cross sectional area. To reduce the effect of this limitation, a pre-compression of 2 gram force was applied to the tissue sample prior to compression in order to create a more uniform loading surface. Finally, the constitutive models in the current study do not take into account the inertial component of force generated during deformation. For more accurate tissue response, inertial effects should be considered in the analysis, given the relatively high loading rates used in the current study.

Future Work

Experimental data will be collected for higher levels of compression, up to 50% engineering strain to increase the range and utility of the current material properties. Additionally, skin from the current Hybrid III ATD will be characterized under compressive loading to determine the compressive characteristics and compare with those of the PMHS. The accuracy of the material properties and the effect of inertial forces on the response of the tissue will be explored using a finite element analysis.

CONCLUSIONS

The mechanical response of the human sub-calcaneal heel pad under compressive loading was studied. The material properties of the tissue were determined up to 20% compression (engineering strain) and at rates between (15-35)s^{-1}. Quasilinear Viscoelastic analysis was validated using the method of isochrones and used to fit 2 nonlinear constitutive models to the experimental data. The R^2 Pearson correlation coefficient indicated that the polynomial model fit the data better than the exponential model. Results for the instantaneous elastic shear modulus were determined and agree with values reported in the literature at similar loading rates. These results may be used for computational models of the foot and design parameters for the construction of more biofidelic ATD's.

REFERENCES

Kuppa, Shashi M., et al. "Axial impact characteristics of dummy and cadaver lower limbs." *16th International Technical Conference on the Enhanced Safety of Vehicles*. 1998.

Miller-Young, Janice E., Neil A. Duncan, and Gamal Baroud. "Material properties of the human calcaneal fat pad in compression: experiment and theory." *Journal of biomechanics* 35.12 (2002): 1523-1531.

Fung YC, Biomechanics: Mechanical Properties of Living Tissues, 277-280, *Springer*, New York, NY, 1993.

Beatty, M. F. "Introduction to nonlinear elasticity." *Nonlinear effects in fluids and solids*. Springer US, 1996. 13-112.

Gefen, Amit, and Susan S. Margulies. "Are in vivo and in situ brain tissues mechanically similar?." *Journal of biomechanics* 37.9 (2004): 1339-1352.

Kerdok, Amy E., Mark P. Ottensmeyer, and Robert D. Howe. "Effects of perfusion on the viscoelastic characteristics of liver." *Journal of Biomechanics* 39.12 (2006): 2221-2231.

Weaver, John B., et al. "Imaging the shear modulus of the heel fat pads." *Clinical biomechanics* 20.3 (2005): 312-

319.
Erdemir, Ahmet, et al. "An inverse finite-element model of heel-pad indentation." *Journal of biomechanics* 39.7 (2006): 1279-1286.

Laksari, Kaveh, Mehdi Shafieian, and Kurosh Darvish. "Constitutive model for brain tissue under finite compression." *Journal of biomechanics* 45.4 (2012): 642-646.

4. Integration of Past and Present Lower Extremity Impact Research

Severe injuries are being reported from occupants of military vehicles exposed to under-body blasts, with lower extremity injuries accounting for a significant portion of these injuries. However, both the etiology and an effective means to mitigate these injuries are not currently known or understood, although whole body accelerations and at least some limited toe-pan intrusion are expected. While other serious injuries may accompany lower extremity injuries in an underbody blast (UBB) event, the direct loading of both the lower extremities and the pelvis make them a key starting point for investigating the injury mechanisms of UBB. Additionally, the ability to evacuate the vehicle following a UBB event in order to avoid further threat by the enemy in live theater makes the prevention of both lower extremity and pelvic injuries a top priority because of their weight-bearing nature and necessity for walking.

Lower extremity injuries are some of the most frequent, severe and debilitating injuries generated by underbody blast. Lower limb injuries sustained in automobile crashes have been heavily researched due to their frequency and high likelihood of impairment and disability. A review of the literature suggests that lower limb injuries account for roughly one-third of all moderate-to-serious injuries sustained by motor vehicle occupants involved in frontal crashes [1-**[3**]. Since intrusion of the foot-well region is often postulated as the primary mechanism of below-knee lower limb injuries, intrusion characteristics such as toe-pan displacement, toe-pan acceleration, intrusion onset rate, intrusion duration, and intrusion initiation time have been examined for their potential to produce lower limb trauma.

The injury mechanisms of the lower limb associated with intrusion of the foot include inertial loading, entrapment, excessive motion of the joints, and subsequent contact with other structures within the occupant compartment [4]. In terms of mechanisms associated with these injuries, the most severe trauma is normally sustained from axial loading of the limb. Biomechanical testing has been conducted to develop basic injury criteria for axial loading of the below-knee structures. For automotive rates of loading, Yoganandan et al. conducted a series of axial impact tests to the human foot-ankle complex and found a mean dynamic force at fracture (calcaneus and distal tibia) to be 15.1 kN [5]. Funk et al. (2002) determined injury risk functions for axial loads to the foot/ankle complex from a study that included axial loads up to approximately 12 kN [6].

The appropriateness of automotive rate tests for UBB applications can be understood by examining the different resulting injuries in each type of event. For example, in Funk et al., 2002, a test series investigating automotive intrusion produced averaged toe-pan velocities of 5 m/s with a load duration of 10ms (approximately 50g, compared to estimates of UBB accelerations of 500+g) [6]. In that study of 43 specimens, this load rate produced 9 talus, 25 calcaneus, 7 pilon, 4 medial malleolus, 8 lateral malleolus, 2 fibula, and 12 tibial plateau fractures. In 2001, Wang reported that underbody blasts can produce accelerations averaging 100g over time spans of 3 to 100 ms [7]. For most tests performed, the acceleration is not reported. Others have reported floor plate velocities produced by mine blasts to reach up to 30 m/s in 6 to 10 ms [8]. A study performed by McKay at loading velocities of 7, 10 and 12 m/s produced injuries similar to the Funk study in 2002; however, each of the tests performed at 10 m/s and above produced calcaneus injuries, with the talus being the second most injured bone. McKay concluded that severity of injury to the tibia and fibula increased with increasing impact velocities, thus suggesting that automotive rate loading is insufficient for determining injury thresholds for UBB [9]. A summary of previous lower extremity tests with sufficient detail for cross-comparison is shown in TABLE 7.

TABLE 7
SUMMARY OF PREVIOUS LOWER EXTREMITY UBB RESEARCH

Study	Boundary Condition	Hammer Mass (kg)	Velocity (m/s)	Max Energy (J)	Force (kN)	Acceleration (G)
Schueler 1995 [10]	Whole body	38	12.5	2968.8	16	250
Yoganandan 1996 [12]	Ballast 16.8kg	25	7.6	722	4.3-11.4	Unreported
Kitagawa 1998 [13]	Fixed end	18	3.99	143.3	7-9	Unreported
Bass 2004 [15]	Free end	N/A	Unreported	200g of C4	>8.6	25-200
McKay 2009 [11]	Femur potted	36.7	7.2-11.8	941-2494	4-6	Unreported
Quenneville 2010 [14]	Free end	3.9	13.9	109.6	15	Unreported
Pandelani, 2010 [25]						
Newell 2012	Potted femur	42	9	1701		Unreported

[27]						

While a lot of biomechanical knowledge already exists for the lower extremities and pelvis, much of the data are limited to automotive rates, meaning the data possess several critical limitations for use in the development of injury countermeasures in the under-body blast environment: these tests have not been developed for rates of loading indicative of the vehicle-blast environment; and they have not included relevant attire (such as combat boots or personal protective equipment). The applicability of these studies and criteria remain a key question to answer in the course of this study. Additionally, while anti-personnel landmine blast studies such as Bass, et al. in 2004 performed tests on PMHS and surrogate limbs exposed to C4 landmine blasts, the loading conditions are not as well defined as an impact test so the results are difficult to compare to UBB conditions and do not provide insight into the response of the whole body. Characterization of how the higher loading rates of UBB affect the response of the lower limb and pelvis will provide valuable information towards understanding the relevant injury mechanisms in UBB events, and is essential in the process of developing a biofidelic anthropomorphic test device (ATD). There is currently no objective test methodology to determine the transmission of forces, nor the risk of injury to the lower extremities due to foot-well intrusion from an under-vehicle blast or to the pelvis due to vertical translation of the seat. This research investigates injury and response of vehicle occupants (both PMHS and ATD) subjected to under body blast (UBB). In order to understand the mechanisms of injury resulting from UBB, laboratory experiments must be performed that recreate the blast-induced intrusion and motion of the vehicle, allow full visualization of the impact event, and include detailed instrumentation of the Post-Mortem-Human-Specimens (PMHS), crash test dummies and vehicle. This paper details a first attempt at whole body testing for a lab-based UBB scenario, while comparing the response of both PMHS and ATD occupants under these high rate loads in matched-pair tests, with particular attention to the lower extremities and pelvis.

Several studies have performed lower extremity impact tests to determine the injury mechanism and injury probability curves for the lower extremities. **Figure 22Figure 22** shows a summary of some of these injury predictors.

Figure 22. Injury Predictors from Previous Lower Extremity Research

Study	Boundary Condition	Loading Condition	Injury Predictor for 50% Injury Probability
McKay 2010 [9]	Potted femur, unbooted	Linear Impactor	5.9 kN axial tibia force, 10.8 m/s velocity
Yoganandan 1997 [5]	Potted proximal tibia, unbooted	Pendulum	0.348*Age+0.415*Axial tibia force=4.4 6.8kN Axial tibia force
Funk 2002 [6]	Potted proximal tibia, unbooted	Linear Impactor	45 YO 50% Male: 8.3 kN 65 YO 50% Male: 6.1 kN 45 YO 5% Female: 5.0 kN 65 YO 5% Female: 3.7 kN
Bass 2004 [15]	Potted mid-femur, booted	AP Landmine Blast	8.6 kN axial force = 50% risk of injury
Quenneville 2011 [14]	Potted tibia, unbooted	Linear impactor	7.9 kN = 10% risk of injury
Henderson 2013 [29]	Potted proximal tibia, unbooted, ballasted	Drop tower	7.34 kN distal tibia force = 50% risk of injury 6.16 kN proximal tibia force = 50% risk of injury

Comparison of Booted versus Unbooted

Little research exists for determining the effect of boots on injury probability, and the research that exists was inconsistent with other literature. Pandelani, et al. (2010) performed several booted and unbooted ATD tests with both the MIL-Lx and Hybrid-III legs at five different velocities. Upper tibia force was compared for each of the tests and the authors concluded that the Hybrid-III leg is more sensitive than the MIL-Lx leg to the presence of a boot [25]. Figure 23 shows a plot of the booted and unbooted upper tibia forces from the MIL-Lx as a function of velocity.

Introduction of an additional compliant element to the loading scenario muddies the boundary conditions, making comparison of results to previous research conclusions difficult. There are limited studies which have compared the response of ATDs and PMHSs with and without boots, and of those studies, the type of boot used was unclear, thus replicating the boundary conditions for such tests is difficult.

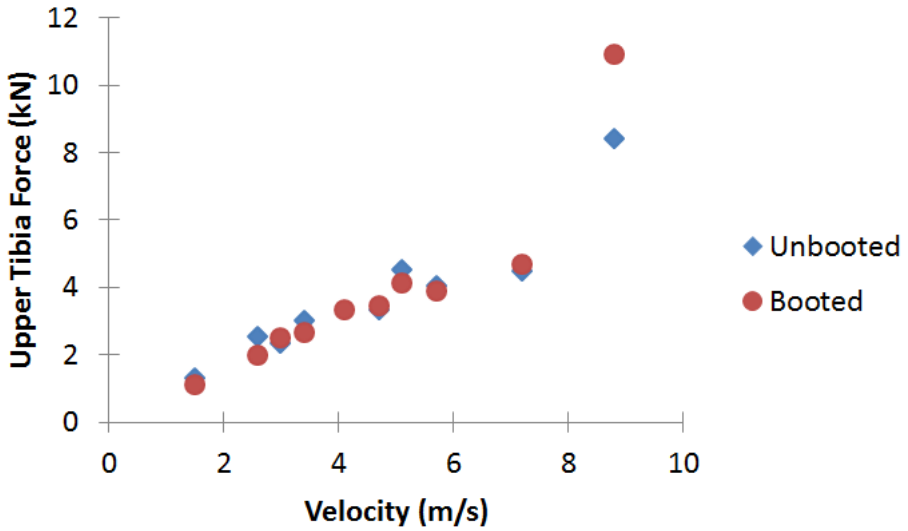

Figure 23. Booted and unbooted MIL-Lx upper tibia forces from Pandelani, et al. [25]

Newell, et al. also performed tests to determine the effect of boots on ATD response. For these tests, the compressive strain of the boot was calculated for PMHS, MIL-Lx and Hybrid-III tests and was found to be significantly larger (44.6%) for Hybrid-III tests than for PMHS tests, in comparison to 3% for MIL-Lx versus PMHS tests. This finding gives reason to suspect the validity of booted Hybrid-III results used for comparison with booted PMHS. This result could potentially be proof of the mass-recruitment issues that develop under higher rates of loading.

To this point no prior work has examined the effects of acceleration on the forces developed in booted or unbooted lower extremities. Thus, a comparison of the data collected by Newell, et al. and Pandelani, et al. is not completely possible due to insufficiency of the data set. Factors such as the rate dependency of the ATD lower extremities being used for comparison as well as the rate dependency of the boot material properties make it difficult to separate the effect of the boot and the effect of the ATD.

Acceleration as an Injury Predictor

Previous injury criteria have focused on measured outputs such as tibia forces for use as injury predictors. However, in live fire environments such injury predictors have limited use. McKay, et al. concluded impact velocity is a useful measure for predicting injury, however differences in boundary conditions such as knee angle, boots, loading rate, or even the time of contact with the impact plate are capable of affecting the injury outcomes [27-[**28**]. This concept is demonstrated by the different injury criterion developed for automotive versus blast loading scenarios. Funk, et al (2002) and Bass, et al (2012) arrive at different force based injury risk functions. McKay and Bir further expanded the range of tibia forces associated with risk of injury by claiming 6.4 kN of load has a 50 percent risk of injury (Figure 26) [11].

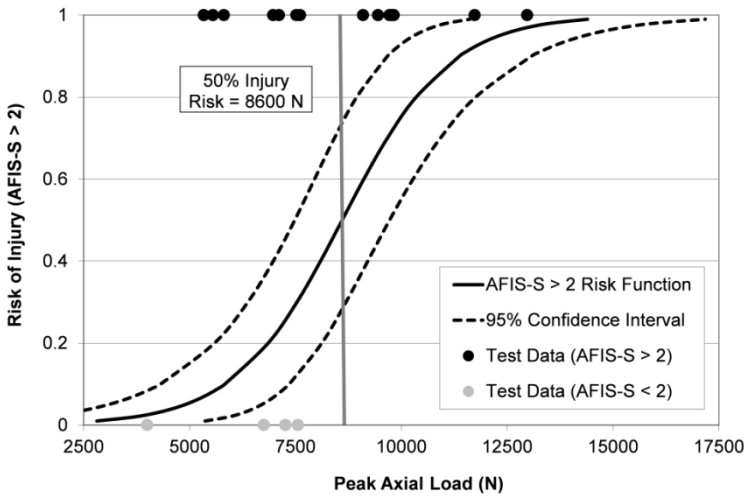

Figure 24. Injury risk function for AFIS-S > 2 injury developed from landmine blast research [30]

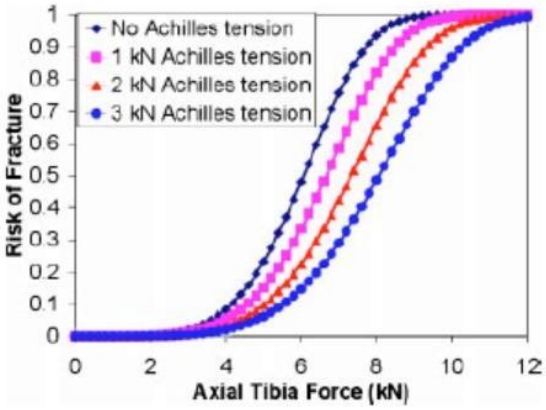

Figure 25. Injury risk function developed by Funk, et al. (2002) [6]

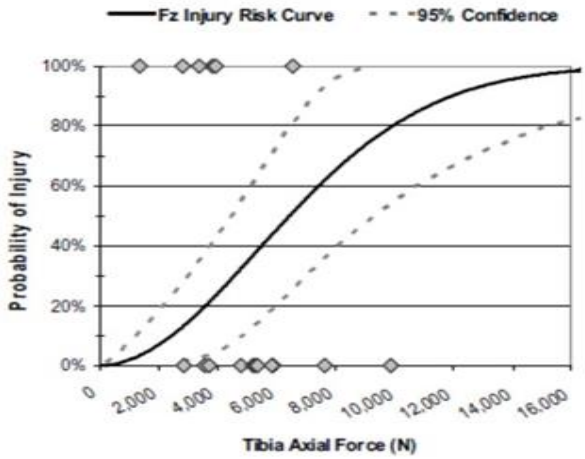

Figure 26. Injury risk curve developed by McKay and Bir (2009) [11]

Data from the studies performed by Funk, et al. in 2000 [6] and Henderson, et al. in 2013 [29], and unpublished data from the Medical College of Wisconsin were combined to gain a better understanding of the factors which affect injury in the lower extremities. A statistical analysis of this data set which combines automotive-rate and UBB-rate lower extremity impact research reveals an interesting relationship between acceleration and probability of injury. While it is possible to develop injury corridors based on the velocity of the impact plate, using acceleration reveals a cleaner relationship. Figure 27 shows the injury corridors based on velocity and time to peak. While the data included in this plot is not normally distributed, one can see that there are several occurrences where similar velocities and times to peak caused both injury and non-injury. Figure 28 shows a more distinct line between injury and non-injury and is based on acceleration and time to peak. Figure 28 was developed using a Weibull distribution parametric survival analysis where $\Pi = 1 - e^{[(\frac{\ln(a)}{c})^{\beta}]}$ and a is the peak acceleration, β is the shape parameter, and c=exp(C_1*T+C_0).

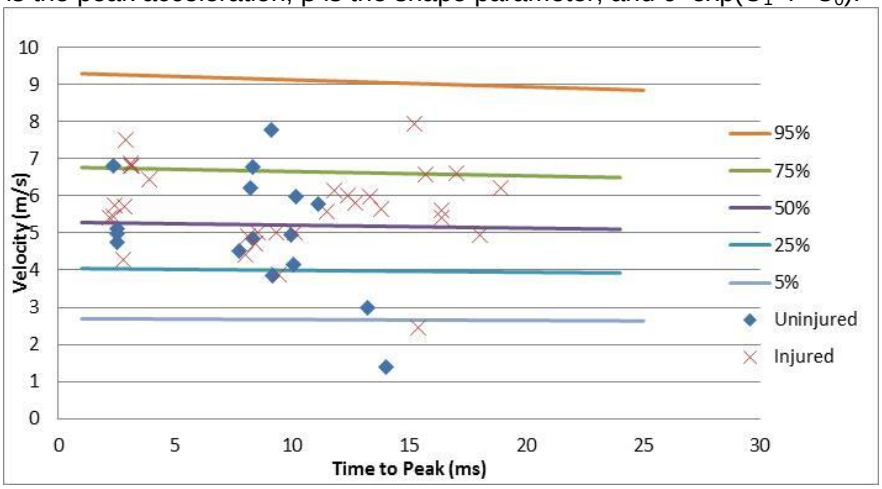

Figure 27. Velocity-based injury corridors developed from previous and current lower extremity research.

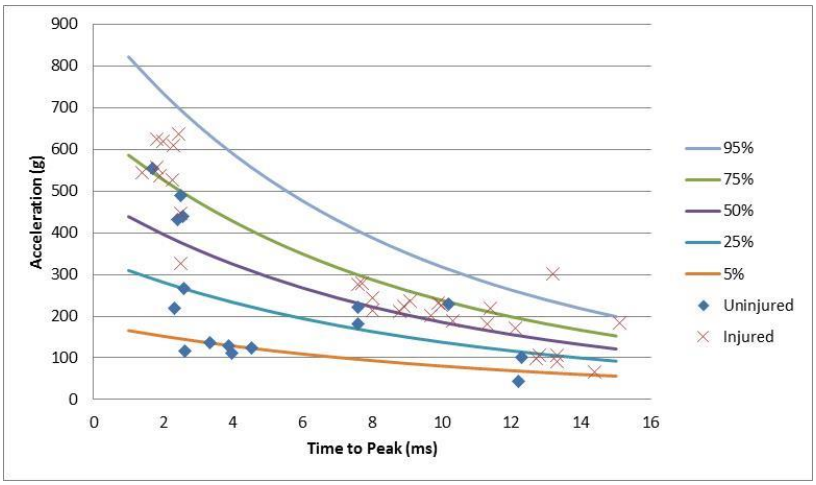

Figure 28. Acceleration-based injury corridors developed from previous and current lower extremity research.

Upon examining Figure 27 and Figure 28, a clearer separation of injury and non-injury seems to exist when using acceleration and time to peak to determine injury probabilities. For the velocity-based injury probability plot, there is significant amount of overlap between injured and non-injured data points. Thus, one should conclude that velocity and time to peak is an insufficient criteria for determining injury probability. While more data is required to draw statistically significant conclusions from this analysis (particularly non-injury data and data between 5 and 8 ms time to peak acceleration), acceleration seems like a more sound injury criteria basis.

ATD Response and Sensitivity to Acceleration and Velocity

Numerous studies have shown the inaccuracies associated with using the Hybrid-III under high rate loading conditions [9[11[27[25]. However, most of the data that exists for determining the response of the lower extremities to UBB loading condition was generated with the Hybrid-III. Figure 29 through Figure 31 show the response of the Hybrid-III and Mil-Lx legs to axial impacts with boots. These plots seem to suggest that the plate impact velocity is a better predictor of force in the lower extremity. However, one must be careful when making assumptions about the boundary conditions of booted tests. While the plate acceleration was used to generate these plots, the actual acceleration that the lower extremity responds too could be much different depending on the material properties and the rate dependency of the boot material. Thus more information is needed to determine the usefulness of these plots.

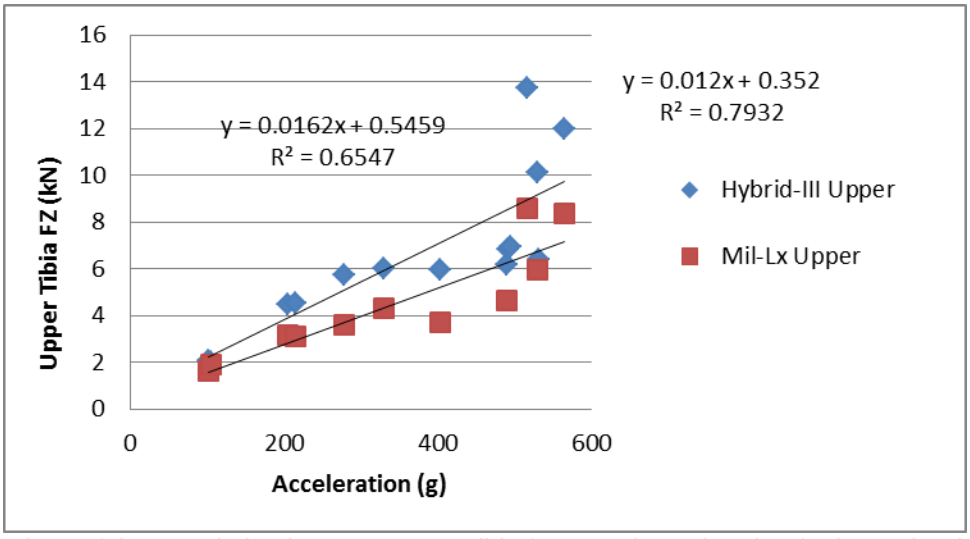

Figure 29. Comparison of the correlation between upper tibia force and acceleration for booted Hybrid-III and MIL-Lx legs.

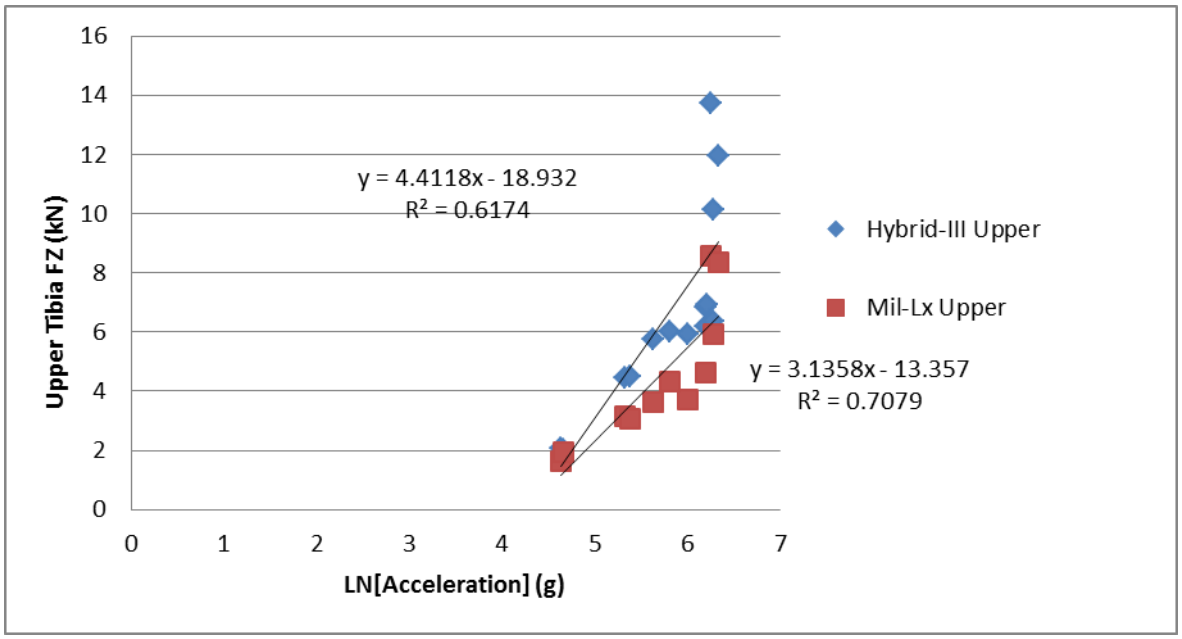

Figure 30. Comparison of the correlation between upper tibia force and the natural log of acceleration for booted Hybrid-III and Mil-Lx legs.

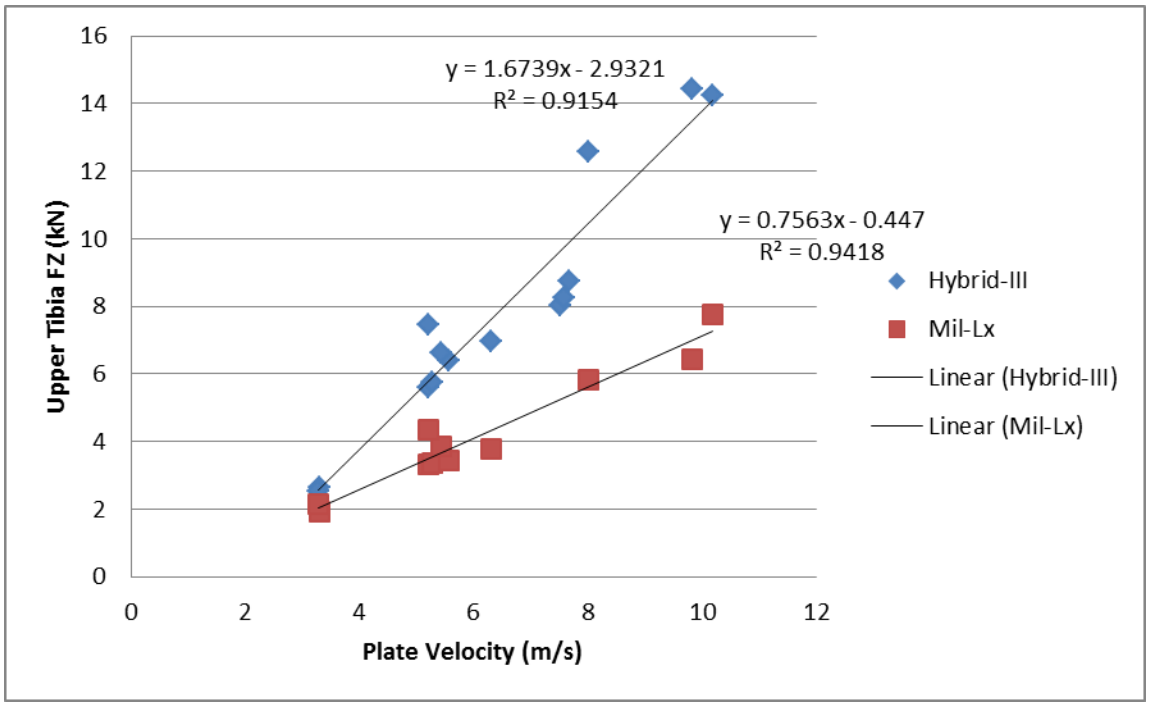

Figure 31. Comparison of the correlation between upper tibia force and plate velocity for Hybrid-III and Mil-Lx legs.

Future Work

While some conclusions may be drawn from this analysis of previous and current experimental data, a better understanding of how the Hybrid-III and other ATD legs respond to different boundary conditions such as acceleration, velocity, and even the mass of the impactor. Furthermore, for this data to be useful, one must also understand the effect of the boot on the ATD and how that differs from how it affects the PMHS. In order to answer some of the outlying questions, a series of drop-tower tests with the Hybrid-III and Mil-Lx legs will be performed, varying the acceleration, hammer velocity, hammer mass, effective mass, platen stroke, and booted/unbooted conditions. Instrumentation will include upper and lower tibia load cells, mid-tibia accelerometers, an in-boot accelerometer, an impact plate accelerometer, and an effective mass accelerometer. Contact between the foot and boot sole, as well as the contact with the platen will be monitored using contact strips. Data from these tests will bring clarity to the understanding of previous work and enable a more-accurate assessment and comparison of existing and future data.

Table 8. Test Matrix for Upcoming Drop-tower Experimentation. Matrix will be performed with both the Hybrid-III and Mil-Lx

Test	Apparel	Acceleration Pulse	Hammer Weight	Stroke (inches)

Condition				
1	Unbooted	200g	Light Hammer	1
2	Unbooted	600g	Light Hammer	1
3	Unbooted	200g	Light Hammer	1
4	Unbooted	600g	Light Hammer	1
5	Unbooted	200g	Heavy Hammer	1
6	Unbooted	600g	Heavy Hammer	1
7	Unbooted	200g	Heavy Hammer	1
8	Unbooted	600g	Heavy Hammer	1
9	Booted	200g	Heavy Hammer	3
10	Booted	600g	Heavy Hammer	3
11	Booted	200g	Heavy Hammer	3
12	Booted	600g	Heavy Hammer	3
13	Booted	200g	Light Hammer	3
14	Booted	600g	Light Hammer	3
15	Booted	200g	Light Hammer	3
16	Booted	600g	Light Hammer	3

References

[1] Otte D, von Rheinbaben H, Zwiipp H, Biomechanics of injuries to the foot and ankle joint of car drivers and improvements for an optimal car floor development, Proceedings of the *Stapp Car Crash Conference,* 922514, 1992.

[2] Crandall et al., The influence of footwell intrusion on lower extremity response and injury in frontal crashes, *Annual Proceedings of the Association for the Advancement of Automotive* Medicine, 39:269-286, 1995.

[3] Kruger H, Heuser G, Kraemer B, Schmitz A, Foot loads and footwell intrusion in an offset frontal crash, *Proceedings of the 14th International Technical Conference on Enhanced Safety of* Vehicles, 94-S4-O-03, 1995.

[4] Crandall J, Kuppa S, Klopp G, Hall G, Pilkey W, Hurwitz S, Injury mechanics and criteria for the human foot and ankle under axial impacts to the foot, *International Journal of Crashworthiness*, 3(2):147-162, 1998.

[5] Yoganandan N, Pintar F, Kumaresan S, Boynton M, Axial impact biomechanics of the human foot-ankle complex, *Journal of Biomechanical Engineering*, 119(4):433-437, 1997.

[6] Funk J, Crandall J, Tourret L, MacMahon C, Bass C, Khaewpong K, Eppinger R, The axial injury tolerance of the human foot/ankle complex and the effect of Achilles tension, *Journal of Biomechanical Engineering*, 124:750-757, 2002.

[7] Wang, J, Bird, R, Swinton, B, Krstic, A, Protection of Lower Limbs Against Floor Impact in Army Vehicles Experiencing Landmine Explosion, *Journal of Battlefield Technology*, 4, 3, 2001.

[8] Ramasamy, A, Hill, A, Masouros, S, Gibb, J, Bull, A, & Clasper, J, Blast-reated Fracture Patterns: A Forensic Biomechanical Approach, *Journal of the Royal Society, 8*, pages 689-698, 2010.

[9] McKay, B, Development of Lower Extremity Injury Criteria and Biomechanical Surrogate to Evaluate Military Vehicle Occupant Injury During an Explosive Blast Event, Wayne State University Dissertation, 2010.

[10] Schueler, F, Mattern, R, Zeidler, F, Scheunert, D, Injuries of the Lower Legs—Foot, Ankle Joint, Tibia; Mechanisms, Tolerance Limits, Injury-Criteria Evaluation of a Recent Biomechanics Experiment-Series. *Proceedings of IRCOBI Conference*, Brunnen, Switzerland, pages 33-45, 1995.

[11] McKay, B, Bir, C, Lower Extremity Injury Criteria for Evaluating Military Vehicle Occupant Injury in Underbelly Blast Events. *Stapp Car Crash Journal*, 53, pages 229-249, 2009.

[12] Yoganandan, N, Pintar, F, Boynton, M, Begeman, P, Prasad, P, Kuppa, S, Dynamic Axial Tolerance of the Human Foot-Ankle Complex, *Proceedings of the 40th Stapp Car Crash* Conference, Albuquerque, New Mexico, pages 207-218, 1996.

[13] Kitagawa, Y, Ichikawa, H, Pal, C, Lower Leg Injuries Caused by Dynamic Axial Loading and Muscle Tensing, *Proceedings of the 16th International Technical Conference on the Enhanced Safety of* Vehicles, Windsor, Ontario, Canada, 1998.

[14] Quenneville, C, Fraser, G, Dunning, C, Development of an Apparatus to Produce Fractures from Short-Duration High-Impulse Loading with an Application in the Lower Leg, *Journal of Biomechanical* Engineering, 132, 1, 2010.

[15] Bass, C, Folk, B, Salzar, R, Davis, M, Harris, R, Rountree, M, Sanderson, E, Development of a Test Methodology to Evaluate Mine Protective Footwear, University of Virginia, Charlottesville, 2004.

[16] Pattimore, D, Ward, E, Thomas, P, Bradford, M, The Nature and Cause of Lower Limb Injuries in Car Crashes, *Stapp Car Crash Conference Proceedings,* Paper No. 912901, 1991.

[17] Dischinger, P, Cushing, B, Kerns, T, Injury Patterns Associated with Direction of Impact: Drivers Admitted to Trauma Centers, *Journal of Trauma*, 35, 3, pages 454-458, 1993.

[18] Siegel, J, et al, Safety Belt Restraints and Compartment Intrusions in Frontal and Lateral Motor Vehicle Crashes: Mechanisms of Injuries, Complications, and Acute Care Costs, *Journal of Trauma*, 34, 5, pages 736-758, 1993.

[19] Organization World Health. *WHO Scientific Group on the Prevention and Management of Osteoporosis*, Geneva: WHO Press, 2000.
[20] Eppinger, R, Marcus, J, Morgan, R, Development of Dummy and Injury Index for NHTSA's Thoracic Side Impact Protection Research Program, Warrendale, Pennsylvania: Society of Automotive Engineers, 1984.
[21] Funk, J, Crandall, J, Calculation of Tibial Loading using Strain Gages, Rocky Mountain Bioengineering Symposium and International ISA Biomedical Sciences Instrumentation Symposium, Terre Haute, Indiana, 2006.
[22] McElhaney, J.H., Dynamic Response of Bone and Muscle Tissue, *Journal of Applied Physiology*, 21, 4, pages 1231-1236, 1966.
[23] Untaroiu, C, Kerrigan, J, Kam, C, Crandall, J, Correlation of Strain and Loads Measured in the Long Bones with Observed Kinematics of the Lower Limb during Vehicle-Pedestrian Impacts, *Stapp Car Crash Journal*, 51, pages 433-467, 2007.
[24] Bir, C, Barbir, A, Dosquet, F, Wilhelm, M, van der Horst, M, Wolfe, G, Validation of Lower Limb Surrogates as Injury Assessment Tools in Floor Impacts Due to Anti-Vehicular Land Mines, *Military Medicine*, 173, 12, pages 1180-1184, 2008.
[25] Pandelani, T, Reinecke, D, Philippens, M, Dosquet, F, Beetge, F, The Practical Evaluation of the Mil-Lx Lower Leg when Subjected to Simulated Vehicle Under Belly Blast Load Conditions, 2010.
[26] Kargus, R, Li, T, Frydman, A, Nesta, J, Methodology for Establishing the Mine/IED Resistance Capacity of Vehicle Seats for Crew Protection, Army Research Lab Adelphi MD, 2008.
[27] Newell, N, Masouros, S, Ramasamy, A, Bonner, T, Hill, A, Clasper, J, Bull, A, Use of Cadavers and Anthropometric Test Devices (ATDs) for Assessing Lower Limb Injury Outcome from Under-Vehicle Explosions, Proceedings of the International Research Council on Biomechanics of Injury, Dublin, Ireland, 2012.
[28] Masouros, S, Newell, N, Bonner, T, Ramasamy, A, Hill, A, West, A, Clasper, J, Bull, A, A Standing Vehicle Occupant is Likely to Sustain a More Severe Injury than One who has Flexed Knees in an Under-Vehicle Explosion: A Cadaveric Study, Proceedings of the International Research Council on Biomechanics of Injury, Dublin, Ireland, 2012.
[29] Henderson, K, Bailey, A, Christopher, J, Brozoski, F, Salzar, R, Biomechanical Response of the Lower Leg under High Rate Loading, Proceedings of the International Research Council on Biomechanics of Injury, Gothenburg, Sweeden, 2013.
[30] Bass, C, Panzer, M, Folk, B, Salzar, R, Funk, J, Harris, R, A new injury criterion for lower extremity injury in mine protective footwear, Journal of Trauma, 2012.
[31] Kuppa, S, Wang, J, Haffner, M, Eppinger, R, Lower Extremity Injuries and Associated Injury Criteria, National Highway Traffic and Safety Administration Paper No. 457, 2007.

5. Purchases

- 16-inch image intensifier high-speed x-ray system
- 94 channel DTS Slice-Pro data acquisition system
- Mindways QCT bone mineral density evaluation software system
- Twelve (12) whole body DoD-approved PMHS
- Ten (10) component DoD-approved pelvi

6. Key Research Accomplishments

- Validation of whole body blast rig design demonstrating our capability to induce theater-level injuries in a secure laboratory environment.
- First instrumented Hybrid-III tests with and without Mil-LX for comparison of ODYSSEY with Live-Fire and GenHull2 results.
- Completion of all cadaveric testing approvals (HRPO).
- Validated lower extremity finite element model capable of predicting injury at UBB load rates.
  Paper and presentation to the Society of Experimental Mechanics (SEM) XII International Congress & Exposition on Experimental & Applied Mechanics: Bailey, AM, Boruah, S, Christopher, JJ, Bennett, BC, Shafieian M, Cronin, DS, Salzar, RS (2012) "Injury Potential of Shock Induced Compressive Waves on Human Bone" 2012 SEM International Congress, Costa Mesa, CA.
- Panzer MB, Henderson K, Salzar RS, Crandall JR (2013) FE Modeling of Lower Extremity Fractures in Occupants Subject to Under-Vehicle Blasts. US National Congress for Computational Mechanics, Raleigh, NC.

-

7. Reportable Outcomes

- A robust, repeatable blast simulator capable of accelerations up to 1800g in less than 1.5 ms is possible for laboratory simulation of underbody blast.
- Preliminary Hybrid-III tests for comparison with previous live-fire and other tests for cross-platform comparison.
- Design of test fixtures with well-characterized boundary conditions for the development of injury thresholds and biofidelity response curves of studied body components.

8. Conclusion

Though only in the first 17 months of this 4.5 year contract, all preliminary steps have been completed allowing the forward progress of this research to begin upon acceptance of the individual task's test protocols. The design of all required test fixtures for each task has been completed and construction started, as has the search for all appropriate PMHS specimens from Army-approved sources.

Appendix 1. Principal Investigator CV

Robert S. Salzar
Curriculum Vitae

Center for Applied Biomechanics
University of Virginia
4040 Lewis and Clark Drive
Charlottesville, Virginia 22911
(434) 296-7288 ext. 135
(434) 296-3453 (fax)
salzar@virginia.edu
www.uva-cab.org

Education

Doctor of Philosophy, Civil Engineering /Applied Mechanics
University of Virginia, 1994
Dissertation - *Optimization of Layered Metal Matrix Composite Cylinders*

Master of Science, Applied Mechanics
University of Virginia, 1990
Thesis - *Stress Concentrations in the Carotid Artery Bifurcation by the Finite Element Method*

Bachelor of Science, Civil Engineering
San Diego State University - Cum Laude, 1986

Work Experience

University of Virginia Center for Applied Biomechanics 2001-Present
Principal Research Scientist, Principal Investigator
Assistant Professor of Emergency Medicine
Responsibilities include all aspects of project management for the Center, including developing proposals, budget projection and management, team coordination, and final reporting. Design and perform shock and ballistic tests on cadaveric specimens, live animal models, and human surrogates. Projects include blast-wave induced brain and thoracic injury detection and prevention, investigating behind armor blunt trauma, brain injury from non-lethal projectiles, developing spinal injury models for impacts, injury mitigation of repeated high frequency shock loadings, and developing injury criteria for orbital fracture. Extensive experience with shock rated instrumentation and high-speed data acquisition, sonomicrometry, and high speed video analysis. Supervision of numerous graduate and undergraduate theses. Coordination of all aspects of biological material handling (BSL-II), including acquisition, storage, testing, and final disposition.

City College of New York, Department of Civil Engineering 1996-2001
Assistant Professor
Director and developer of the Civil Engineering Department network computer lab. Supervisor of lab technician and manager of daily operations. Faculty advisor of ASCE. Liaison to New York Association of Consulting Engineers. Liaison to MOLES. Executive board member of the Biomechanical Engineering Program. Steel Bridge Club Advisor. Organizer of New York City-wide Civil Engineering Career Fair with cooperation with the Met-section ASCE-YMF. Board member of NASA in New York Day Planning Committee.

Comptek Structural Composites, Inc 2001
Engineering Associate

Developed solutions to strengthening problems in buildings, old and new, using fiber reinforced plastics. Developed tools for analysis as well as design criteria for broad introduction of these materials into common use.

Naval Air Warfare Center, Aircraft Division — Summer 1998
U.S. Navy Summer Faculty Researcher
Performed metallurgical analyses on inter-metallic composites. Investigated failures on F/A-18E and V-22 tactical aircraft.

National Research Council, NASA-Lewis Research Center — 1995-1996
NRC Resident Research Associate
Post-doctoral studies that included research on inter-metallic composites for aerospace applications, and software development.

University of Virginia, Department of Civil Engineering — 1994-1995
Research Associate
Principal scientist in developing an algorithm for the optimization of residual stresses in metal matrix composites using the multiple compliant interfacial layer concept for NASA-Lewis Research Center. Supervised two University undergraduate students in research.

University of Virginia, Department of Civil Engineering — Fall 1993
Instructor
Lectured, developed assignments and exams for Engineering Mechanics

University of Virginia, Department of Civil Engineering — 1990-1993
Research Assistant
Developed the OPTCOMP computer software package for the reduction of residual stresses in metal matrix composites through the optimization of interfacial layer properties for NASA-Lewis Research Center. Extended solution procedure to include arbitrarily laminated composite tubes.

University of Virginia, Department of Civil Engineering — 1988-1990
Teaching Assistant
Assisted in the teaching of Engineering Graphics, FORTRAN, CAD, Advanced Strength of Materials, Structural Stability, and Pre-stressed Concrete Design. Also assisted in the grading of student assignments including exams.

Testing Engineers of San Diego — 1987-1988
Special Investigations Engineer
Developed and applied forensic test methodologies pertaining to a variety of construction related problems.

Academic / Professional Honors

- Reviewer for:
  - Journal of Critical Technologies in Shock and Vibration
  - Journal of Neurotrauma
  - International Journal of Solids and Structures
  - Composites Part B, Engineering
  - Composites Science and Technology
  - Journal of Biomechanics
  - Society of Automobile Engineering Journal
  - Traffic Injury Prevention
  - Aviation, Space, and Environmental Medicine
  - Experimental Mechanics
- Member of CISIT Scientific International Committee review board, 2009-present
- U.S. Navy Summer Faculty Research Program, 1998
- Biomedical Research cited in Sigma Xi's American Scientist Magazine, 1997
- NRC Research Associate Fellowship, NASA-Lewis Research Center, 1995-1996

- Contributor to The Fatal Cruise of the Argus, Naval Institute Press, 1996
- Dean's Fellow, University of Virginia, 1988-1992
- Outstanding Graduate in Civil Engineering, San Diego State University, 1987
- Certified Engineer in Training (EIT), California, 1986

Associations/Registrations

- Orthopaedic Trauma Association
- Association for the Advancement of Automotive Medicine (AAAM)
- American Society of Civil Engineers
- American Society of Mechanical Engineers
- Sigma Xi, The Society for Scientific Research
- Chi Epsilon, The National Civil Engineering Honor Society

Publications

A. Refereed Journal Publications

A1. Rooks T, Brozoski F, Pintar F, Salzar R, Bass C, Schmidt A, Chancey C (2013) Development of Injury Risk Curves and Associated Injury Assessment Risk Curves for Pelvic Fracture in Vertical Loading Environments. Stapp Car Crash Journal (under review).

A2. Salzar, RS, Lau,S, Lessley, D, Sochor, M, Shaw, C, Kent, R, Crandall, R (2012) Thoracic Response to Shoulder-Belt Loading: Comparison of Table-Top and frontal Sled Tests with PMHS. Traffic Injury Prevention, 14:2, 159-167.

A3. Rafaels KA, Bass CR, Panzer MB, Salzar RS, Woods WA, Feldman SH, Walilko T, Kent RW, Capehart BP, Foster JB, Derkunt B, Toman A (2012) Brain injury risk from primary blast. J Trauma Acute Care Surg, 73(4):895-901.

A4. Kent, R, Lopez-Valdes, F, Lamp, J, Lau, S, Parent, D, Kerrigan, J, Lessley, D, Salzar, R, Sochor, M, Bass, C, Maltese, M (2012) Biomechanical response targets for physical and computational models of the pediatric trunk. Traffic Injury Prevention (Mar 30 Epub ahead of print).

A5. Bass, CR, Peterson, R, Ziemba, AAE, Salzar, RS, Lucas, S, Pierce, E, Schmidt, A (2012) Human Measurements and Injury Specification Strategy for Repeated Impacts in High Speed Planing Boats. (Submitted to Journal of Ship Design).

A6. Bass, CR, Panzer, MB, Folk, JB, Salzar, RS, Funk, JR, Harris, RM, Rountree, MS, Waclawik, S (2012) A New Injury Criterion for Lower Extremity Injury in Mine Protective Footwear. (submitted to Journal of Trauma).

A7. Palm, EJ, Bass, CR, Panzer, MB, Shridnarani, J, Salzar, RS, Rafaels, KA, Walilko, T, Weiss, G, Perritt C, Haynes, N, Masters, K. (2012) Submitted to Journal of Occupational and Environmental Medicine.

A8. Christopher, J.J., Sochor, M.R., Pellettiere, J.A., Salzar, R.S. (2012) Assessment of Ear- and Tooth-Mounted Accelerometers as Representative of Human Head Response, Submitted to SAE International Motorsports.

A9. Salzar, RS, Lievers, WB, Frimenko, RE, Seamon, J, Keller, T, Subit, DL, Gochenour, TH, Sochor, M, Crandall, JR (2011) Fracture Tolerance of the Patellofemoral Joint in Frontal Knee Impacts of 75 and 35 Year Old Males. International Journal of Crashworthiness, 16:4: 397-409.

A10. Rafaels, KA, Bass, CR, Salzar, RS, Panzer, M, Woods, W, Feldman, S, Cummings, TJ, Capehart, B. (2011) Survival Risk Assessment for Primary Blast Exposures to the Head. Journal of Neurotrauma, 28(11):2319-28.

A11. Lamp, JF, Salzar, R, Kerrigan, J, Parent, D, Lopez-Valdez, F, Lau, S, Lessley, D, Kent, R, Luck, J, Loyd, A, Bass, C. (2010) Expansion and Evaluation of Data Characterizing the Structural Behavior of the Pediatric Abdomen. Ann Adv Automot Med. 2010; 54:89-96.

A12. Bass, CR, Salzar, RS, Lucas, SR, Rafaels, KA, Damon, AM, Crandall, JR. (2010) Re-evaluating the neck injury index (NII) using experimental PMHS tests. Traffic Injury Prevention, 11(2): 194-201.

A13. Bass, CR, Meyerhoff, K, Damon, AM, Bellizzi, AM, Salzar, RS, Rafaels, KA (2010) Drosophila Melanogaster Larvae as a Model for Blast Lung Injury. Journal of Trauma, 69(1):179-84.

A14. Damon, AM, Lessley, DJ, Salzar, RS, Bass, CR, Shen, F, Paskoff, G, Shender, B. (2010) Kinematic Response of the Spine During Simulated Aircraft Ejections. Aviation, Space, and Environmental Medicine, 81(5): 453-459.

A15. Lessley, DJ, Salzar, RS, Crandall, JR, Kent, RW, Bolton, JR, Bass, CR, Guillemot, H, Forman, JL. (2010) Kinematics of the thorax under dynamic belt loading conditions. International Journal of Crashworthiness, 15(2):175-190.

A16. Rafaels, KA, Bass. CR, Panzer, MB, Salzar, RS. (2010) Pulmonary Injury Risk Assessment for Long-Duration Blasts: A Meta-Analysis. Journal of Trauma, 69(2):368-374.

A17. Salzar, RS, Ash, JH, Lucas, SR, Planchak, C, Dalton, A, Emond, B, Getz, JE. (2010) Forensic Analysis and Injury Prediction in Small Craft Collisions. Journal of Ship Production and Design, 26(2): 1-9.

A18. Kent, RW, Salzar, RS, Kerrigan, JR, Parent, DP, Lessley, DJ, Sochor, M, Luck, JF, Loyd, A, Song, Y, Nightingale, R, Bass, CR, Maltese, MR. (2009) Pediatric Thoracoabdominal Biomechanics. Stapp Car Crash Journal, 53: 373-401.

A19. Kent, RW, Woods, WA, Salzar, RS, Damon, AM, Bass, CR. (2009) The transient relationship between pressure and volume in the pediatric pulmonary system. Journal of Biomechanics, 42(11): 1656-63.

A20. Lucas, SR, Bass, CR, Crandall, JR, Kent, RW, Shen, FH, Salzar, RS, (2009) Viscoelastic and failure properties of spine ligament collagen fascicles. Biomechanics and Modeling in Mechanobiology, 8(6): 487-498.

A21. Salzar, RS, Genovese, D, Bass, CR, Bolton, JR, Guillemot, H, Damon, AM, Crandall, JR. (2009) Load path distribution within the pelvic structure under lateral loading. International Journal of Crashworthiness, 14(1): 99-110.

A22. Salzar, RS, Bass, CR, Lessley, DJ, Crandall, JR, Kent, RW, Bolton, JR. (2009) Viscoelastic response of the thorax under dynamic belt loading. Traffic Injury Prevention, 10(3): 290-296.

A23. Salzar, RS, Bolton, JR, Crandall, JR. (2009) Ejection Injury to the Spine in Small Aviators: Sled Tests of Manikins vs. Postmortem Specimens. Aviation, Space, and Environmental Medicine, 80(7): 621-628.

A24. Bass, CR, Rafaels, KA, Salzar, RS, Carboni, M, Kent, RW, Lloyd, MD, Lucas, SR, Meyerhoff, K, Planchak, C, Damon, AM, Bass, GT. (2008) Thoracic and lumbar spinal impact tolerance. Accident Analysis and Prevention, 40(2): 487-495.

A25. Bass, CR, Rafaels, KA, Salzar, RS. (2008) Pulmonary injury risk assessment for short duration blasts. Journal of Trauma, 65(3): 604-15.

A26. Lucas, SR, Bass, CR, Salzar, RS, Oyen, ML, Planchak, MS, Ziemba, MS, Shender, BS, Paskoff, G. (2008) Viscoelastic properties of the cervical spine under fast strain rate deformations. Acta Biomaterialia, 4: 117-125.

A27. Salzar, RS, Bass, CR, Pellettiere, J. (2008) Improving Earpiece Accelerometer Coupling to the Head. SAE Transactions: Journal of Passenger Cars-Mechanical Systems, 1367-1381. Based on SAE Paper 2008-01-2978.

A28. Bass, CR, Lucas, SR, Salzar, RS, Oyen, M, Planchak, C, Shender, B, Paskoff, G. (2007) Failure Properties of Cervical Spinal Ligaments Under Fast Strain Rate Deformations. Spine, 32(1): E7-E13.

A29. Bass, CR, Planchak, CJ, Salzar, RS, Lucas, SR, Rafaels, KA, Shender, BS, Paskoff, G. (2007) The temperature-dependent viscoelasticity of porcine lumbar spine ligaments. Spine, 32(16): E436-442.

A30. Bass, CR, Salzar, RS, Lucas, SR, Davis, M, Donnellan, L, Folk, B, Sanderson, E, Waclawik, S. (2006) Injury Risk in Behind Armor Blunt Thoracic Trauma. International Journal of Occupational Safety and Ergonomics, (12)4: 429-442.

A31. Kent, RW, Bass, CR, Woods, WA, Salzar, RS, Lee, SH, Melvin, J. (2006) The role of muscle tensing on the force-deflection response of the thorax and a reassessment of frontal impact thoracic biofidelity corridors. Journal of Automobile Engineering. Proceedings of the Institution of Mechanical Engineers, 220(D7): 853-868.

A32. Lucas, SR, Bass, CR, Planchak, CJ, Salzar, RS, Shender, BS, Paskoff, G. (2006) Temperature and age effects on high rate viscoelasticity of cervical spinal components. Proceedings of the 5th World Congress of Biomechanics, Munich, Germany, abstract in J. Biomech. 39(1): S151.

A33. Salzar, RS, Bass, CR, Kent, RW, Millington, S, Davis, M, Lucas, S, Rudd, RW, Folk, B, Donnellan, L, Murakami, D, Kobayashi, S. (2006) Development of injury criteria for pelvic fracture in frontal crashes. Traffic Injury Prevention, 7(3):299-305.

A34. Kent, RW, Bass, CR, Woods, WA, Sherwood, CP, Madeley, NJ, Salzar, RS, Kitagawa, Y. (2003) Muscle tetanus and loading condition effects on the elastic and viscous characteristics of the thorax. Traffic Injury Prevention, 4(4): 297-314.

A35. Salzar, RS. (1999) Influence of Autofrettage on Metal Matrix Composite Reinforced Armaments. Composites Part B: Engineering Journal, 30(8): 841-847.

A36. Salzar, RS. (1999) Design Considerations for Rotating Laminated Metal Matrix Composite Shafts. Composites Science and Technology, 59(6): 883-897.

A37. Salzar, RS. (1998) Optimization of Material Processing Profiles. Composites Part B: Engineering Journal. 29B: 235-244.

A38. Salzar, RS, Pindera, M, Barton, F. (1996) Elastic-Plastic Analysis of Layered Metal Matrix Composite Cylinders, Part I. Journal of Pressure Vessel Technology, 118: 13-20.

A39. Salzar, RS, Pindera, M, Barton, F. (1996) Elastic-Plastic Analysis of Layered Metal Matrix Composite Cylinders, Part II. Journal of Pressure Vessel Technology, 118: 21-26.

A40. Salzar, RS, Thubrikar, MJ, Eppink, RT. (1995) Pressure-induced mechanical stress in the carotid artery bifurcation: a possible correlation to atherosclerosis. Journal of Biomechanics, 28(11): 1333-1340.

A41. Salzar, RS. (1995) Functionally Graded Metal Matrix Composite Tubes. Composites Engineering, 5: 851.

A42. Salzar, RS. (1995) Functionally Graded Metal-Matrix Composite Tubes. Composites Engineering, 5(7): 891-900.

A43. Salzar, RS, Barton, FW. (1994) Residual-Stress Optimization in Metal-Matrix Composites Using Discretely Graded Interfaces. Composites Engineering, 4(1): 115-128.

A44. Pindera, M, Salzar, RS, Williams, T. (1993) An Evaluation of a New Approach for the Thermoplastic Response of Metal Matrix Composites. Composites Engineering, 3: 1185.

A45. Salzar, RS, Thubrikar, M, Eppink, R. (1993) Pressure Induced Wall Stress and Atherosclerosis in the Carotid Artery Bifurcation (abstract). Annals of Biomedical Engineering, 21.

A46. Salzar, RS, Thubrikar, M, Williams, T. (1993) Pressure induced Wall Stress and Atherosclerosis in the Carotid Artery Bifurcation. Annals of Biomedical Engineering, 21.

A47. Salzar, RS, Thubrikar, M, Eppink, R. (1991) Pressure-Induced Mechanical Stress and Atherosclerosis in the Carotid Bifurcation. Annals of Biomedical Engineering, 19: 587.

A48. Thubrikar, MJ, Salzar, RS, Eppink, RT. (1990) Correlation between intramural stress and atherosclerotic lesions in human carotid-artery bifurcation. Arteriosclerosis, 10: 5, A821-A821.

B. Conference Publications and Abstracts

B1. Panzer MB, Henderson K, Salzar RS, Crandall JR (2013) FE Modeling of Lower Extremity Fractures in Occupants Subject to Under-Vehicle Blasts. US National Congress for Computational Mechanics, Raleigh, NC.

B2. Subit D, Arregui C, Salzar R, Crandall J (2013) Pediatric, Adult and Elderly Bone Material Properties. IRCOBI Conference on the Biomechanics of Impact, Gothenburg, Sweden.

B3. Boruah S, Henderson K, Subit D, Salzar R, Shender B, Paskoff G (2013) Response of Human Skull Bone to Dynamic Compressive Loading. IRCOBI Conference on the Biomechanics of Impact, Gothenburg, Sweden.

B4. Gabler L, Stone J, Mourad P, Crandall J, Salzar R (2013) Region Specific Viscoelastic Properties of the Adult Rat Brain under Indentation following Traumatic Brain Injury. . IRCOBI Conference on the Biomechanics of Impact, Gothenburg, Sweden.

B5. Bailey A, Christopher J, Henderson K, Brozoski F, Salzar R (2013) Comparison of Hybrid-III and PMHS Response to Simulated Underbody Blast Loading Conditions. . IRCOBI Conference on the Biomechanics of Impact, Gothenburg, Sweden.

B6. Henderson K, Bailey A, Christopher J, Brozoski F, Salzar R (2013) Biomechanical Response of the Lower Leg under High Rate Loading. IRCOBI Conference on the Biomechanics of Impact, Gothenburg, Sweden.

B7. Ganpule S, Alai A, Salzar R, Chandra N (2013) Response of post-mortem human head under primary blast loading conditions – effect of blast overpressures. Proceedings of the American Society of Mechanical Engineers 2013 International Mechanical Engineering Congress & Exposition, San Diego.

B8. Forman J, del Pozo de Dios E, Symeonidis I, Duart J, Kerrigan J, Salzar R, Balasubramanian S, Segui-Gomez M, Kent R (2012) Fracture Tolerance Related to Skeletal Development and Aging Throughout Life: 3-point Bending of Human Femurs. IRCOBI Conference on the Biomechanics of Impact.

B9. Bailey AM, Boruah S, Christopher JJ, Shafieian M, Salzar RS, Cronin DS (2012) Finite Element Analysis of the Injury Potential of Shock-Induced Compressive Waves on Human Bone. Ohio State Injury Biomechanics Symposium.

B10. Boruah S, Subit D, Salzar RS (2012) Bone material properties of the adult human skull. 83rd Annual Scientific Meeting of the Aerospace Medical Association, Atlanta, GA.

B11. Christopher JJ, Salzar RS, Sochor M, Pellettiere J (2012) Assessment of Ear and Tooth Mounted Accelerometers as Representative of Human Head Response. Ohio State Injury Biomechanics Symposium.

B12. Gabler L, Crandall J, Salzar R, Shafieian M, Stone J (2012) Validation of spherical indentation methodology to characterize material properties of brain tissue. Ohio State Injury Biomechanics Symposium.

B13. Bailey, AM, Boruah, S, Christopher, JJ, Bennett, BC, Shafieian M, Cronin, DS, Salzar, RS (2012) "Injury Potential of Shock Induced Compressive Waves on Human Bone" 2012 SEM International Congress, Costa Mesa, CA.

B14. Christopher, J.J., Sochor, M.R., Pellettiere, J.A., Salzar, R.S.(2011) "Assessment of Ear- and Tooth-Mounted Accelerometers as Representative of Human Head Response," IMIS Conference, Indianapolis, IN.

B15. Rafaels, KA, Bass, CR, Panzer, MB, Salzar, RS, Woods, WA, Feldman, S, Walilko, T, Kent, RW, Capehart, BP, Shridharani, JK, Toman, A. (2011) Brain Injury Risk from Primary Blast. 2011 BMES Annual Meeting, Hartford, CT.

B16. Salzar, RS, Lessley, DJ, Sochor, M, Shaw, CG, Kent, RW, Crandall, JR. (2011) Thoracic Response to Shoulder Belt Loading: Comparison of Table-top and Frontal Sled Tests with PMHS. IRCOBI Conference on the Biomechanics of Impact.

B17. Palm, EJ, Bass, CR, Panzer, MB, Shridnarani, J, Salzar, RS, Rafaels, KA, Walilko, T, Weiss, G, Perritt C, Haynes, N, Masters, K. (2010) Test Methodology for the Assessment of Blast Trauma Behind Military Helmets. Presented at the Personal Armor Safety Symposium (PASS), Washington, DC.

B18. Lamp, J, Salzar, RS, Kerrigan, JR, Parent, DP, Lopez-Valdez, FJ, Lau, S, Lessley, DJ, Kent, RW, Luck, J, Loyd, A, Bass, CR, Zuby, D, Arbelaez, R. (2010) Expansion and Evaluation of Data Characterizing the Structural Behavior of the Pediatric Abdomen. Proceedings of the AAAM.

B19. Bass, CR, Rafaels, KA, Panzer, M, Wood, G, Shridharani, J, Palm, E, Capehart, B, Salzar, RS. (2010) Brain vs. Pulmonary Blast Injury Tolerance and the Effect of Blassitic Protective Vests. Meeting of the Department of Defense Explosives Safety Board.

B20. Lucas, SR, McGowan, JR, Salzar, RS, Planchak, C, Getz, JE. (2009) Biomechanical Assessment of Small Craft Collisions. 2010 Chesapeake Power Boat Symposium Proceedings, 2, Annapolis, MD.

B21. Panzer, M, Bass, CR, Salzar, RS, Pellettiere, J, Myers, B. (2009) Evalutation of Ear-Mounted Sensors for Determining Impact Head Acceleration. IRCOBI Conference on the Biomechanics of Impact.

B22. Rafaels, KA, Shridharani, J, Bass, CR, Salzar, RS, Walilko, TJ, Panzer, MB. (2010) Blast Wave Attenuation: Ballistic Protective Helmets and the Head. Presented at the Personal Armor Safety Symposium (PASS), Washington, DC.

B23. Lessley, DJ, Kent, RW, Crandall, JR, Salzar, RS, Shaw, CG. (2009) Internal vs. External Chest Deformation Response to Shoulder Belt Loading, Part 1: Table-Top Tests. Paper 2009-01-0393, Society of Automotive Engineers.

B24. Bass, CR, Damon, AM, Lucas, SR, Salzar, RS, Paskoff, G, Shender, BS. (2008) High Strain Rate Material Characterization of the Thoracic and Lumbar Spine. 79th Annual Scientific Meeting of the Aerospace Medical Association, Boston MA.

B25. Bass, CR, Salzar, RS, Ash, JH, Ziemba, A, Lucas, SR, Peterson, R, Pierce, E. (2008) Models for Assessing Spinal Dynamics and Injury from Repeated Impact in High Speed Planing Boats. Paper 2008-01-0782, Society of Automotive Engineers.

B26. Bass, CR, Crandall, JR, Salzar, RS, Rafaels, KA, Damon, AM, Lucas, SR. (2008) Assessing the Neck Injury Index (NII) Using Experimental Cadaver Tests. IRCOBI Conference on the Biomechanics of Impact.

B27. Lessley, DJ, Salzar, RS, Crandall, JR, Kent, RW, Bolton, JR, Bass, CR, Forman, JL. (2008) Kinematics of the Thorax under Dynamic Belt Loading Conditions. Proceedings of the International Crashworthiness Conference.

B28. Lucas, SR, Salzar, RS, Bass, CR. (2008) Viscoelastic Properties of Spine Ligament Collagen Fascicles. Proceedings of the ASME Summer Bioengineering Conference, Marco Island, Fl.

B29. Rafaels, K, Bass, CR, Salzar, RS. (2008) Pulmonary Injury Risk Assessment for Long Duration Blasts. PASS Conference, Brussels, Belgium.

B30. Salzar, RS, Bass, CR, Pellettiere, J. (2008) Improving Earpiece Accelerometer Coupling to the Head. Paper 2008-01-2978, Society of Automotive Engineers.

B31. Salzar, RS, Bass, CR, Lessley, DJ, Crandall, JR, Kent, RW, Bolton, JR. (2008) Viscoelastic Response of the Thorax under Dynamic Belt Loading. IRCOBI Conference on the Biomechanics of Impact.

B32. Salzar, RS, Genovese, D, Bass, CR, Bolton, JR, Guillemot, H, Damon, AM, Crandall, JR. (2008) Load path distribution within the pelvic structure under lateral loading. Proceedings of the International Crashworthiness Conference.

B33. Untaroiu, CD, Salzar, RS, Guillemot, H, Crandall, JR. (2008) Pelvic response under lateral impact loading: the force transmission path and the strain distribution of pubic rami. Southeastern Meeting of the American Society of Biomechanics.

B34. Untaroiu, CD, Salzar, RS, Guillemot, H, Crandall, JR. (2008) The Strain Distribution and Force Transmission Path through Pubic Rami during Lateral Pelvic Impacts. ASME International Mechanical Engineering Congress and RD&D Congress, IMECE2008-67791.

B35. Bass, CR, Salzar, RS, Ash, JH, Ziemba, A, Lucas, SR, Peterson, R, Pierce, E, Price, B. (2007) Dynamics models for the assessment of spinal injury from repeated impact in high speed planing boats. IRCOBI Conference on the Biomechanics of Impact.

B36. Bass, CR, Donnellan, L, Salzar, RS, Lucas, SR, Folk, B, Davis, M, Rafaels, KA, Planchak, C, Meyerhoff, K, Ziemba, A, Alem, N. (2006) A New Neck Injury Criterion in Combined Vertical/Frontal Crashes with Head Supported Mass. IRCOBI Conference on the Biomechanics of Impact.

B37. Bass, CR, Donnellan, L, Salzar, RS, Lucas, SR, Folk, B, Davis, M, Rafaels, KA, Planchak, C, Meyerhoff, K, Ziemba, A, Alem, N. (2006) Injuries in Cadaveric Tests Simulating Rotary Wing Aviators in Vertical/Frontal Crashes with Head Mounted Mass, Aerospace Medical Association Conference. Orlando, FL.

B38. Bass, CR, Rafaels, KA, Salzar, RS, Meyerhoff, K, Planchak, C, Stringer, B, Goyne, C, Waclawik, S. (2006) Developing a Test Methodology for Assessing Nonpenetrating Blast Trauma in Explosive Ordnance Disposal (EOD) Suits. Proceedings of the Eighth Biennial International Symposia on Personal Armour Systems, Sept 18-22, Leeds, UK, p. 199-208.

B39. Bass, CR, Rafaels, KA, Salzar, RS. (2006) A New Injury Criteria for Blast. Personal Armour Systems Symposium (PASS), Leeds, UK.

B40. Bass, CR, Ziemba, A, Lucas, SR, Salzar, RS. (2006) Evaluation of Criteria for Assessing Risk of Impact Injury in High Speed Craft. ABCD Symposium on Human Performance. Panama City, FL.

B41. Bass, CR, Rafaels, KA, Salzar, RS. (2006) Pulmonary injury risk assessment for short-duration blasts. Proceedings of the Eighth Biennial International Symposia on Personal Armour Systems, Sept 18-22, Leeds, UK, p. 233-248.

B42. Lucas, SR, Bass, CR, Salzar, RS, Planchak, C, Ziemba, A, Shender, BS, Paskoff, G. (2006) Age-Dependent Material Properties of Soft Tissues in the Spine. Aerospace Medical Association Conference. Orlando, FL.

B43. Lucas, SR, Bass, CR, Salzar, RS, Shender, B, Paskoff, G. (2006) High Rate Viscoelastic Properties of Human Cervical Spinal Intervertebral Discs. American Society of Biomechanics Annual Meeting. Blacksburg, VA.

B44. Bass, CR, Donnellan, L, Salzar, RS, Lucas, SR, Folk, B, Davis, M, Rafaels, KA, Planchak, C, Meyerhoff, K, Ziemba, A, Alem, N, Crowley, J. (2005) A New Neck Injury Criterion for Rotary Wing Aviators in Vertical/Frontal Crashes with Head Mounted Mass, Aerospace Medical Association Conference. Kansas City, MO.

B45. Bass, CR, Salzar, RS, Ziemba, A, Lucas, SR, Peterson, R, Price, B, Labreque, J. (2005) Evaluation of Injury Criteria for High Speed Planing Craft. SAVAIC Conference. New Orleans, LA.

B46. Bass, CR, Salzar, RS, Ziemba, A, Lucas, SR, Peterson, R, Price, B, Labreque, J. (2005) Injury Specification Strategy for Occupants in High-Speed Planing Craft. SAVIAC Conference. New Orleans, LA.

B47. Bass, CR, Salzar, RS, Ziemba, A, Lucas, SR, Peterson, R. (2005) The modeling and measurement of humans in high speed planing boats under repeated vertical impacts. IRCOBI Conference on the Biomechanics of Impact.

B48. Lucas, SR, Bass, CR, Salzar, RS, Folk, J, Donnellan, L, Paskoff, G, Shender, B. (2005) Material Properties and Failure Characteristics of Cervical Spinal Ligaments under High-Rate Loading. Aerospace Medical Association Conference. Kansas City, MO.

B49. Lucas, SR, Bass, CR, Salzar, RS, Planchak, C, Ziemba, A, Shender, B, Paskoff, G. (2005) Failure Properties of Cervical Spinal Ligaments under High-Rate Loading. American Society of Biomechanics / International Society of Biomechanics Conference. Cleveland, OH.

B50. Bass, CR, Folk, B, Salzar, RS, Davis, M, Donnellan, L, Harris, R, Rountree, M, Gardner, M, Harcke, T, Rouse, E, Oliver, W, Sanderson, E, Waclawik, S, Holthe, M, Hauck, B. (2004) Development of a Test Methodology To Evaluate Mine Protective Footwear. Personal Armor Systems Symposium (PASS) The Hague, NL.

B51. Bass, CR, Kent, RW, Salzar, RS, Millington, SA, Davis, M, Folk, B, Lucas, SR, Donnellan, L, Murakami, D, Kobayashi, S. (2004) Development of Injury Criteria for Pelvic Fracture in Frontal Crashes. IRCOBI Conference on the Biomechanics of Impact.

B52. Kent, RW, Bass, CR, Woods, WA, Salzar, RS, Melvin, J. (2004) The Role of Muscle Tensing on the Force Deflection Response of the Thorax and a Reassessment of Frontal Impact Thoracic Biofidelity Corridors. IRCOBI Conference on the Biomechanics of Impact.

B53. Lucas, SR, Bass, CR, Salzar, RS, Folk, J, Donnellan, L, Paskoff, G, Shender, B. (2004) Viscoelastic Characterization of Cervical Spinal Ligaments. American Society of Biomechanics Conference. Portland, OR.

B54. Bass, CR, Lucas, SR, Salzar, RS, van Rooij, L, Pilkey, WD, Peterson, R, Martin, S. (2003) Human Biodynamic Response to High Speed Craft Shock Loading. SAVIAC Conference.

B55. Bass, CR, Lucas, SR, Salzar, RS, van Rooij, L. (2003) Computational Modeling of High Speed Boat Occupants. MAAC Conference. Norfolk, VA.

B56. Bass, CR, Salzar, RS, Davis, M, Lucas, SR, Donnellan, L, Folk, B, Sanderson, E, Waclawik, S. (2003) Injury Risk in Behind Armor Blunt Thoracic Trauma. Personal Armor Systems Symposium. The Hague, Netherlands.

B57. Bass, CR, Rountree, S, Ling, G, Sanderson, E, Andrefsky, W, Chichester, C, Salzar, RS, Davis, M, Harris, R. (2002) Head and Thoracic Injury Risk in Humanitarian Deminers. UXO Conference, Orlando, FL, September.

B58. Bass, CR, Salzar, RS, Lucas, SR, Donnellan, L, Folk, B, van Rooij, L, Pilkey, WD. (2002) Medical consensus working group on shock mitigation for high speed planing boat occupants. United States Special Warfare Command. San Diego, CA.

B59. Bass, CR, Salzar, RS, Pilkey, WD. (2001) Biodynamic Analysis of Injury and Shock Mitigation in Naval High-Speed Planing Craft, Shock and Vibration Symposium (SAVIAC), Ft. Walton Beach, FL, November.

B60. Pindera, M, Salzar, RS, Williams, T. (1994) Optimization of Residual Stresses in MMC's Using Compensating/Compliant Interfacial Layers, Part II - OPTCOMP User's Guide, NASA Contractor Report 195337, NASA-Lewis Research Center.

B61. Salzar, RS, Barton, FW. (1994) Inelastic Response of Metal Matrix Composite Tubes. Space '94, The 4th International Conference and Exposition on Engineering, Construction, and Operations in Space, Albuquerque, New Mexico.

B62. Pindera, M, Salzar, RS, Williams, T. (1993) An Analytical/Numerical Correlation Study of the Multiple Concentric Cylinder Model for the Thermoplastic Response of Metal Matrix Composites, NASA Contractor Report 191142, NASA-Lewis Research Center.

B63. Salzar, RS, Barton, FW. (1993) Residual Stress Optimization in Metal Matrix Composites Using Discretely-Graded Interfaces (abstract) Proceedings Meet'N'93, Joint ASCE-ASME-SES, Charlottesville, Virginia.

B64. Pindera, M, Williams, T, Salzar, RS, Arnold, S. (1992) Optimization of Residual Stresses in Metal Matrix Composites Using the Multiple Concentric Cylinder Model. NASA Conference Publication 10104, Proceedings of the 5th Annual HITEMP Review, 2: 34.

B65. Salzar, RS, Barton, FW, Ramsey, R. (1992) Optimum Design of Laminated Composites, Proceedings Space '92, ASCE Engineering, Construction, and Operations in Space III, Denver, Colorado.

B66. Salzar, RS, Thubrikar, M, Eppink, R. (1991) Pressure-Induced Mechanical Stress and Atherosclerosis in the Carotid Artery Bifurcation (abstract). Annals of Biomedical Engineering, 19: 587.

C. Workshops

C1. Salzar, RS, Sochor, M, Leasure, JM, Pellettiere, J (2010) Head vs. Helmet: Acceleration as a Blast Dosimeter. Presented to the Accelerative Injury Workshop, Army Research Lab, Aberdeen MD.

C2. Pellettiere JA, Salzar, RS. (2010) Novell Techniques for Measurement of Human Head Acceleration. Presented to ISN Workshop of Biomedical Experiments. Hamburg, Germany.

C3. Bass, CR, Woods, WA, Salzar, RS, Rafaels, KA. (2006) Brain Injury from Blast. Poster presented at the Defense Advanced Research Projects Agency (DARPA), March 27, 2006.

C4. Lucas, SR, Bass, CR, Salzar, RS, Folk, JB, Donnellan, LE, Paskoff, G, Shender, BS. (2004) Viscoelastic Characterization of Cervical Spinal Ligament. Poster presented at the Injury Biomechanics Symposium, The Ohio State University.

C5. Kent, RW, Bass, CR, Woods, WA, Sherwood, CP, Madeley, NJ, Salzar, RS, Crandall, JR. (2002) The Use of a Postmortem Porcine Model to Study the Effect of Muscle Tetanus on Thoracic Force-Deflection Response. Proceedings of the 30th International Workshop on Human Subjects for Biomechanical Research, National Highway Traffic Safety Administration, U.S. D.O.T.

C6. Salzar, RS, Bass, CR, Darvish, KK. (2001) Sonomicrometry in Impact Biomechanics. Proceedings of the 29th International Workshop on Human Subjects for Biomechanical Research, National Highway Traffic Safety Administration, U.S. D.O.T.

D. Presentations and Lectures

D1. Invited Lecture (2013) The Imperial College – London (Blast Brain Biomechanics)

D2. Invited Lecture (2012) Annual Meeting of Orthopaedic Trauma Association, Minneapolis, MN.

D3. Invited Lecture (2012) Department of Orthopaedics – Grand Round Lecture, University of Virginia.

D4. Invited Lecture (2010). History of Blast Research at UVA. Delivered to the University of Nebraska School of Engineering.

D5. Recreational Boat Occupant Kinematics in Crash Scenarios. Invited Lecture to the National Association of State Boating Law Administrators, NTSB Academy, Ashburn, VA.

D6. International IRCOBI Conference on the Biomechanics of Impact, Bern, Switzerland, 2008

D7. Combat Helmet Recorder for Enhanced Detection and Treatment of Traumatic Brain Injuries, Haymarket, Virginia, 2007

D8. 2005 Military/Civilian Transportation Safety Workshop, Ft. Eustis, Virginia, 2005

D9. International IRCOBI Conference on the Biomechanics of Impact, Graz, Austria, 2004

D10. 29th Annual Workshop on Human Subjects for Biomechanical Research, San Antonio, Texas (2001)

D11. ICCE3, The Third International Conference on Composites Engineering, New Orleans, Louisiana (1996)

D12. ICCE2, The Second International Conference on Composites Engineering, New Orleans, Louisiana (1995)

D13. 7th Annual Review of the Advanced High Temperature Engine Materials Technology Program (HITEMP), Cleveland, Ohio (1994)

D14. ICCE1, The First International Conference on Composites Engineering, New Orleans, Louisiana (1994)

D15. Space '94, The 4th International Conference on Engineering, Construction, and Operations in Space, Albuquerque, New Mexico (1994)

D16. Meet'N'93, Joint ASCE-ASME-SES, Charlottesville, Virginia (1993)

D17. Space '92, ASCE Engineering, Construction, and Operations in Space III, Denver, Colorado (1992)

D18. Annual Fall Meeting of the Biomedical Engineering Society, Charlottesville, Virginia (1991)

D19. Applied Mechanics Seminar Series, University of Virginia, Charlottesville, Virginia (1991)

D20. Surgical Research Conference, University of Virginia, Charlottesville, Virginia (1990)

E. Edited Volumes

E1. Lower Leg Biomechanics by Salzar R, Crandall J, Bailey A, and Lievers B. Accidental Injury – Biomechanics and Prevention; Third Edition, Editors: Naraya Yoganandan, Alan Nahum, and John Melvin. Springer, New York, NY, 2013.

APPENDIX 2. HRPO Permissions

From: Brosch, Laura R Dr CIV USA MEDCOM USAMRMC [Laura.Brosch@us.army.mil]
Sent: Wednesday, August 01, 2012 4:06 PM
To: Salzar, Robert (rss2t)
Cc: Gupta, Raj K Dr DoD Af US USA MEDCOM USAMRMC; Chancey, Valeta C Dr CIV USA MEDCOM USAARL; McEntire, Barney J Mr CIV USA MEDCOM USAARL; Brozoski, Frederick T Mr CIV USA MEDCOM USAARL; Emerson, Jill D Ms CIV US USA MEDCOM USAARL; Vasquez, Kimberly B Ms CTR US USA MEDCOM USAARL; Bennett, Jodi H Ms CIV USA MEDCOM USAMRMC; Donahue, Sarah L Dr CIV US USA MEDCOM USAMRMC; Brosch, Laura R Dr CIV USA MEDCOM USAMRMC; Hall, LaMont J LTC MIL USA ASA ALT; Vallone, Michael A Mr CIV USA MEDCOM USAMRAA
Subject: A-17347 Approval of Cadaver Activity "Development of Injury Thresholds Pertaining to Under-Body Blasts," in Support of Tasks 1-4, Proposal 11196007, Award W81XWH-12-2-0042 (UNCLASSIFIED)

Classification: UNCLASSIFIED
Caveats: NONE

SUBJECT: Approval of Cadaver Activity, "Development of Injury Thresholds Pertaining to Under-Body Blasts," Submitted by Robert S. Salzar, PhD, University of Virginia, in Support of Tasks 1, 2, 3 and 4 in accordance with Proposal Log Number 11196007, Award Number W81XWH-12-2-0042, USAMRMC ORP Log Number A-17347

1. The U.S. Army Medical Research and Materiel Command (USAMRMC) Office of Research Protections (ORP) received documents in support of Proposal Statement of Work (SOW) Task XX or the planned DA-Organization activity on 22 May 2012.

2. The test protocol (version 1.0, dated 20 May 2012) and associated documents have been reviewed for applicability of the U.S. Army Policy for Use of Human Cadavers for Research, Development, Test and Evaluation (RDT&E), Education, or Training (referred to herein as the "Army policy"). The involvement of cadavers in this activity constitutes a sensitive use as defined within the Army policy.

a. The activity involves the exposures to blast-level forces of instrumented human cadavers/cadaver specimens to determine the responses of the lower extremity, pelvis and thorax. This multi-phased project will provide data to inform the identification of injury criteria specific to these body regions that will be applicable to UBB scenarios as well as information to characterize the whole body movements necessary for validation of the WIAMan test dummy.

b. The number of cadaver and specimens that will be involved is as follows: Task 1 will use up to 21 pelves and 4 whole bodies; Task 2 will use up to 16 lower extremities; Task 3 will use up to 10 whole bodies; and Task 4 will use up to 3 whole bodies.

c. Cadavers and specimens will be obtained from the following sources provided donor mark the appropriate check-boxes on donation forms from: the LifeLegacy Foundation, the International Institute for the Advancement of Medicine, and the Biological Resource Center, Inc. Cadavers and specimens may also be obtained from the Commonwealth of Virginia State Anatomical Program provided donors' next of kin provide approval as specified in the Center for Applied Biomechanics Standard Operating Procedure, Sourcing and Shipping of Biological Material (SOP B10.1, Nov 2010).

3. The USAMRMC ORP has determined that requirements of the Army policy have been satisfied. This activity is approved and may be implemented pending authorization by local authorities.

4. Please note the following reporting requirements and responsibilities. Send actions as described below to the hrpo@amedd.army.mil, referencing both the proposal log number and USAMRMC ORP log number listed in the "Subject" line above.

a. The activity must be conducted in accordance with the approved test protocol and other governing documents.

b. In the event of activity modifications, the Principal Investigator must send a description of the change(s) to the USAMRMC ORP prior to implementation. A change to the approved SOW requires ORP approval prior to implementation.

c. Problems related to the conduct of the activity involving cadavers or the procurement, inventory, use, storage, transfer, transportation, and disposition of cadavers must be reported promptly to the USAMRMC ORP. Examples of problems include but are not limited to: loss of confidentiality of cadaveric donors, breach of security, significant deviation from the approved protocol, failure to comply with state laws and/or institutional policies, and public relations issues. The USAMRMC ORP will report the problem to the CG, USAMRMC and to TSG of the Army.

5. The Commander/Director/Head of the DA organization conducting or supporting the activity, the USAMRMC ORP, or designees, must be permitted to observe the activity upon request and/or audit activity records to ensure compliance with the approved protocol or applicable regulatory requirements.

6. Do not construe this correspondence as approval for any contract funding. Only the Contracting Officer or Grants Officer can authorize expenditure of funds. It is recommended that you contact the appropriate contract specialist or contracting officer regarding the expenditure of funds for your project.

7. Further information regarding this review may be obtained by contacting Sarah L. Donahue, PhD, MPH, CIP, at 301-619-1118 or Sarah.L.Donahue@us.army.mil

LAURA R. BROSCH, PhD
Director, Office of Research Protections Director, Human Research Protection Office U.S. Army Medical Research and Materiel Command

Note: The official copy of this approval memo is housed with the protocol file at the Office of Research Protections, Human Research Protections Office, 504 Scott Street, Fort Detrick, MD 21702. Signed copies will be provided upon request.

Classification: UNCLASSIFIED
Caveats: NONE

Appendix 3. Personnel Receiving Pay from Research Effort

J Blakey
J Bolton
J Crandall
T Gillispie
S Heltzel
M McCardell
T Miller
B Overby
J Poplin
D Roethlisberger
R Salzar
M Sochor

Grad Students:
Brandon Perry
Sourabh Boruah
Lee Gabler